Functional Roles of the Gap Junction Protein, Connexin43.4, During Vertebrate Development

A DISSERTATION
SUBMITTED TO THE FACULTY OF THE GRADUATE SCHOOL
OF THE UNIVERSITY OF MINNESOTA
BY

Julia M. Hatler

IN PARTIAL FULFILLMENT OF THE REQUIREMENTS
FOR THE DEGREE OF
DOCTOR OF PHILOSOPHY

Advisor: Dr. Ross Johnson

May 2009

Acknowledgements

I write this thesis knowing that there are many people who have been mentors as well as good friends to me over the years…

I thank Ross, my graduate advisor – for thoughtful scientific conversations, excellent professional and personal advice, and many stories (some longer than others) along the way. If I had to "bet my baseball glove" on one of the best mentors a graduate student could encounter, Ross would be among the finest.

I thank Jeff Essner, our long-time collaborator – for always acknowledging my scientific contributions and encouraging me to think freely and come up with lots of hypotheses.

I thank Alison Krufka, my undergraduate mentor – for sparking scientific curiosity in me and for her unique way of convincing me that attending graduate school was the right choice: she advised me that should I enroll in a graduate program, I would find a spouse there, see below…

I thank Ellen Kennedy, my non-science, yet academic mentor – for always keeping my passion for science in a global context and exemplifying how professional achievements and various degrees often take one on interesting and unexpected paths.

I thank Davin, my husband – for always recognizing the important things in life and for being a patient, steadfast friend. And, perhaps most importantly, for thinking like a scientist and helping me to appreciate the importance of amino acids.

I thank Bev and Ron, my parents – for constant, unwavering support and encouragement. And for their willingness to tell their friends and relatives that "no, our daughter still doesn't have a "real" job…yes, she's still in school…" while always reminding me how proud they are.

Dedication

To my family and friends

and

To Dabber Shunts

For bringing friends together and helping us all keep life in perspective

Abstract

During early embryonic development, compartments of cells must send and receive signals in order to coordinate activities such as proliferation, migration and differentiation. Cells regulate these activities inpart through cell-to-cell communication by sharing small signaling molecules and ions via Connexin (Cx)-based gap junction (GJ) channels that connect the cytoplasms of adjacent cells. Mouse knockout models of Cx proteins have demonstrated the necessity for GJ communication during development; cx45 knockouts are embryonic lethal and cx43 null embryos exhibit defects in heart development. However, the mechanisms by which GJ communication regulate early embryonic development, particularly in terms of axis specification and patterning, remain largely unexamined.

Here, the role of zebrafish Cx43.4 (the ortholog of mammalian Cx45) in patterning the asymmetric left-right (L-R) axis of zebrafish was examined. L-R patterning is directed by ciliary beating that generates a leftward fluid flow in the mammalian node or in Kupffer's vesicle (KV), the related structure in zebrafish. Leftward nodal flow is required for normal asymmetric organ placement and function. Cx43.4 expression was detected in KV and morpholino (MO) knockdown of Cx43.4 resulted in randomized organ distribution and reversed asymmetric gene expression. The major finding of these knockdown experiments is that Cx43.4 is required for the morphogenesis of KV. Additionally, Cx43.4 hemichannels, rather than GJ communication, are sufficient to rescue the

defects in asymmetric patterning. Finally, the function of Cx43.4 hemichannels, together with purinergic receptors, is required for the morphogenesis of the KV epithelium. These novel findings have important implications for both the communication and L-R development fields, as well as suggesting new roles for Cx proteins in the early development of a variety of epithelial tissues.

Table of Contents

Acknowledgements i
Dedication ii
Abstract iii
Table of Contents v
List of Tables vi
List of Figures vii
List of Abbreviations ix

Chapter I: Left-Right Patterning and Connexin Biology 1

Chapter II: A Gap Junction Connexin is Required in the Vertebrate Left-Right Organizer 25
- Summary 26
- Introduction 27
- Results 30
- Discussion 41
- Materials and Methods 47

Chapter III: Connexin 43.4 Hemichannel Function is Required for Kupffer's Vesicle Lumen Formation 68
- Summary 69
- Introduction 70
- Results and Discussion 72
- Materials and Methods 83
- Acknowledgements 87

Chapter IV: Summary and Discussion 106

Chapter V: Knockdown of Zebrafish Connexin43.4 Perturbs Angiogenesis Through an Affect on Netrin Signaling 115
- Summary 116
- Introduction 118
- Results 125
- Discussion 139
- Materials and Methods 144

Appendix I: Reprint Permissions 174

Bibliography 176

List of Tables

Chapter V:

Table 1: Circulation defects in Cx43.4-deficient embryos at 30 hpf 168

Table 2: Circulation defects in Cx43.4-deficient embryos at 50 hpf 169

Table 3: Circulation defects in Cx44.2-deficient embryos at 30 hpf 170

Table 4: Circulation defects in Cx44.2-deficient embryos at 50 hpf 171

Table 5: Co-injection of Cx43.4 and Cx44.2 MOs affect the circulation at 30 hpf 172

Table 6: Co-injection of Cx43.4 and Cx44.2 MOs affect the circulation at 50 hpf 173

List of Figures

Chapter 1:

The mammalian embryonic node 20

Connexins and gap junctions 22

Chapter II:

Figure 1: Cx43.4 is specifically required for L-R patterning 50

Figure 2: Cx43.4 is expressed in a spatio-temporal manner to be competent for KV function 52

Figure 3: Molecular markers support a role for Cx43.4 in KV function 54

Figure 4: Midline integrity is maintained in Cx43.4 morphants 56

Figure 5: KV cells are specified in Cx43.4 morphants, though ciliary defects exist 58

Figure 6: KV lumen formation is impaired in Cx43.4 morphants 60

Figure 7: Human *cx45* mRNA partially rescues heart looping 62

Supplementary Figure 1: Cx44.2 is not required for L-R patterning 64

Supplementary Figure 2: Cx43.4 is expressed in KV 66

Chapter III:

Figure 1: Cx43.4 is required for KV morphogenesis 88

Figure 2: Human Cx45 can partially rescue defects in KV lumen formation 90

Figure 3: Cx43.4 hemichannels are sufficient to rescue L-R patterning defects 92

Figure 4: $P2Y_5$ MO phenocopies KV lumen development defect and acts synergistically with Cx43.4 94

Figure 5: Proposed model of Cx43.4 hemichannel function in KV Morphogenesis 96

Supplementary Figure 1: Cx43.4 is not expressed in DFCs at the shield stage 98

Supplementary Figure 2: Junctional complexes are not altered in Cx43.4 morphants 100

Supplementary Figure 3: Expression of Cx-fusion proteins in 293T cells 102

Supplementary Figure 4: Cx43.4-mediated dye uptake in 293T cells is sensitive to Ca_{2+} levels 104

Chapter V:

Figure 1: Multiple Connexin isoforms are expressed in the notochord 148

Figure 2: Cx-deficient embryos have abnormal circulation 150

Figure 3: Cx43.4 morphants have slower heart rates at 48 hpf 152

Figure 4: Cx43.4- and Cx44.2-deficient embryos have defects in angiogenesis 154

Figure 5: *cadh5* expression is reduced in the PCV of Cx morphant embryos 156

Figure 6: Cx43.4 is not expressed in the developing vasculature of Tg*(fli:egfp)* embryos 158

Figure 7: Vascular-specific *shh* signaling cascade in Cx-deficient embryos 160

Figure 8: *net1b* expression is upregulated in Cx morphants 162

Figure 9: Increased *net1b* staining is partially rescued by Cx43.4 DNA 164

Figure 10: Quantitative PCR reveals differences in gene expression in Cx43.4 morphants 166

List of Abbreviations

BBS	Bardet-Biedl syndrome
CNS	central nervous system
Cx	connexin
DA	dorsal aorta
DFC	dorsal forerunner cell
dpf	days post-fertilization
EGFP	enhanced green fluorescent protein
FGF	fibroblast growth factor
GJ	gap junction
hpf	hours post-fertilization
ISV	intersegmental vessel
KIF	kinesin superfamily protein
KV	Kupffer's vesicle
L-R	left-right
MO	morpholino
NVP	nodal vesicular particle
PAV	parachordal vessel
PCV	posterior cardinal vein
RT-PCR	reverse transcriptase-polymerase chain reaction
Tg	transgenic
TGF-β	transforming growth factor β
VEGF	vascular endothelial growth factor
ZO-1	zona occludens-1

Chapter I

Left-Right Patterning and Connexin Biology

Left-Right (L-R) Asymmetry

During early vertebrate development, the overall body plan is established with respect to the anterior-posterior, dorsal-ventral, and left-right (L-R) axes. While most vertebrates have a symmetrical external body plan, the internal patterning and function of organs have distinct L-R asymmetries. This type of asymmetric patterning is conserved both across and within species. For example, asymmetry is observed from snails to humans, and all normal individuals within a given species have the same pattern of L-R asymmetry. In snails, while the external foot and head are bilaterally symmetrical, the direction of snail shell coiling, which reflects the internal body plan, is asymmetric. It has been estimated that greater than 90% of living snail species show dextral, or right-handed shell coiling, rather than the reversed, sinistral coil (Schilthuizen & Davison, 2005).

In humans and other vertebrates, as in invertebrates, there are symmetrical external features that are often paired, such as the eyes and limbs. As expected, the internal body plan has numerous examples of visceral asymmetry, particularly across the L-R axis. For example, the heart, stomach, and spleen are found on the left side, while the gallbladder and liver are located toward the right. Normal asymmetric organ patterning is termed situs solitus, while the congenital condition, situs inversus, describes a mirror-image reversal.

Precise asymmetric patterning is thought to be required for the ability to package numerous organs within the thorax and abdomen. Additionally, functional asymmetry exists across the hemispheres of the brain and is necessary for the specialization of different compartments of the central nervous system. Consistent with normal asymmetric patterning being critical for organ function, heterotaxy – the misplacment of at least one organ with respect to the others – is most often associated with congenital heart defects, polysplenia, and anomalies within the gastrointestinal tract (Peeters & Devriendt, 2006).

Interestingly, despite the defects and congenital diseases associated with abnormal L-R patterning, the rare occurrence of situs inversus (1 out of 6,000-8,000 newborns) has limited detrimental physiological consequences (Peeters & Devriendt, 2006). This observation sets up the interesting question: Why is L-R asymmetry maintained in such a precise way within a species, given that complete organ reversal has few negative ramifications? It would seem that random establishment of the L-R axis would be just as evolutionarily favorable as a particular situs. While the answer to this question remains elusive, research over the past decade has shed light on how L-R asymmetry is established.

Nodal Flow Directs Left-Right Asymmetry

The high conservation of L-R asymmetry across species and the congenital defects associated with mis-patterning suggest that there is an

underlying genetic mechanism(s) by which the L-R axis is established. Hints as to which genetic components influence L-R patterning came from observations of patients with the disease Kartagener's syndrome. The symptoms of Kartagener's syndrome include male sterility, frequent respiratory infections, and chronic sinusitis. These disease characteristics are all associated with defects in ciliary function, and mutations in dynein that render cilia immotile are common in families with Kartagener's syndrome (McGrath & Brueckner, 2003). Interestingly, 50% of patients with Kartagener's syndrome also display situs inversus, suggesting that a ciliary-based mechanism may direct the formation of L-R asymmetry.

Additional evidence to link ciliary function with L-R patterning was provided by a mouse knockout of a microtubule-dependent motor, Kinesin superfamily protein (KIF). In these knockout embryos, the lack of KIF3B resulted in L-R asymmetry defects and the complete absence of cilia within the embryonic node (Nonaka et al., 1998). Further studies found that the nodal cilia of wildtype animals were motile and capable of moving extracellular fluid in a net leftward direction, termed nodal flow (Fig. 1a,b). Importantly, fluid flow was not observed in *kif3B*$^{-/-}$ embryos, suggesting that cilia-driven nodal flow is critical for L-R patterning.

An elegant experimental system was devised by Nonaka et al. to test directly whether nodal flow is a symmetry-breaking event. Remarkably, when mouse embryos were cultured in medium with reversed, rightward artificial fluid

flow across the embryonic node, most of the embryos displayed situs inversus (Nonaka et al., 2002). In further support of the importance of nodal flow for L-R development, artificial leftward fluid flow was able to rescue L-R defects in mutant mice lacking nodal flow due to the presence of immotile cilia.

It has been known for some time that orthologous embryonic node structures are present in multiple species and that these presumptive L-R "organizers" contain monocilia and express a dynein (*lrd*), which is essential for ciliary motility (Essner et al., 2002). However, whether nodal flow as a symmetry-breaking event in L-R patterning is conserved across these species has been controversial. Growing evidence from multiple species (in addition to mice), including zebrafish (Essner et al., 2005; Kramer-Zucker et al., 2005), *Xenopus* (Schweickert et al., 2007), and rabbit (Okada et al., 2005), suggests that nodal flow is a conserved feature of L-R asymmetry. It remains to be determined, however, whether nodal flow breaks symmetry in these species, as it seems to in the mouse, or whether it serves to amplify a previous asymmetry present in the early embryo.

How does nodal flow direct L-R patterning?

Since the discovery of nodal flow just over a decade ago, much research has focused on understanding the signal transduction mechanism of cilia-driven fluid flow in directing L-R patterning (Basu & Brueckner, 2008). There are currently two models to explain how fluid flow is transmitted into L-R

information: either through a chemical or mechanical mechanism. While support exists for each of these models (described below), whether one mechanism (or both) is (are) the primary mode by which nodal flow directs a left-sided signal remains unclear.

First, the chemical model proposed that some unknown morphogen or signaling molecule was moved by the extracellular fluid flow, creating a gradient of the signal that would be higher on the left side of the node than on the right. In support of this model, nodal vesicular particles (NVPs) were identified in the mouse node. These membranous spheres are released into the node in a fibroblast growth factor (FGF)-dependent manner and are thought to be swept by the nodal flow to the left side of the node where they release their signaling contents, Sonic hedgehog and retinoic acid (Tanaka et al., 2005).

Second, a mechanical mechanism whereby the force of nodal flow would be sensed differently on the left side compared to the right side could be utilized to transmit nodal flow into a downstream signal. Indeed, two populations of cilia have been identified in the mammalian node: one thought to be motile and to produce fluid flow, while the other class is immotile and could sense and respond to the flow. These immotile cilia are localized to the periphery of the node and contain the cation channel, polycystin-2 (McGrath et al., 2003). Interestingly, mice lacking polycystin have defects in L-R asymmetry, suggesting that the nodal cilia expression of polycystin may act as a sensor for normal patterning.

In the kidney, the polycystin proteins function as mechanosensors. Upon the bending of cilia, polycystin is required to facilitate the influx of Ca^{2+}, with the increase in Ca^{2+} being transmitted to neighboring cells via gap junctions. A similar mechanism could be envisioned in the embryonic node during the establishment of the L-R axis. Indeed, a left-sided Ca^{2+} wave is observed in the mesodermal tissue surrounding the node structures of both mice (McGrath et al., 2003) and zebrafish (Sarmah et al., 2005). Finally, increased intracellular Ca^{2+} in cells adjacent to the node is dependent on polycystin-2 (McGrath et al., 2003), suggesting that polycystin-2 is able to transduce fluid flow into a downstream signal.

Nodal flow directs asymmetric gene expression

How then does the Ca^{2+} wave induced by nodal flow result in asymmetric organ patterning and function? A conserved, left-sided TGF-β signaling pathway is thought to transmit the directionality introduced by nodal flow to organ precursors (Raya & Belmonte, 2006). In all vertebrates studied, *nodal* (a member of the TGF-β family) expression is restricted to the left lateral mesoderm of the early embryo. Downstream of Nodal, the transcription factor Pitx2 is activated on the left side of the embryo. Pitx2 is responsible for promoting changes in cell morphology, survival, and growth that ultimately result in asymmetric organ development (Mercola, 2003).

Interestingly, the conservation of the left-sided nodal signaling cascade has recently gained additional support in invertebrates, following the isolation of *nodal* and *pitx* genes in snails. Consistent with loss-of function studies in vertebrates, pharmacological inhibition of the nodal signaling pathway in the snail resulted in L-R defects, reflected in reversed, sinistral shell coiling (Grande & Patel, 2009).

Although much is known about the roles of cilia-induced nodal flow and the left-sided gene expression cascade, a number of important questions remain unresolved. How the asymmetric signal is transmitted from the node to the lateral mesoderm is not well-understood (further discussion included in Chapter II). As previously alluded to, the extent to which the laterality program is a conserved mechanism also remains unclear. Specifically, with respect to conservation, one of the least understood questions is whether nodal flow serves as the primary L-R determining factor or whether it amplifies a prior L-R determinant. In *Xenopus*, for example, H^+-V-ATPase is asymmetrically localized prior to node function at the early cleavage stages, and H^+-V-ATPase is required for L-R patterning in *Xenopus*, chick, and zebrafish (Adams et al., 2006). Future studies will be necessary to determine whether H^+-V-ATPase, or other transcripts, are asymmetrically expressed in mammals prior to nodal flow and whether they are similarly required for L-R patterning.

Zebrafish as a model system for studying L-R asymmetry

The zebrafish model system has many advantages that allow investigations using both cell biological and genomic approaches into the mechanisms that regulate L-R patterning. A single zebrafish pair can produce hundreds of synchronized embryos by natural spawning, and these embryos develop externally and are optically clear. These features allow for ease in observing the development and function of the orthologous embryonic node structure, Kupffer's vesicle (KV), and the asymmetric patterning of organ systems within living embryos. In addition, external development allows for easy accessibility to structures like KV for physical manipulations and data collection. The ability to efficiently knock down protein levels in zebrafish embryos by injection of antisense morpholino (MO) oligonucleotides allows for studies of specific gene function (Nasevicius & Ekker, 2000). Finally, there is strong conservation of gene identity and function from zebrafish to higher vertebrates (Shin & Fishman, 2002), so developmental mechanisms that operate in zebrafish are likely to have relevance in other organisms as well.

Kupffer's vesicle morphogenesis is required for nodal flow and normal L-R development

Previous studies in zebrafish have identified KV as the orthologous L-R organizer (Essner et al., 2005; Kramer-Zucker et al., 2005). KV is a transient "organ" that shares many features with the mammalian node. Similar to cells of the node, KV cells also form a tight epithelium with each cell containing a motile

monocilium. The vortical movement of these cilia produces a counter-clockwise fluid flow that is required for normal L-R patterning. In contrast, the morphologies of KV and the mammalian node display some differences. While, the mammalian node is a triangular shaped, concave pit containing a single epithelial cell layer that is covered by a thin membrane (to create a space for nodal flow), KV is an inflated sphere with the interior lumen space lined by the ciliated epithelium (Lee & Anderson, 2008). Additionally, each of the cells lining KV has a cilium pointing toward the lumen, while only the ventral surface of the mouse node contains cilia.

Although there are morphological differences in the overall layouts of the zebrafish and mouse L-R organizers, the primary function of these tissues – production of nodal flow – is conserved (Essner et al., 2005; Kramer-Zucker et al., 2005). Interestingly, upon closer examination of KV, it was noted that the proportion of KV cilia is enriched in the dorsal hemisphere (Kreiling et al., 2007). This organization is strikingly similar to the mouse node, which lends further support to the conserved mechanism of leftward fluid flow within these structures (Lee & Anderson, 2008).

The morphogenesis and full lumen formation of KV is required for normal patterning and the steps leading to KV development have recently been studied. In brief (further discussion in Chapter III), future KV precursor cells undergo a mesenchymal to epithelial transition (MET), establish apical-basal

polarity and develop cilia, and finally, the apical cell surfaces expand away from one another to form a fluid-filled luminal space (Amack et al., 2007).

While the complete mechanism and genetic players are not yet known, a growing number of genes that affect various stages of KV morphogenesis exist in the literature. Prior to the MET, KV precursor cells undergo migration, which is dependent on beta-catenin expression and an increase in intracellular Ca^{2+} (Schneider et al., 2008). Two transcription factors, *spt* and *ntl*, are required for maintenance of cell-cell associations during early KV cell specification and subsequent lumen formation, respectively (Essner et al., 2005; Amack et al., 2007). Depletion of Bardet–Biedl syndrome (BBS) genes results in ciliary degeneration and KV fails to inflate, although the mechanism leading to BBS regulation of inflation is unknown (Yen et al., 2006). Although each of these examples affects a different stage of KV morphogenesis, the end result is the same: KV does not develop into a fully inflated, luminal sphere that can support cilia-driven fluid flow. An important area of future study will be do identify how, if at all, these (and other as yet unidentified) genes fit together in a common KV morphogenesis program.

Other important questions in the field of KV morphogenesis include: How are nodal cilia properly localized in order to generate a productive flow? In order for fluid flow to have a net leftward direction (or counterclockwise in the case of KV), the cilia must be oriented toward the posterior in the plane of the apical cell membrane as well as being tilted toward the posterior (Nonaka et al.,

2005). Could planar cell polarity signaling play a role in this process? Finally, given the observation that KV cilia organization resembles that of the mammalian node (Lee & Anderson, 2008), it will be interesting determine whether any of the mechanisms that regulate KV morphogenesis also affect development and/or function of the mouse node.

Cell communication mediated by gap junctions

Cell-to-cell communication is important for the regulation of myriad developmental processes such as proliferation, migration, growth control, differentiation, and morphogenesis. Communication can be indirect through signals transmitted via the extracellular matrix as an intermediate or direct from the cytoplasm of one cell to its neighbors. The direct transmission of small molecules less than ~1000 Daltons occurs through unique collections of transmembrane channels termed gap junctions (GJs).

In vertebrates, GJs are comprised of Connexin (Cx) protein subunits (Fig. 2a), of which there are approximately 20 family members in mammals (Willecke et al., 2002) and additional numbers in zebrafish (Eastman et al., 2006; Cruciani & Mikalsen, 2007). Orthologs are also present in invertebrates and are termed Innexins. A GJ channel is formed when a Cx hexamer (termed a hemichannel or connexon) surrounding an aqueous pore (Fig. 2b) docks with another hexamer in the membrane of an apposing cell (Fig. 2c) (Kumar & Gilula, 1996). Numerous cell-cell channels aggregate within a plasma

membrane domain and the resulting intercellular space is reduced to a narrow gap of approximately 2-3 nm, hence the term gap junction.

GJ communication is present in nearly all differentiated animal cells, and the level of communication between cells can be precisely regulated. For example, the number of cell-cell channels within a GJ plaque or the activity of these channels (i.e. the open probability) can be modulated in response to various cell signaling events. Cx mRNA levels can be increased in response to hormone (Saez et al., 2003) or growth factor signaling (Ai et al., 2000) with a corresponding increase in cell coupling. Alternatively, communication can be inhibited following the ubiquitination of Cxs at the plasma membrane (Leithe & Rivedal, 2004), which results in rapid protein turnover, with half lives on the order of 1-2 hours in some cases.

GJ communication can also be regulated on the order of minutes without an apparent reduction in channel number by means of a gating mechanism, which affects the open probability of GJ channels (Moreno & Lau, 2007). Most Cxs have multiple phosphorylation sites, and certain phosphorylation events, particularly those mediated by MAPK, are implicated in channel gating (Solan & Lampe, 2009).

Physiological roles of gap junction communication

Almost all adult mammalian cells rely on GJs for communication, and the importance of Cx function for the regulation of tissue and organ physiology has

been underscored by recent mouse knockout studies and the analysis of human diseases. For example, knockout of Cx37 results in female sterility due to defects in oocyte maturation (Simon et al., 1997), and loss of Cx50 leads to cataract development (White et al., 1998). In addition to the mouse studies, many human conditions including Charcot-Marie-Tooth disease, deafness, and skin disorders have been linked to mutations in various Cx genes (Willecke et al., 2002). These observations reveal the extensive requirement for Cxs across many tissue types and suggest that Cxs fulfill a variety of functions within nearly all cells.

Gap junctions in development

There are many cellular events during embryonic development that are stimulated by signals and require the coordination of groups of cells, so GJs have long been thought of as critical for development. Again, mouse knockout studies have revealed many requirements for Cxs during development. For example, embryonic lethality due to cardiovascular deficiencies is observed in Cx45 knockout animals (further discussion in Chapter V), and Cx43 knockout mice have defects in heart outflow tract morphogenesis (Huang et al., 1998). Although there are numerous examples that clearly demonstrate a requirement for Cxs during development, how Cxs and/or GJ communication function during development remains largely unknown.

In addition to the examples of Cx function in the development of cardiovascular organ systems, GJ communication has also been implicated in early embryonic patterning events, although this is less understood (further discussion in Chapter II). During early embryogenesis, cell-cell interactions are critical for the establishment of the overall body plan and the major axes of the organism. An important aspect of axis patterning is that populations of cells are differentially specified (e.g. dorsal versus ventral compartments). GJ communication could serve to coordinate the response of a population of cells to certain signals, ensuring that they remain distinct from other cells destined for a different fate. This is exemplified by differences in GJ communication between dorsal and ventral cells of the developing *Xenopus* embryo (Krufka et al., 1998).

Gap Junctions and Left-Right Asymmetry

Of particular relevance to the studies presented here, GJs have also been implicated during patterning of the L-R axis. Characterization of patients with laterality defects uncovered mutations in the Cx43 sequence (Britz-Cunningham et al., 1995). However, additional patient studies by other groups failed to confirm these early findings (Gebbia et al., 1996; Debrus et al., 1997), and it remains unclear whether Cx43 mutations are a cause of laterality defects or a correlative observation.

Because of the study by Britz-Cunningham et al., and prior to the discovery of nodal flow (discussed above), it was postulated that GJ communication could provide an effective mechanism for an initial asymmetric cue to be transmitted to entire cell fields (Levin & Nascone, 1997). Early studies in *Xenopus* (Levin & Mercola, 1998) and chick (Levin & Mercola, 1999) using pharmacological inhibitors of GJ communication revealed defects in L-R patterning. However, the efficacy and specificity of these inhibitors has been questioned due to the presence of off-target effects, e.g. the insecticide, lindane, induces oxidative stress (Caruso et al., 2005). Perhaps more convincing evidence to support a role for Cxs in L-R patterning came from the use of a dominant-negative Cx construct injected into dorsal blastomeres of the *Xenopus* embryo (Levin & Mercola, 1998) and chick embryos cultured in the presence of antisense oligonucleotides to reduce *cx43* expression (Levin & Mercola, 1999).

A more recent study has investigated the role of Cx43-based GJs during L-R patterning in rabbits, again using pharmacological GJ blockers. The results suggest that FGF-activated signals are passed through GJs from the midline to the lateral mesoderm in order to repress left-sided gene expression prior to nodal flow (Feistel & Blum, 2008). Interestingly, it seems that GJ communication is attenuated in response to nodal flow, which results in the release of FGF-mediated inhibition and the subsequent activation of left-sided gene expression.

These studies have provided important evidence that Cxs play a role during L-R patterning but many questions still remain. Importantly, given the controversial reports on human laterality patients and Cx43 mutations, it is unclear whether conservation of Cx43 function in L-R patterning exists from *Xenopus,* chick and rabbits to humans. Also, the use of drug inhibitors to block GJ communication does not enable a precise evaluation of the spatio-temporal requirement of Cx function nor the specific Cx isoform required within the early embryo. Additionally, given our expanded knowledge of the role of the ciliated node structures since the publication of the early studies in chick and *Xenopus*, a major question is whether Cxs could be involved in nodal flow or whether they strictly function outside of the node as the study in rabbits would indicate.

Important remaining questions

Although GJs have been studied for over 40 years and there are numerous examples of the importance of Cxs for embryonic development, there are still many important questions remaining. In particular, most interpretations of the function of Cxs during development have focused on their roles in the formation of GJs and intercellular communication. However, the nature of the signals that pass through GJs to regulate developmental processes are not clear.

Additionally, a growing body of literature suggests that Cxs may have other roles, independent of their intercellular communication function within a GJ. An interesting alternative role for Cx proteins is related to the regulation of

cell adhesion. First, Cxs and the adhesion molecules, cadherins, share a number of binding partners including zona occludens-1 (ZO-1) and catenin family members (Wei et al., 2004). Second, depletion of N-cadherin reduces GJ coupling (perhaps not surprisingly if cells are no longer in contact) and, interestingly, Cx43 siRNA knockdown also reduces the amount of plasma membrane N-cadherin (Wei et al., 2005). These observations provide evidence that GJs and adherens junctions are closely associated. Finally, in a recent study examining radial migration of neurons in the developing mouse embryo, a developmental role for Cx-mediated adhesion was observed. Neuronal migration was inhibited in the absence of Cx43, and this migratory defect could be rescued by a communication-deficient Cx43 construct even when the C-terminal tail (a site of signaling via phosphorylation and protein-protein interactions) was eliminated (Elias et al., 2007).

Another GJ-independent role for Cx function involves undocked hemichannels in the plasma membrane. Hemichannels that are not associated with a GJ have been detected in multiple cell systems, and these hemichannels can be opened experimentally (Goodenough & Paul, 2003). How then, might Cx hemichannels function physiologically? Ca^{2+} waves have been observed in numerous cell types, and they are associated with Cx expression. GJ inhibitors do not always block these Ca^{2+} waves, suggesting that the Cx requirement is independent of GJ function (Goodenough & Paul, 2003).

It is now clear that there are two classes of Ca^{2+} wave propagation, one dependent on GJ communication and a second involving an extracellular pathway. This extracellular pathway can be blocked with suramin and apyrase to degrade ATP. The non-GJ model involves the release of ATP through Cx hemichannels that stimulates purinergic receptors and the downstream activation of IP_3 (Goodenough & Paul, 2003). In further support of this model, a recent study has used several experimental approaches to show that ATP release coincides with Cx43 hemichannel opening (Kang et al., 2008). It is interesting to speculate that the Ca^{2+} wave in the cells adjacent to KV may be mediated by a similar hemichannel-dependent mechanism of ATP release.

The goals of this thesis

Cx expression is found across cell and tissue types and is known to be important for development. However, there are few examples of how Cxs or GJs function during embryonic patterning and no clear mechanisms have been elucidated. With respect to L-R patterning, the focus of the studies presented here, a requirement for GJs has been proposed. However, as described above, there are many important questions remaining. This thesis seeks to address the following questions:

1) Are Cxs required in the early stages of embryonic development?
2) Do changes in Cx expression (in time and space) suggest different functional roles during development?

3) Is Cx function a general requirement for L-R patterning?

4) Do different Cx isoforms play different roles during L-R patterning?

5) How precisely do Cxs function during L-R patterning?

6) What is the mechanism by which Cx43.4 functions to create a functional epithelium?

7) Is the role of Cx43.4 hemichannels sufficient to explain all of this Cx's function in L-R patterning?

8) Is the role of Cx43.4 in lumen formation found more broadly in terms of epithelial development?

Figure 1:

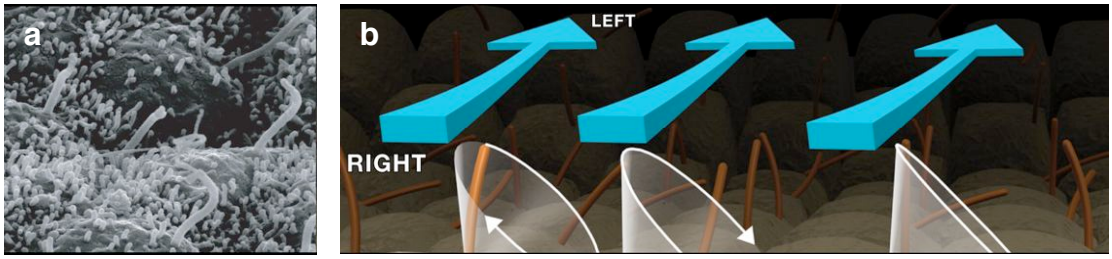

Reprinted from (Hirokawa et al., 2006), with permission from Elsevier
License Number: 2173190339757

Figure 1:

The mammalian embryonic node. (a) A scanning electron micrograph of the ciliated cells in the rabbit ventral node. (b) Ciliary motility creates a leftward extracellular fluid flow.

Figure 2:

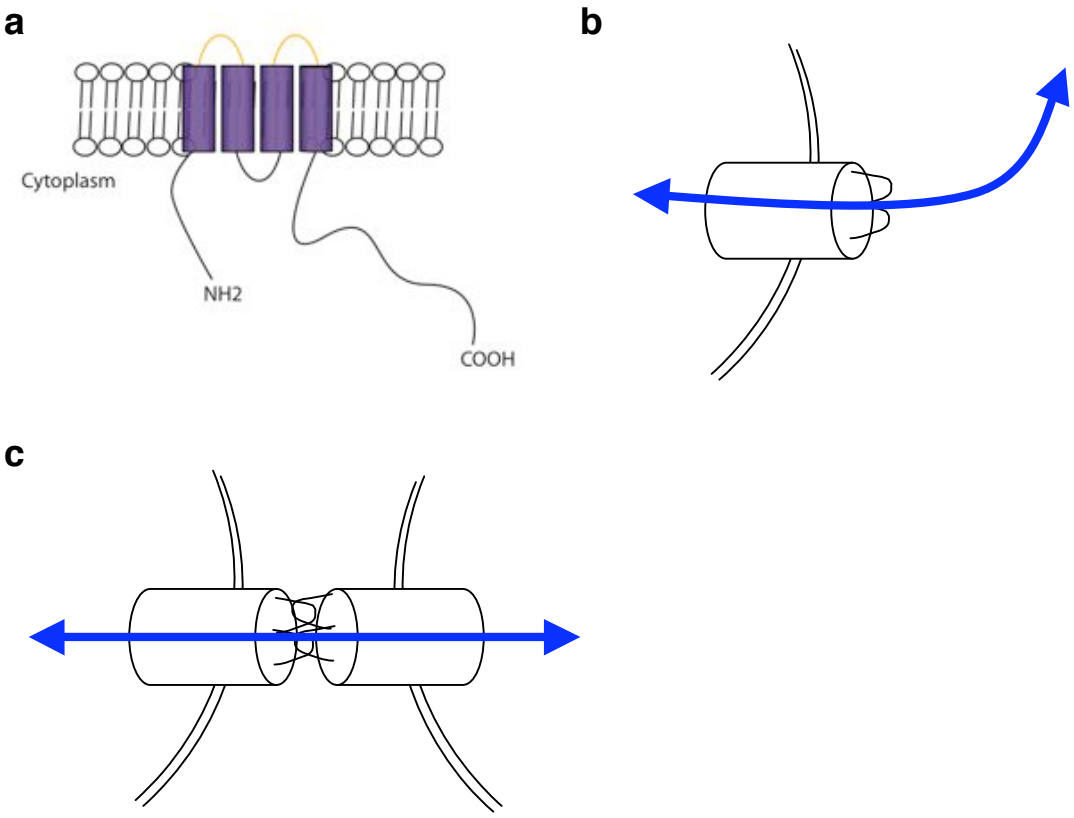

Figure 2:

Connexins and gap junctions. (a) Cx proteins contain four hydrophobic, membrane-spanning regions, two extracellular loops that are important for hemichannel docking, and both the N- and C- termini are located cytoplasmically. (b) Six Cx subunits are assembled to form a hemichannel and are inserted into the plasma membrane. These hemichannels can be opened experimentally to the extracellular environment. (c) One hemichannel docks with a similar hemichannel on an adjacent cell membrane to form an aqueous GJ channel, which directly connects the cytoplasm of neighboring cells.

Chapter II

A Gap Junction Connexin is Required in the Vertebrate Left-Right Organizer

SUMMARY

Early patterning of vertebrate embryos involves the generation of asymmetric signals across the left-right (L-R) axis that are necessary to establish the position and function of internal organs. This patterning is directed by a conserved nodal/lefty signaling cascade on the left side of the embryo, thought to be asymmetrically directed by ciliary beating that generates a leftward fluid flow in the mammalian node or in Kupffer's vesicle (KV), the related structure in zebrafish. Following morpholino knockdown of Cx43.4, asymmetric gene expression and global organ distribution are randomized, consistent with the expression of Cx43.4 in KV. Randomization is recapitulated in mosaic embryos in which Cx43.4 is depleted preferentially in KV cells, showing that Cx43.4 is specifically required in KV for proper L-R axis formation. The mechanistic basis for the laterality anomalies in Cx43.4-deficient embryos is a primary morphogenesis defect reflected in non-inflated and poorly developed KVs that lack definitive lumens. Additionally, the role of Cx43.4 appears to be conserved given that its ortholog, human Cx45, is able to functionally compensate for zebrafish Cx43.4 during L-R patterning. This is the first report linking Cx function in the ciliated, node-like cells of KV with normal L-R axis development.

INTRODUCTION

While vertebrates typically exhibit external symmetry across the left-right (L-R) axis, the distribution of internal viscera and function of particular organs are strikingly asymmetric. Internal L-R asymmetry is a tightly regulated patterning process such that all normal individuals within a species display a precise morphological and functional arrangement. The failure to establish the L-R axis during early embryogenesis leads to heterotaxy, which is associated with organ laterality defects, including congenital heart disease and spleen abnormalities (Bisgrove et al., 2003).

Much progress has been made toward understanding the mechanisms that lead to proper asymmetric patterning, including identification of a conserved, left-sided TGF-β signaling cascade (Meno et al., 1996). In the mouse, direction and propagation of this signaling cascade requires the action of motile monocilia within the embryonic node (Basu & Brueckner, 2008). These monocilia rotate in a counter-clockwise direction to produce nodal flow, which is the movement of extracellular fluid in a net leftward direction (Nonaka et al., 1998). Although many genes have been implicated in the known mechanisms that drive L-R patterning (e.g. cilia-driven nodal flow, left-sided gene expression, and midline function), the primary L-R determinant remains debated (Yost, 2003; Levin, 2005; Raya & Belmonte, 2006). However, the presence of motile monocilia in the orthologous L-R organizing structures of mouse, chick, *Xenopus,* and zebrafish (Essner et al., 2002) highlights the

conservation of nodal cell function and leftward fluid flow for L-R patterning and suggests that extensive mechanistic conservation exists among at least some species.

Zebrafish have served as a useful model for understanding L-R patterning as they provide a number of advantages for pursuing these conserved mechanisms. In particular, the ability to easily access, manipulate, and monitor the ciliated cells of KV in live embryos has resulted in a model outlining the distinct steps in the development of this structure (Amack et al., 2007). KV is a transient structure that arises from the dorsal forerunner cells (DFCs). DFCs are a population of mesenchymal cells that migrate ahead of the shield (zebrafish organizer) during epiboly and eventually involute to reside within the developing tailbud (Cooper & D'Amico, 1996). At this site, they differentiate into the ciliated epithelial cells that line the lumen of KV. Surgical disruption of KV showed that a critical developmental window exists from 3-7 somites when ciliary function and nodal flow are required for normal L-R patterning (Essner et al., 2005). In the present study, we demonstrate that a Cx protein is required for the DFCs to develop into KV and undergo morphogenesis into a fully functional epithelial lumen capable of generating an asymmetric signal.

Recent mouse knockouts of connexins (Cx), the protein subunits of vertebrate gap junctions (GJs), have clearly demonstrated that Cx-based communication is required for normal organ function and, in some cases, for

proper development (Wei et al., 2004). For example, Cx45 null embryos die at embryonic day 10 (Kruger et al., 2000; Kumai et al., 2000), and Cx43 knockouts exhibit defects in heart development (Reaume et al., 1995). However, the mechanisms by which Cxs might regulate early embryonic development and patterning remain largely unexamined.

Since Cx proteins are required for development, we theorized that GJ channels also play an early role in embryonic patterning. Specifically, GJ channels could function during development through the direct, cell-cell transfer of small signaling molecules, such as ions, cAMP, and IP_3 in regulating the migration, differentiation, and physiology of cells (Wei et al., 2004).

Here, we show that morpholino (MO) depletion of Cx43.4 randomizes L-R patterning. These defects can be rescued by co-injection of MOs and Cx43.4 mRNA, showing that the L-R phenotype is a specific consequence of Cx43.4 knockdown. Consistent with Cx43.4 localization in KV cells, targeted knockdown of Cx43.4 within KV cells leads to randomization. This indicates that Cx43.4 function within KV cells is necessary for L-R patterning. KV cells were correctly specified following Cx43.4 depletion given that cilia were present, although they were shorter in morphants than in controls. However, following MO knockdown, Cx43.4 morphant KVs failed to inflate and morphogenetic defects were apparent. Taken together, these results indicate that the laterality defects associated with Cx43.4 depletion are a result of defects during KV morphogenesis.

RESULTS

Cx43.4 knockdown randomizes left-right asymmetry

We sought to determine the role of Cx43.4 in embryonic patterning given that it is highly expressed during gastrulation and somite-forming stages in zebrafish (Essner et al., 1996). Interestingly, when antisense MO methods (Nasevicius & Ekker, 2000) were utilized to knock down the level of Cx43.4, morphant embryos displayed heart laterality defects that indicated a L-R patterning defect. Normally, the heart tube loops from the left to the right side of the embryo. This morphogenesis can be visualized by *in situ* hybridization using a cardiac myosin light chain (*cmlc2*) probe (Fig. 1A). However, upon MO depletion of Cx43.4, heart looping was abnormal in 47% of embryos (notably, 39% reversed and 8% midline; Fig. 1B, C), compared with only 7% aberrant looping in embryos injected with a mismatched control MO (Fig. 1C). The effects of Cx43.4 knockdown on heart looping were not significantly different from the theoretical maximum of 50% reversal upon randomization, (χ^2 (1, N = 64) = 0.360, $p > 0.5$). Knockdown of a closely related connexin family member, Cx44.2, however, produced insignificant effects on heart looping (Fig. S1A), suggesting that Cx43.4 plays a more significant role in L-R specification despite the localization of *cx44.2* transcripts to KV (Fig. S1B). Therefore, the remaining studies focused on the role of Cx43.4, and not Cx44.2, during L-R development.

To determine whether Cx43.4 is required for global embryonic L-R patterning processes versus a more limited function during later heart

morphogenesis, other known asymmetric organ systems were examined. 100% of control embryos (n=13) had normal positioning of the gallbladder on the right and pancreas on the left at 6 days post fertilization (Fig. 1D). However, heterotaxia was observed in the developing guts of 51% (n=39) of morphant embryos (Fig. 1E) with embryos displaying reversal of the gallbladder and/or the pancreas. These data, along with the analysis of asymmetric central nervous system (CNS) patterning below, indicate that the laterality of multiple organ systems is affected in Cx43.4-deficient embryos and suggest a requirement for Cx43.4 during early establishment of the L-R axis.

Cx43.4 is expressed in and around KV

To explore further the role of Cx43.4 in asymmetric patterning, we next asked if its localization supports a function for Cx43.4 during LR development. As previously reported (Essner et al., 1996), *cx43.4* was expressed throughout the somite-stage embryo with higher expression observed posteriorly and in the notochord. Interestingly, the DFCs do not display expression of *cx43.4* during gastrulation (Essner et al., 1996), suggesting a later role for Cx43.4 during KV development. Consistent with this, *cx43.4* transcripts were identified in KV cells of 10-somite stage embryos (Fig. S2). Protein localization was also analyzed to determine whether it coincided with mRNA expression. For this analysis, KV was identified using antibodies for acetylated tubulin to label cilia in the tail region of 10-somite stage embryos. Co-labeling with polyclonal Cx43.4

antibodies (Desplantez et al., 2003) showed distinct puncta within the ciliated area of KV and throughout the surrounding tail tissue (Fig. 2A). Notably, Cx43.4 puncta were not co-localized with cilia or Hoechst-labeled nuclei and were often found between nuclei, suggesting that the Cx43.4-positive plaques are localized to regions of cell-cell apposition. The expression of Cx43.4 in KV cells during the developmental stage when KV cilia are actively producing nodal flow is consistent with a requirement for Cx43.4 during L-R development.

We also analyzed the effects of MO injection on Cx43.4 localization. Upon injection of Cx43.4 MOs, the punctate staining in KV and elsewhere throughout the embryo was abolished (Fig. 2B), demonstrating extensive MO knockdown efficacy. Overall, Cx43.4-depleted embryos were grossly normal at 24 hours post fertilization (hpf) (data not shown) and high survival rates were observed, averaging 86% (after normalizing uninjected controls to 100%). This suggests that the observed disruption of L-R patterning in Cx43.4 morphants represents a direct requirement for Cx43.4 in KV (or tissues near KV) and not a secondary effect given the normal patterning of other embryonic axes.

Cx43.4 is specifically required for LR patterning

To rule out off-target effects of Cx43.4 MO injection, the specificity of the morphant L-R phenotype was verified by a rescue approach. Cx43.4 MOs were co-injected with *in vitro* transcribed, MO-insensitive *cx43.4* mRNA at the one-cell stage and heart looping was analyzed at 30 hpf. In these experiments, injection of MOs alone resulted in 40% of the embryos (n=178) displaying

aberrant heart looping, while Cx43.4 mRNA injected alone had no effect. Co-injection of MOs and 100 pg of rescuing mRNA significantly reduced the percentage of embryos with aberrant heart looping from 40% to 23% (n=148, $p<0.04$) (Fig. 2C). These results indicate that the effects of Cx43.4 MO injection on L-R development are specifically related to Cx43.4 depletion and are not a side effect of the MO injection procedure.

Cx43.4 functions in KV during LR patterning

Given the widespread distribution of Cx43.4 puncta observed by immunofluorescence, it is possible that Cx43.4 is not required in KV itself. Cx43.4 could influence L-R patterning through its expression in the lateral mesoderm and/or notochord. To address whether Cx43.4 expression is required specifically in KV cells, mosaic animals were produced by an experimental method that is unique to zebrafish. Because the DFCs maintain cytoplasmic bridges to the yolk between the 256- and 1,000-cell stages while other blastomeres do not, MO injection into the yolk at these stages knocks down expression in a KV cell-specific manner (Amack & Yost, 2004). After DFC-targeted knockdown of Cx43.4, defects in heart looping were seen in 34% of embryos (Fig. 2D), which is quantitatively comparable to previously reported defects in DFC-targeted knockdowns of a ciliary dynein, *lrdr1*, (Essner et al., 2005) and the transcription factor, *ntl* (Amack & Yost, 2004). In our hands, DFC-targeted *ntl* depletion produced comparable alterations in heart looping to

knockdown of Cx43.4 (Fig. 2D) and served as a positive control. This mosaic analysis provides strong evidence of a tissue-autonomous requirement for Cx43.4 in KV during establishment of the L-R axis.

Previous reports in the literature have implicated Cx43-based GJ communication in L-R patterning of *Xenopus* and chick embryos (Levin & Mercola, 1998, 1999). However, the role of Cx43 in L-R patterning may not be conserved; Cx43 knockout mice do not show laterality defects and it is unclear whether human patients with laterality defects also have Cx43 point mutations (Britz-Cunningham et al., 1995; Debrus et al., 1997). In the present study, consistent with the lack of *cx43* expression in KV cells (data not shown), abnormal looping in DFC-targeted Cx43 morphant embryos was not significantly different than in uninjected control embryos (Fig. 2D, $p > 0.4$). This suggests that Cx43 is not required within the cells of KV for normal L-R development and serves as a control for the specificity of Cx43.4 function in KV.

Asymmetric gene expression patterns are consistent with a role for Cx43.4 function in KV

To determine whether the KV tissue-autonomous role of Cx43.4 influenced downstream signaling events, we analyzed the expression of genes in an evolutionarily conserved, left-sided TGF-β cascade known to direct asymmetric organ development. One of the first asymmetrically expressed genes, *spaw*, is activated in the left-lateral mesoderm adjacent to KV at 10-12 somites (Long et al., 2003). Left-sided *spaw* expression is dependent on an

intact KV with normal nodal flow. Initiation of *spaw* expression in 12-somite stage Cx43.4 morphants was predominantly bilateral (66%, n = 35; Fig. 3A-E), while 82% of control embryos expressed *spaw* on the left side. These data suggest that cells lateral to KV in Cx43.4-deficient embryos are capable of receiving a signal and activating *spaw* expression, however the directionality of activation is impaired.

The embryonic midline, comprising the notochord and floor plate of the CNS, is required to restrict asymmetric gene expression to the left or right sides of the embryo. Disruption of the midline or of repressive signaling from this midline barrier results in bilateral expression of normally asymmetrically expressed genes (Danos & Yost, 1996; Meno et al., 1998), similar to the *spaw* expression pattern in 12-somite stage Cx43.4 morphant embryos. Since Cx43.4 is expressed in the notochord, we next examined the signaling barrier function of the midline in Cx43.4-deficient embryos to determine if it was intact. No apparent differences in the expression of *ntl* in the notochord domain were detected when comparing controls (Fig. 4A,C) and Cx43.4 morphants (Fig. 4B,D) at 10 or 20 somites, suggesting that the midline was continuous. Additionally, at 20 somites, *spaw* expression was randomized (Fig. 3F), rather than being expressed bilaterally as observed at 12 somites (Fig. 3E). Resolution of early bilateral *spaw* expression to randomization at 20 somites provides further evidence, of a functional nature, that the midline barrier is intact in Cx43.4-deficient embryos and is capable of restricting asymmetric gene

expression to one side of the embryo. Taken together, the *spaw* expression data at two developmental time points suggest that Cx43.4 morphants do not have defects in midline barrier function, but KV function is altered.

We next analyzed the asymmetric expression of genes that are downstream of *spaw* signaling. *lefty1* is normally expressed in the left, dorsal diencephalon (Fig. 3G) and can be used as a marker for asymmetry in the CNS at the 20-somite stage. Upon Cx43.4 knockdown, *lefty1* was expressed on the left in only 22% of embryos, while all of the control embryos that had activated *lefty1* displayed normal, left-sided expression (Fig. 3H,I). Importantly, right-sided or bilateral expression patterns were never seen in controls, whereas 33% of Cx43.4 morphant embryos had reversed, right-sided *lefty1* expression. Cx43.4 knockdown also resulted in randomization of *lefty2* (Fig. 3J-L), a gene normally expressed in the left side of the developing heart field at 20 somites. Notably, bilateral *lefty2* expression was observed only in rare cases (4 out of 64). Overall, the low percentage of Cx43.4 knockdown embryos with bilateral *spaw, lefty1,* or *lefty2* expression at 20 somites is consistent with maintenance of midline integrity. Together, these data provide strong evidence that Cx43.4 functions specifically in KV to help direct asymmetric gene expression rather than in establishment or maintenance or the midline barrier function.

Cx43.4 is required for KV ciliary development, but not KV cell specification

Since mosaic analysis following DFC-targeted MO injections showed that Cx43.4 is required in KV cells and gene expression data indicated a role for Cx43.4 in KV function, we next asked whether Cx43.4 is required for KV cell specification, differentiation, morphogenesis or function. Based on immunofluorescence methods, KV cilia in 10-somite control embryos were notably well-developed and the distribution of cilia encompassed a circular area (Fig. 5A). In Cx43.4 morphant embryos, however, although ciliated cells had developed in a distinct region of the tail, they occupied a smaller and more irregularly shaped area (Fig. 5B). These results are similar to previously published ciliary characteristics in *ntl* mutant and morphant embryos (Amack et al., 2007) and suggest that Cx43.4 is similarly required for complete KV morphogenesis.

To quantify the differences between control and morphant cilia, additional analyses were performed using ImageJ software. Morphant cilia, although similar in number compared to controls (Fig. 5C), were significantly shorter than the average wildtype cilium (Fig. 5D). The analysis of nodal cilia showed that KV cells are specified and have begun a differentiation program in order to acquire this specialized cell structure, the cilium. Additionally, since no significant differences were seen in the number of cilia, KV cell progenitors

(DFCs) likely migrated to the correct position in the embryo and were then specified correctly.

Since KV cilia in Cx43.4 morphant embryos were shorter compared to controls, we next asked whether Cx43.4 was required for ciliary motility and production of a net leftward fluid flow. Fluorescently-labeled beads were injected into inflated KVs of live 10-somite stage embryos and video microscopy was used to track their movement. In wildtype embryos, as previously reported, (Essner et al., 2005; Kramer-Zucker et al., 2005) the beads circulated in a counter-clockwise direction, driven by motile monocilia (data not shown). Interestingly, while attempting to inject beads into KVs of Cx43.4-deficient embryos, we found that 94% of the knockdown embryos (n=38) did not possess a luminal KV space observable by DIC microscopy (Fig. 6A-C). In contrast, only 3% of mismatched control MO injected embryos lacked an inflated KV. To determine whether the Cx43.4 MO injection produced a developmental delay, the posterior region of Cx43.4 morphants was observed until 16 somites with no recovery of lumen inflation observed. Thus, a fundamental part of the Cx43.4 knockdown phenotype is a lack of KV inflation. Our interpretation is that without an inflated luminal space, the cilia in KV are likely unable to generate a net leftward flow, thus rendering KV incapable of directing normal asymmetric development.

Human Cx45 can functionally compensate for zebrafish Cx43.4 in L-R development

Finally, we addressed whether the role of Cx43.4 in KV cells during L-R patterning is conserved. The expression pattern of zebrafish Cx43.4 resembles that of mammalian Cx45 during somitogenesis (Kruger et al., 2000; Kumai et al., 2000), and the two connexins are highly related by sequence and phylogeny (Cruciani & Mikalsen, 2006; Eastman et al., 2006). Additionally, physiological analyses of Cx43.4 channel properties (Barrio et al., 1997; Desplantez et al., 2003) provide evidence for substantial functional conservation. Therefore, we asked whether human Cx45 could functionally compensate for Cx43.4 during L-R patterning.

Control experiments showed that when 80 pgs of in vitro synthesized human *cx45* mRNA were injected into single-cell embryos, there were no significant L-R heart looping aberrations (Fig. 7). As in earlier experiments, more than 40% of Cx43.4 morphants displayed aberrant heart looping. However, when *cx45* mRNA was co-injected with Cx43.4 targeting MOs, the percentage of embryos with aberrant heart looping was significantly reduced to only 25% (Fig. 7). This level of rescue is comparable to that observed after injection of rescuing zebrafish *cx43.4* mRNA (Fig. 2D), suggesting that human Cx45 can effectively compensate for Cx43.4 during L-R patterning. Additionally, we note that Cx45 null mice have specific defects in positioning of the atrium and ventricle of the heart (Kumai et al., 2000), which are reminiscent

of a laterality defect. These observations are consistent with the idea that Cx45 orthologs have a conserved role in L-R patterning.

DISCUSSION

A role for Cx43.4 in development

It is well known that GJs equip neighboring cells for communication by providing cell-to-cell channels that allow small molecules to pass directly between cells. As a result, these pathways have been envisioned as a means of signaling and coordinating cells during various developmental processes. Particularly relevant to this study, GJ communication has been viewed as critical for normal patterning during early embryogenesis. For example, future dorsal cells can be distinguished from their ventral counterparts in 32- and 64-cell *Xenopus* embryos by a difference in GJ communication (Warner et al., 1984; Olson et al., 1991); and beta-catenin, a key player in early embryonic development, is the endogenous regulator of the increase in communication in dorsal cells (Krufka et al., 1998). Moreover, previous studies have implicated GJs during L-R patterning in both chick and *Xenopus* embryos (Levin & Mercola, 1998, 1999). However, neither the precise spatio-temporal requirements of Cxs during L-R patterning nor the extent of mechanistic conservation of Cx function among species are yet clear.

Here, we sought to capitalize on the experimental advantages of the zebrafish embryo, in order to evaluate the developmental role of Cx43.4, which is highly expressed in early embryos, specifically in cells of KV, the zebrafish L-R organizer. We show that Cx43.4 is specifically required for L-R patterning. The high level of penetrance leading to nearly 50% randomization after MO

knockdown underscores the significance of this requirement. Importantly, DFC-targeted MO injection allowed for the analysis of mosaic embryos and the first observation that Cx function is required within a specific tissue, KV, during L-R axis development. Although KV cells are still specified in Cx43.4-deficient embryos and develop cilia, a functional lumen fails to develop. This indicates that Cx43.4 is required for KV morphogenesis – at a specific place and time within the embryo – during early L-R patterning. Additionally, it appears that this function could be conserved in vertebrate development, as human *cx45* mRNA was sufficient to rescue the L-R defects associated with zebrafish Cx43.4 depletion, and knockout of Cx45 in mice produces heart morphogenesis anomalies that are indicative of looping defects (Kumai et al., 2000).

Other potential roles of connexin proteins during embryonic patterning

We stress that the present findings do not exclude the possibility that Cxs play other roles, as well, during embryonic patterning. In fact, it is likely that this is the case. Previous studies in the chick and *Xenopus* suggested that although Cx43 is not required specifically within the L-R organizer, it does play a role during L-R development (Levin & Mercola, 1998, 1999). Evidence supports a model where GJs comprised of Cx43 could function in the blastomeres to establish an electrical gradient that would distinguish the future left side from the right (Levin, 2005). Support came from experiments using dominant negative constructs and less specific drug treatments. The model

proposed that some unknown L-R determinant would segregate along the electrical gradient and would then influence asymmetric gene expression depending on its local concentration on a given side of the embryo. Thus, Cx43 could function prior to or in conjunction with KV in a manner that is distinct from the role of Cx43.4 within the L-R organizer. (Note that these are not closely related connexins, despite the similar terminology.)

In order for KV to develop and function, the KV precursor cells, DFCs, must migrate to the correct position in the embryo during gastrulation and then undergo differentiation. This subpopulation of cells migrates together, and it is possible that Cxs other than Cx43.4 are required for DFC migration, similar to the involvement of Cx43 during neural crest cell migration (Lo et al., 1999). Neural crest cells migrate in streams away from the neural tube during development and give rise to many tissues, including certain cells within the nervous system and heart. Neural crest cells have been shown to express Cx43 and be well-coupled, even during migration. In the absence of Cx43, neural crest cell migration is altered (Huang et al., 1998). In the present experiments, embryos depleted of Cx43.4 displayed a similar number of KV cilia (presumably one per cell) as control embryos, suggesting that DFC migration and early KV cell specification are not dependent on Cx43.4.

Yet another potential role for Cxs in L-R patterning comes from the observation that the cilia on the epithelial cells of KV beat in a coordinated fashion. In airway epithelia, the coordinated beating of cilia is also required,

specifically for the efficient clearance of mucus. In these epithelial cells, the coordination is thought to be dependent on GJ communication (Boitano et al., 1992). Coordinated ciliary beating likely relies on elevated Ca^{2+} within cells that is generated by mechanical stimulation (e.g., by means of the normal flow of mucus across the epithelium) and propagated to neighboring cells via GJs. A similar model could be envisioned in the ciliated KV epithelium, where GJ communication could coordinate ciliary beating in order to create a functional leftward fluid flow, without which KV would be rendered incapable of directing L-R asymmetry. The data presented here do not eliminate a possible role for Cx43.4 in coordinating KV ciliary beating. However, in Cx43.4 morphant embryos, it is likely that any effects on ciliary motility would be masked due to the uninflated KV structure, which would render fluid flow ineffective regardless of an effect on ciliary function.

Finally, once the cells derived from DFCs have differentiated and nodal flow has been established in KV, a left-sided signaling wave is observed in the cells adjacent to KV. That is, some type of signal inside the epithelial lumen of KV needs to ultimately reach lateral mesodermal cells adjacent to KV and subsequently activate the Nodal signaling cascade. Cxs could also be required for the spread of this signal. In fact, this communication question ranks as one of the most fundamental in terms of understanding the process of L-R patterning, not only in zebrafish, but in higher vertebrates as well. Thus, although we have gained important insights into L-R patterning as a result of

the present analysis of Cx43.4, we have much to learn about the role of Cxs in development, including roles in embryonic patterning.

Cx43.4 is required for KV morphogenesis

What then is known about KV development and how might a Cx function in this process? First, it is clear that for the motile KV cilia to function optimally and produce a robust, leftward fluid flow, they must operate within a fully inflated luminal space. Recent studies have begun to examine the various processes that lead to KV development (Amack et al., 2007), although the precise genes involved in this morphogenetic event and the mechanistic details remain unclear.

The formation of cilia is an early step in KV development that precedes lumen expansion (Amack et al., 2007). In Cx43.4-deficient embryos, KV cells are specified and cilia are present. However, we observed defects in the length of KV cilia, suggesting that Cx43.4 is required for this early phase of KV development. Interestingly, recent work has implicated fibroblast growth factor (FGF) signaling in the regulation of cilia length (Neugebauer et al., 2009). Moreover, membrane permeability through the activation of Cx43 and Cx45 hemichannels (channels located on the plasma membrane but not docked as in a GJ) is specifically increased upon FGF signaling (Schalper et al., 2008), and FGF can stimulate ATP release via Cx43 hemichannels (De Vuyst et al., 2007). These observations suggest that, in a similar way, Cx43.4 and FGF signaling

may function together in KV to regulate cilia length, a necessary step for the production of fluid flow. Alternatively, the defects in KV cilia length could be consistent with a requirement for Cx43.4 during KV cell development and may represent a secondary effect of inflation deficiencies in KV.

After the acquisition of cilia, KV cells display expanded apical membrane surfaces as the lumen of KV begins to inflate (Amack et al., 2007). The transcription factor, *ntl*, is known to be required for KV lumen formation (Amack & Yost, 2004; Essner et al., 2005), and the defects associated with *ntl* depletion are strikingly similar to the results described here for Cx43.4. Furthermore, we have previously shown that *ntl* mutant embryos have reduced levels of Cx43.4 expression (Essner et al., 1996). These observations suggest that Cx43.4 is one of the transcriptional targets of *ntl*, possibly even a key player with an impact on downstream events, during the KV morphogenesis program. Future experiments will be directed at understanding the precise function of Cx43.4 during KV morphogenesis with the goal of identifying the critical point at which KV lumen formation fails in the absence of Cx43.4.

MATERIALS AND METHODS

Morpholino Injections

The following morpholinos (MOs) were obtained from GeneTools (Eugene, OR) and were injected into one- to four-cell stage embryos as described (Nasevicius & Ekker, 2000):

Cx43.4 MO: 5'-TCAAGAAGTACCACCGTCTCAGTCC-3'

Cx43.4 mismatched MO: 5'-TCAtGAAcTACCACCGTCaCAGaCC-3'

Cx44.2 MO: 5'-AACGTGTCAAGAAGCTCCAACTCAT-3'

Cx43 MO: 5'-AGGGAGTTCTAGCTGGAAAGAAGTA-3'

ntl-MO, 5´–GACTTGAGGCAGGCATATTTCCGAT–3´

Fluorescein-labeled MOs of the same sequences listed above were injected at the mid-blastula stage to knock down expression specifically in the dorsal forerunner cells (DFCs) according to published methods (Amack & Yost, 2004). Embryos were screened by fluorescence microscopy at the shield stage for fluorescence in the DFCs, which was lacking in other embryonic cells.

mRNA Rescue

The Cx43.4 coding sequence was cloned using the following 5' primer 5'-ATGAGtTGGAGcTTcCTaACGCGGTTGTTG-3'. This fragment was generated with silent mutations (shown in lower case letters) to prevent recognition by start codon-targeting MOs and cloned into the vector, pT3TS. A human Cx45 plasmid was provided by E. Beyer (Kanter et al., 1994) (University of Chicago). Full-length, capped mRNA was synthesized using Ambion's mMessage

Machine (Austin, TX) transcription kit. Cx43.4 or human Cx45 mRNA was injected into one-cell embryos at doses ranging from 20-200 pg/embryo. For MO-mRNA co-injection experiments, a dose of 60 or 100 pg/embryo was used.

In situ Hybridization

Whole-mount in situ hybridization was performed as described (Essner et al., 2005). *cx43.4* probes were used as before (Essner et al., 1996). The *cx44.2* antisense probe was synthesized from the full length *cx44.2* coding sequence. Antisense RNA probes used to analyze L-R patterning events were *cmlc2* (Yelon et al., 1999), *spaw* (Long et al., 2003), *lefty1* (Bisgrove et al., 1999), and *lefty2* (Bisgrove et al., 1999). The midline was analyzed with *ntl* antisense probes.

Whole-Mount Immunohistochemistry

Cilia in KV were labeled with anti-acetylated tubulin (Sigma T7451, St. Louis, MO) as described (Essner et al., 2002). Cx43.4 rabbit polyclonal antibodies (Desplantez et al., 2003) were used at 10 μg/ml. To stain nuclei, Hoechst dye (Molecular Probes 33342, Carlsbad, CA) was added to the wash solution at a concentration of 10 μg/ml. Embryos were mounted in Prolong Antifade (Molecular Probes, Carlsbad, CA) and z-series images were collected using either a Nikon C1si confocal microscope or a Zeiss fitted with an Apotome and analyzed using ImageJ software (NIH, Bethesda, MD).

Nodal Flow Analysis

0.5 μm fluorescent latex beads (Polysciences, Inc., Warrington, PA) were diluted in PBS and injected in KVs of 8-12 somite stage embryos as described (Essner et al., 2005).

Figure 1:

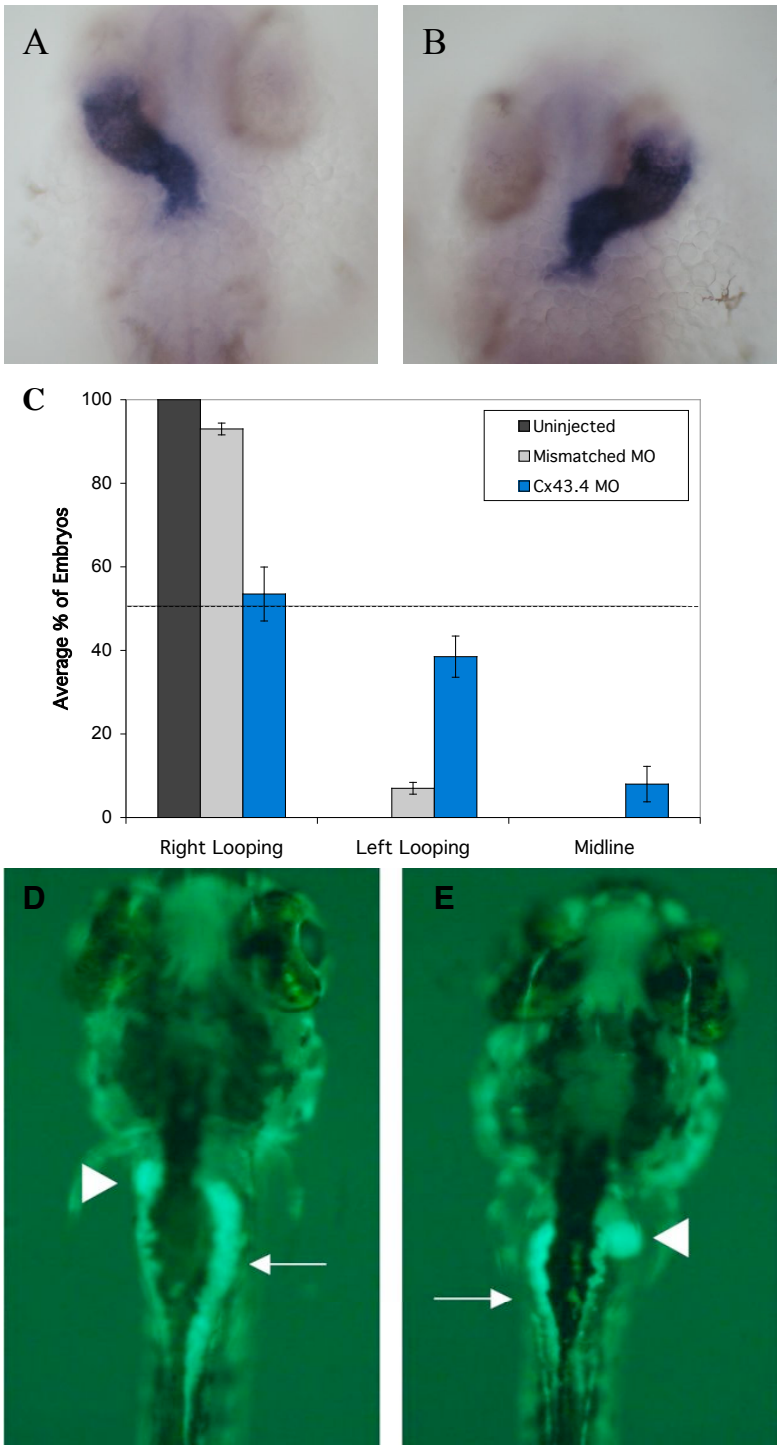
A
B
C
100
80
60
40
20
0
Average % of Embryos
Uninjected
Mismatched MO
Cx43.4 MO
Right Looping
Left Looping
Midline
D
E

Figure 1:

Cx43.4 is specifically required for L-R patterning. Dorsal views of 30 hpf embryos processed for *in situ* hybridization with a cardiac myosin light chain probe show normal looping of the heart tube towards the right in controls (A) and aberrant looping to the left in Cx43.4 morphants (B). (C) Quantification of heart looping in four independent knockdown experiments is represented as means +/- s.e.m. The dotted line in all graphs shows the theoretical maximum value for randomization. (D) Ventral view of autofluorescence in the gut of a 5 dpf larva, specifically the gallbladder (arrowhead) and pancreas (arrow); compare with (E) the Cx43.4 morphant where these organs are reversed.

Figure 2:

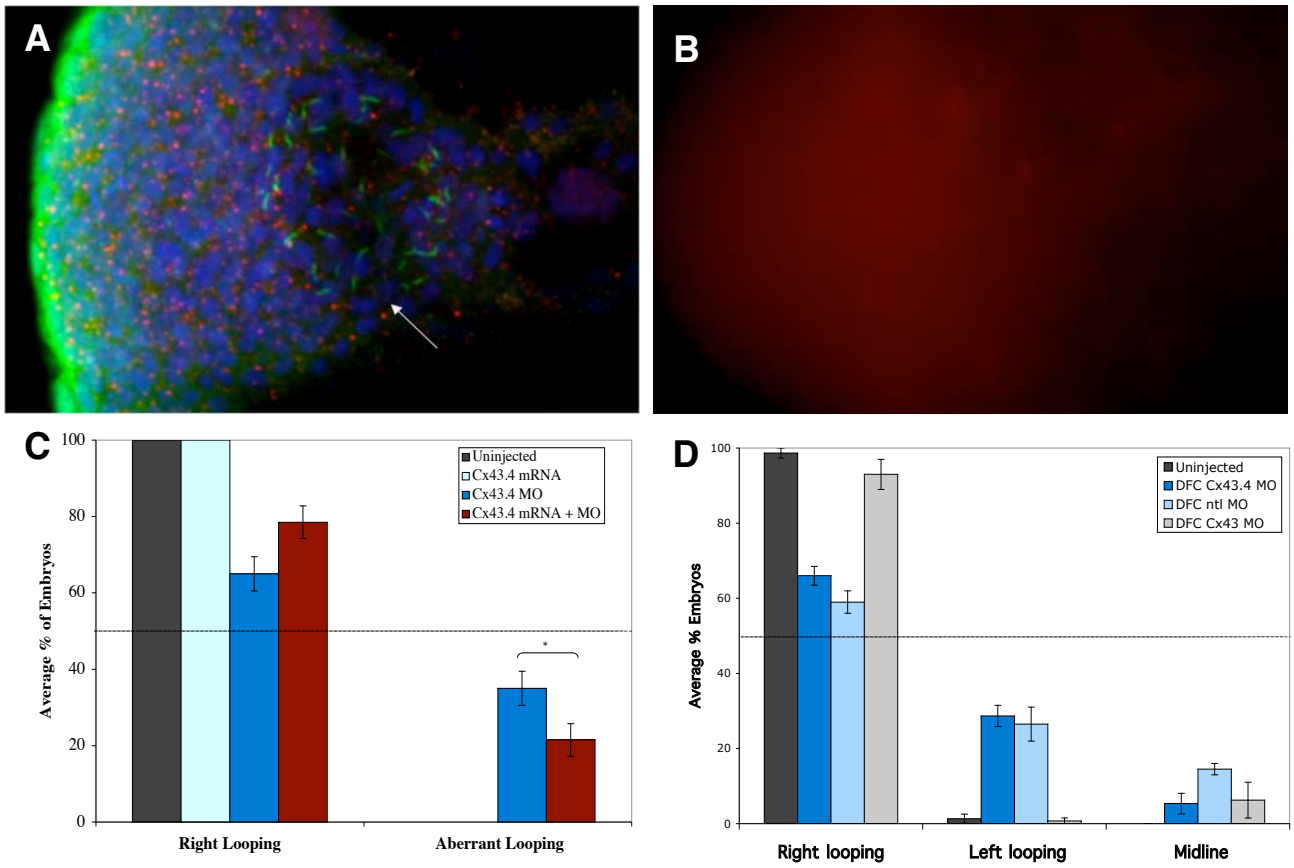
A
B
C
Average % of Embryos
100
80
60
40
20
0
Uninjected
Cx43.4 mRNA
Cx43.4 MO
Cx43.4 mRNA + MO
*
Right Looping
Aberrant Looping
D
Average % Embryos
100
80
60
40
20
0
Uninjected
DFC Cx43.4 MO
DFC ntl MO
DFC Cx43 MO
Right looping
Left looping
Midline

Figure 2:

Cx43.4 is expressed in a spatio-temporal manner to be competent for KV function. Confocal fluorescence imaging (A,B) shows Cx43.4 labeling (red) in puncta that are distinct from the nuclei and cilia of KV cells. Note also significant Cx43.4 labeling in the surrounding tail bud tissue. (B) Cx43.4 MO efficacy is shown by the lack of staining (red), punctate or otherwise, in knockdown embryos. (C) Defects in heart laterality are partially rescued by co-injection of *cx43.4* mRNA, *p=0.04. (D) DFC-targeted injections of Cx43.4 MOs have a significant heart reversal phenotype. (C,D) Data are averages of three independent experiments and are represented as means +/- s.e.m.

Figure 3:

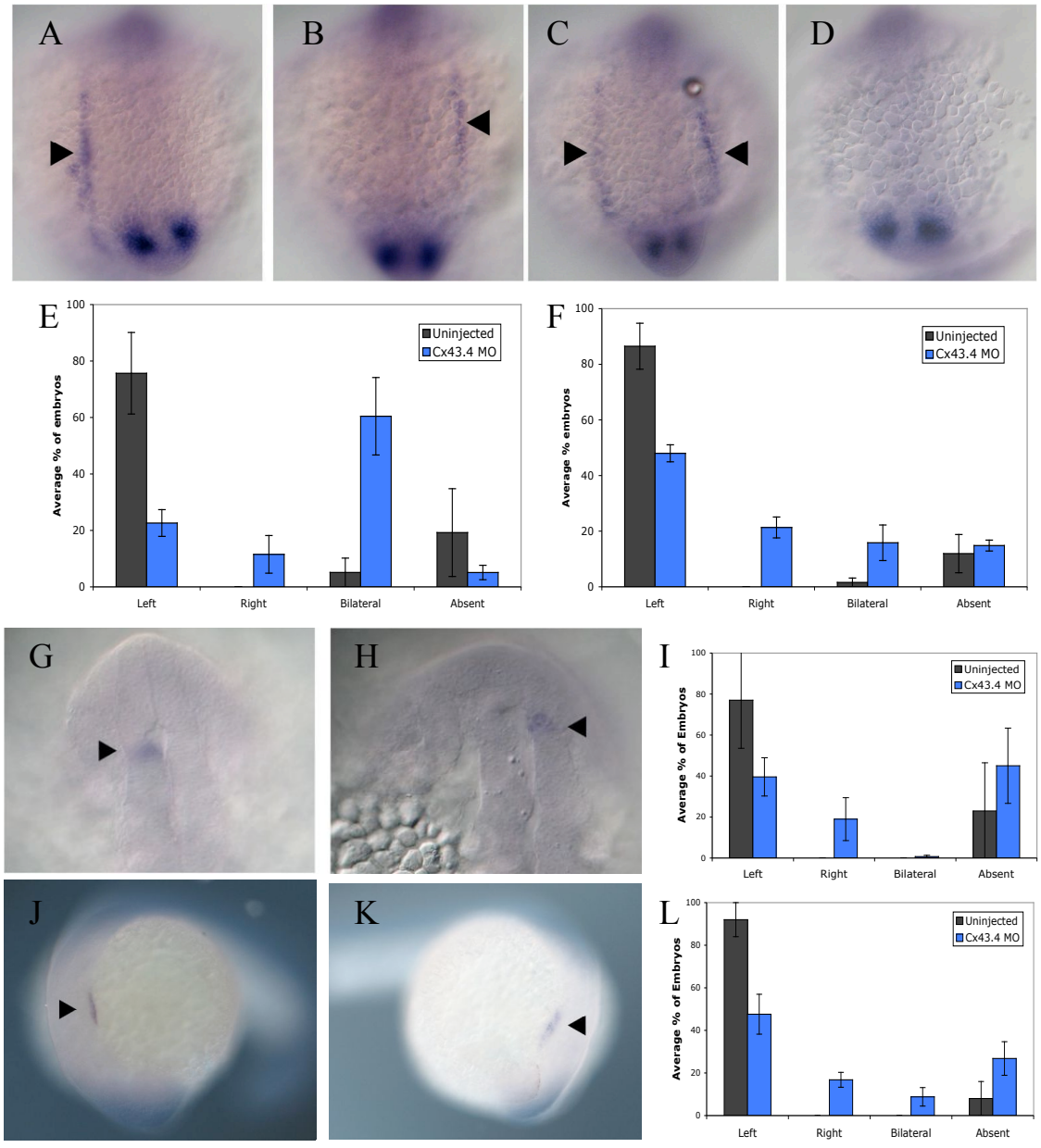
A
B
C
D
E
Average % of embryos
Uninjected
Cx43.4 MO
Left
Right
Bilateral
Absent
F
Average % embryos
G
H
I
Average % of Embryos
J
K
L

Figure 3:

Molecular markers support a role for Cx43.4 in KV function. In situ hybridizations are used to probe for expression of genes in the L-R signaling cascade. (A-D) 12-somite Cx43.4 morphant embryos probed for *spaw* expression (arrowheads, throughout) show left, right, bilateral, and absent expression, respectively. *spaw* expression data are quantified (E) at 12 somites and (F) at 20 somites. 20-somite embryos probed with *lefty1* show (G) normal expression in wildtype and (H) reversed expression in a DFC-targeted Cx43.4 knockdown embryo. (I) *lefty1* data are summarized. (J) 20 somite embryos probed with *lefty2* show a (K) reversal in the developing heart field of the Cx43.4 morphant. (L) Quantification of *lefty2* expression was compiled from three independent experiments. Graphs in (E, F, I, L) represent means +/- s.e.m. from three independent experiments.

Figure 4:

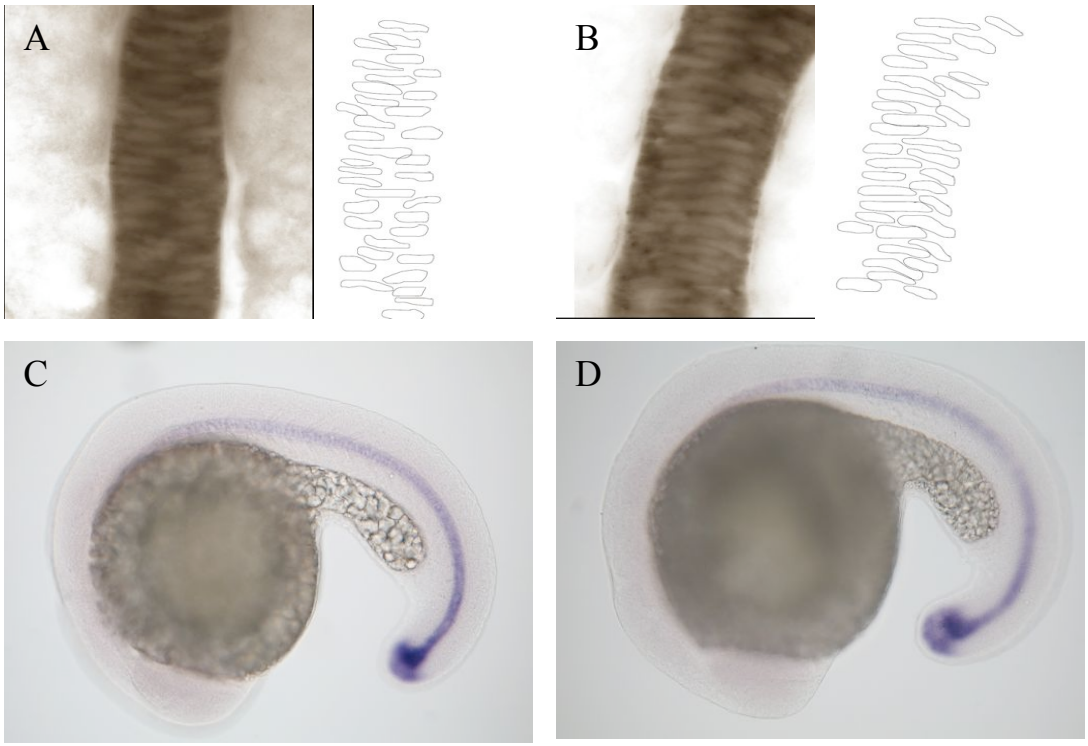

Figure 4:

Midline integrity is maintained in Cx43.4 morphants. *In situ* hybridization with a *ntl* probe (A-D). (A) 10-somite stage uninjected and (B) Cx43.4 morphant embryos both have an intact, continuous midline. For clarity, individual nuclei were outlined in Photoshop (right of A and B). (C) 20-somite stage control and (D) Cx43.4-deficient embryos express *ntl* along the midline.

Figure 5:

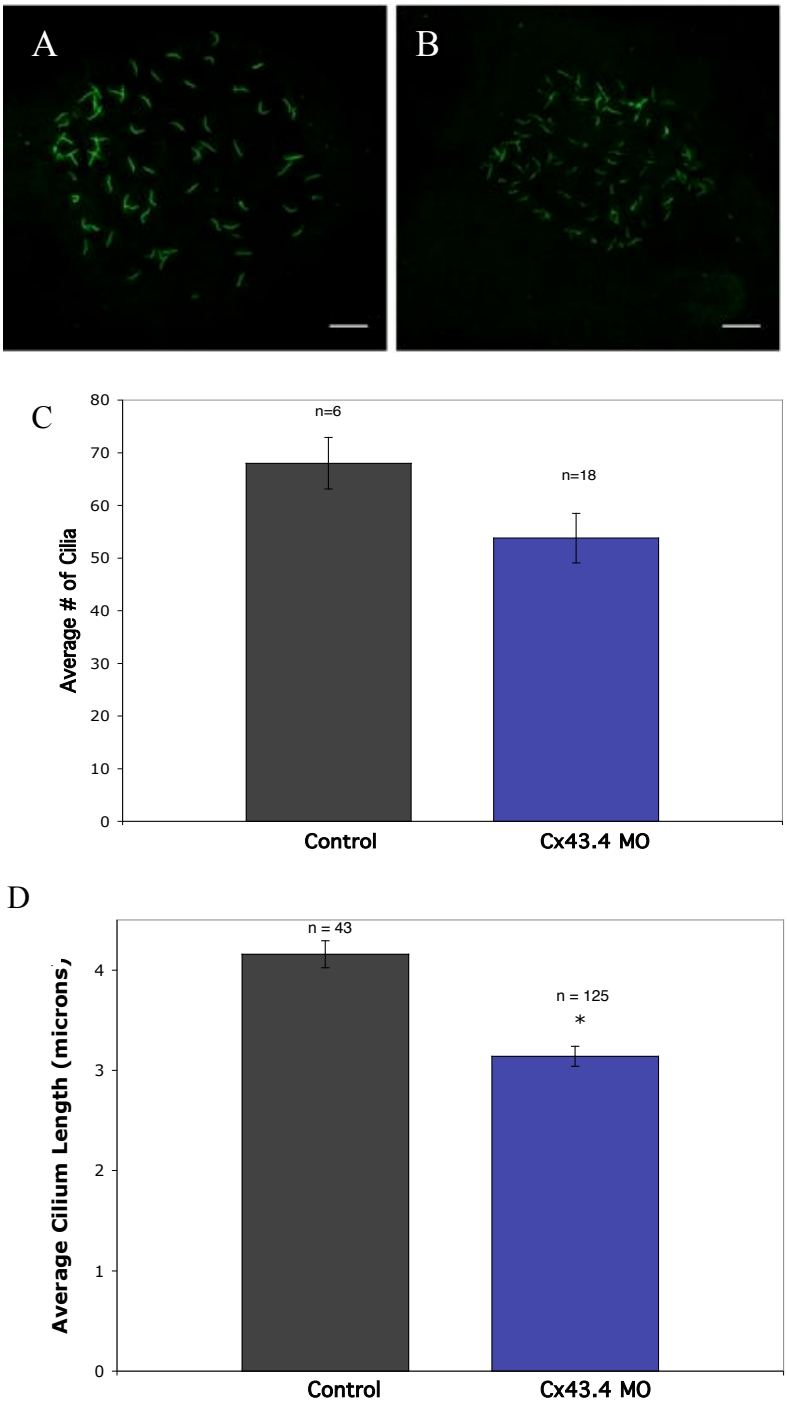
A
B
C
n=6
n=18
Average # of Cilia
80
70
60
50
40
30
20
10
0
Control
Cx43.4 MO
D
n = 43
n = 125
*
Average Cilium Length (microns)
4
3
2
1
0
Control
Cx43.4 MO

Figure 5:

KV cells are specified in Cx43.4 morphants, though ciliary defects exists. Confocal fluorescence imaging (A,B) of KV cilia labeled with acetylated tubulin antibodies. Scale bar = 10 microns. (A) Uninjected, control embryos have well-developed cilia in a circular pattern, while (B) Cx43.4 morphants have disorganized, smaller ciliated KVs. Multiple fluorescence images of 10-somite stage KVs labeled with acetylated tubulin antibodies were analyzed using ImageJ software (C,D) and data were plotted as means +/- s.e.m. (C) The average number of cilia per KV was similar between uninjected and Cx43.4 morphant embryos, p=0.13. (D) The average cilium in Cx43.4 morphant embryos was significantly shorter than a wildtype cilium, * $p=3 \times 10^{-7}$.

Figure 6:

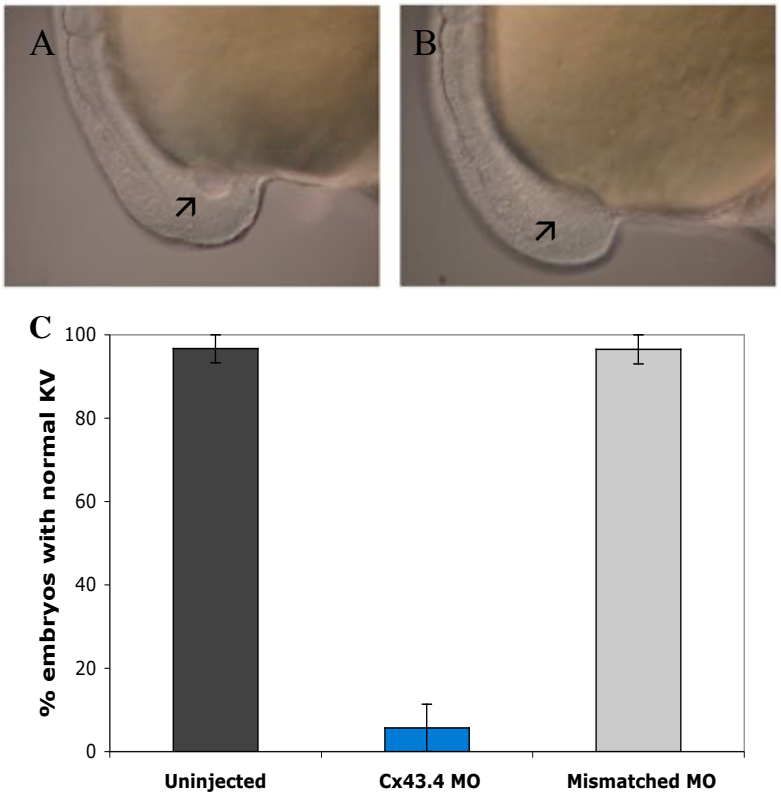
A
B
C
% embryos with normal KV
100
80
60
40
20
0
Uninjected
Cx43.4 MO
Mismatched MO

Figure 6:

KV lumen formation is impaired in Cx43.4 morphants. DIC microscopy (A,B) of 10-somite stage embryos. (A) KV inflation is observed in control embryos, while (B) Cx43.4 morphants do not have detectable KVs (arrows in A and B point to KV location). (C) The percentage of embryos with normal KVs as analyzed by DIC microscopy from three independent experiments are represented as means +/- s.e.m.

Figure 7:

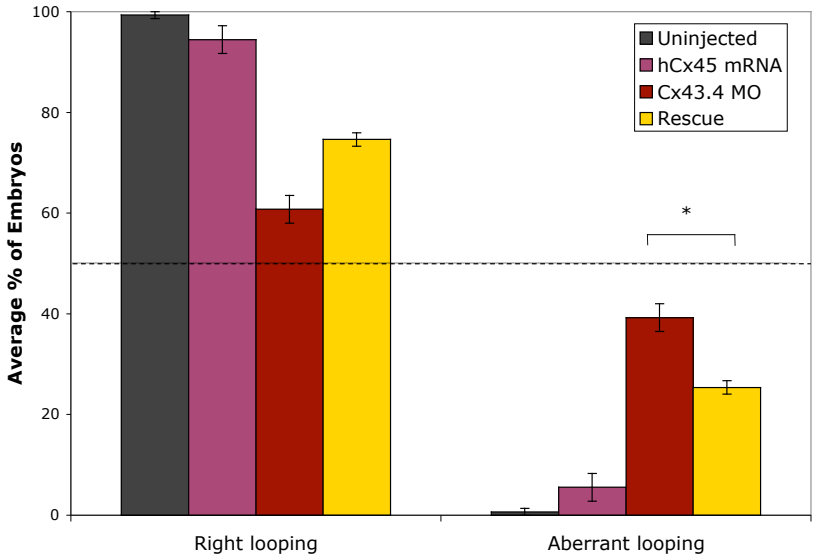
100
80
60
40
20
0
Average % of Embryos
Uninjected
hCx45 mRNA
Cx43.4 MO
Rescue
*
Right looping
Aberrant looping

Figure 7:

Human *cx45* mRNA partially rescues heart looping. Quantification of three independent experiments shows no alterations in heart looping when human *cx45* mRNA is injected alone. Co-injection of human *cx45* mRNA with Cx43.4 MOs significantly rescues aberrant heart looping, *p=0.01.

Supplementary Figure 1

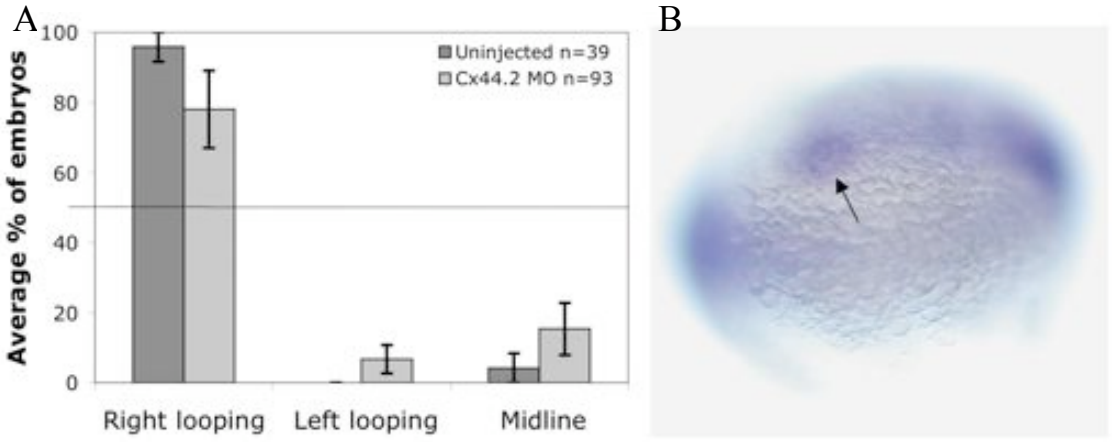

Supplementary Figure 1

Cx44.2 is not required for L-R patterning. (A) Aberrant heart looping in Cx44.2-deficient embryos is not significantly different from uninjected control embryos. (B) Ventral view of a 10-somite stage embryo processed by for *in situ* hybridization with *cx44.2* antisense probes shows *cx44.2* expression in KV (arrow).

Supplementary Figure 2

Supplementary Figure 2

Cx43.4 is expressed in KV. In situ hybridization analysis shows that *cx43.4* transcripts are expressed in KV (arrow) of a 10-somite stage embryo.

Chapter III

Connexin43.4 Hemichannel Function is Required for Kupffer's Vesicle Lumen Formation

SUMMARY

Cilia-driven, leftward nodal flow within the left-right (L-R) organizers of multiple species is known to be required for the establishment of L-R asymmetry. The process by which these ciliated epithelia develop is not well-understood. Recent research in zebrafish has begun to address the genetic components and mechanisms leading to the morphogenesis of the L-R organizer, Kupffer's vesicle (KV) (Amack et al., 2007). Previous results have shown a requirement of the gap junction (GJ) protein, Cx43.4, during KV development (Hatler et al., manuscript submitted). Here, morpholino knockdown revealed that Cx43.4 is required for KV lumen formation and inflation. Examination of KV structure using a membrane marker revealed defects in morphogenesis, e.g., smaller, irregularly-shaped and noninflated KVs in the knockdowns. Interestingly, the specific action of Cx43.4-based hemichannels, rather than cell-cell communication through GJs, is sufficient to produce normal L-R patterning, a novel finding in the communication field. Additional evidence points to the function of purinergic receptors within KV cells during lumen expansion. Our knockdown of a P2Y receptor in KV cells, with or without knockdown of Cx43.4, supports a model where hemichannels and P2Y receptors are required in apical membranes of KV cells to drive fluid into the developing KV lumen, rendering the ciliated cells capable of generating asymmetry.

INTRODUCTION

Recently, the key developmental stages leading to a functional KV containing a lumen were described (Amack et al., 2007). KV precursor cells, the dorsal forerunner cells (DFCs), migrate to a central location within the tailbud at the end of gastrulation. At this location, they undergo a mesenchymal to epithelial transition (MET) and begin a differentiation program. This differentiation leads to the acquisition of a specialized epithelial cell fate, where each cell contains a single motile cilium. Next, developing KV cells establish apical-basal polarity and the apical membranes cluster together. Finally, the clustered apical surfaces begin to separate and the developing lumen subsequently expands. While these analyses have expanded our knowledge of KV morphogenesis, it is not clear how KV cells coordinate the steps of morphogenesis.

It has been theorized that gap junction (GJ) communication serves to coordinate cellular behavior during development. GJs allow for the direct passage of small molecules, ions, and signals between neighboring cells through intercellular channels composed of Connexin (Cx) protein subunits. Prior to docking with a neighboring cell to form a GJ channel, six Cx subunits, termed a hemichannel, are located at the plasma membrane. While hemichannels can be opened to the extracellular environment experimentally in tissue culture cells (Li et al., 1996), physiological roles for hemichannels are

largely unknown and whether they open naturally in vivo has been debated (Goodenough & Paul, 2003; Spray et al., 2006).

Here we report that when Cx43.4 is depleted in zebrafish embryos, a mutant form of the Cx, which is able to form hemichannels, is capable of rescuing the embryos and providing for normal L-R patterning. Cx hemichannels have not previously been shown to play essential roles in early development. Other data presented here support a model for the role of hemichannels in KV morphogenesis and raise the question of whether similar mechanisms will be found broadly distributed in other developing epithelia (further discussion in Chapter IV).

RESULTS

Cx43.4 is required for KV morphogenesis

We have previously shown that Cx43.4 is required for complete KV cell development and lumen formation (Hatler, et al., manuscript submitted). To analyze KV cell morphology in more detail, an antibody against aPKCζ, a recently identified marker of KV cells was used to evaluate the stages of KV development (Amack et al., 2007). Normally at 2-3 somites, KV cells have become polarized, begun to develop short cilia, and apical cell membranes have coalesced into a single focus of intense PKC staining (Fig. 1a-c). However, many Cx43.4 morphant embryos (50%, n=8) failed to show a single cluster of PKC staining, although ciliary development was comparable to controls at this stage. PKC-positive cells in morphant KVs often formed a linear assembly of apical cell staining (Fig. 1d-f), or in some cases, a more severe, dispersed arrangement where the majority of apical surfaces, labeled with PKC, failed to make physical contact with one another. Despite the disruption in apical clustering, the cells of KV still displayed PKC expression following Cx43.4 knockdown, suggesting that the MET has occurred normally. These results indicate that Cx43.4 is required for tight apical clustering at an early stage of KV morphogenesis.

Later KV development at the 4-somite stage is characterized by the initial formation of a lumen within the epithelium. In uninjected control embryos, the apical surfaces of KV cells, marked by PKC staining, have separated from each

other to form the spherical, fluid-filled KV (Fig. 1g-i). In contrast, the majority of Cx43.4 morphant embryos had small, disorganized KVs that failed to complete inflation. Interestingly, some Cx43.4 morphant embryos had multiple vesicular areas of PKC staining that corresponded to multi-ciliated areas, apparently each one a mini-KV structure (Fig. 1j-l). This multiple-KV phenotype is consistent with the most severe apical clustering defects in which more than one group of PKC-positive cell-cell contacts initiated lumen formation. This observation is indicative of a failure in the coordination of KV cells in the absence of Cx43.4.

In order to quantify the defects in lumen formation following Cx43.4 knockdown, ImageJ software was used to measure the area defined by those cells that were PKC-positive and had developed cilia at the 4-somite stage. Uninjected control embryos had an average KV area of 3,283 square microns (Fig. 2a,d), while Cx43.4 morphant embryos had a significantly reduced KV area of 830 square microns (Fig. 2b,d). KV area measurements are representative of the size of the lumen, and the significant reduction in size clearly shows that Cx43.4 is required for complete KV lumen expansion.

Overall, the defects in KV lumen formation in Cx43.4-deficient embryos would likely render fluid flow within the uninflated luminal space non-functional. Therefore, the primary defect associated with L-R patterning problems in Cx43.4 knockout embryos is a lack of KV lumen morphogenesis. An alternative interpretation would be that the lack of apical clustering results from fewer cells

participating in lumen formation. However, this seems less likely since there are similar numbers of cells contributing to KV in Cx43.4-deficient embryos compared to controls (based on previous ciliary analysis in Hatler, et al., submitted).

To determine whether the quantifiable defects in lumen formation were specific to Cx43.4 MO knockdown, rescue experiments were performed. For these experiments we took advantage of previously published results showing that human *cx45* mRNA was able to functionally compensate for zebrafish Cx43.4 in patterning the L-R axis (Hatler, et al., manuscript submitted). Here, we asked whether Cx43.4 was similarly required in a conserved process of lumen formation. When human *cx45* mRNA was co-injected with Cx43.4 targeting MOs, KV area was partially rescued to an average of 1,551 square microns from 830 microns with MOs alone (Fig. 2c,d). These results show that Cx43.4 is specifically required for KV lumen formation. Additionally, these findings provide functional evidence of a conserved role for Cx45 orthologs in the development of the KV lumen space.

Cx43.4 is not required in the DFCs

Given the defects in KV lumen formation, we next asked whether Cx43.4 functions within KV cells or in the precursor cells, the dorsal forerunner cells (DFCs). Previous results showed that *cx43.4* transcripts were not expressed in a subset of cells in the caudal embryonic shield (Essner et al., 1996), which correspond to the precursors of KV. This suggests that DFCs likely do not

express *cx43.4* during epiboly. To determine whether DFCs express Cx43.4 protein that was not detected at the mRNA level, epiboly stage embryos were probed with Cx43.4-specific antibodies. Cx43.4 protein is localized to punctate structures throughout the embryo at the shield stage and at 90% epiboly. However, when the shield and midline were co-labeled with *ntl* antisense probes (Supplementary Information, Fig. S1a) and processed by *in situ* hybridization, the DFC population, located at the margin of the blastoderm, was devoid of Cx43.4-positive punctate structures (Supplementary Information, Fig. S1b). These results suggest that the spatio-temporal regulation of Cx43.4 expression is tightly regulated throughout the developmental progression of KV. Furthermore, previous DFC-targeted experiments (Hatler, et al., manuscript submitted) and the localization data presented here are consistent with a role for Cx43.4 later in KV development and/or function rather than during the migration or specification of DFCs.

Cx43.4 is not required for KV cell epithelial specification

To understand how Cx43.4 regulates KV lumen formation, we focused on general aspects of tube or lumen biogenesis. We hypothesized that Cx43.4 functionally interacted with proteins of adherens junctions and/or tight junctions in order to maintain cell-cell contacts and provide a tight barrier by which secreted extracellular fluid would be maintained within the developing lumen space. It has previously been shown that cadherins can be closely associated

with Cxs (Wei et al., 2004) and that the mammalian ortholog, Cx45, interacts with zona occludens-1 (ZO-1) (Kausalya et al., 2001). It is possible that Cx43.4 acts in a similar manner in KV cells. We analyzed the localization of ZO-1 during KV development and found it to also be a specific marker of differentiated KV cells at 4 somites that co-localizes with PKC in wildtype embryos (Supplementary Information, Fig. S2a-c). In Cx43.4 morphant embryos, there were no apparent differences in ZO-1 expression or localization when compared to control embryos (Supplementary Information, Fig. S2d-f). Even in embryos where dramatic defects in KV morphology were observed, such as multiple KV structures, ZO-1 continued to co-localize with PKC (Supplementary Information, Fig. S2g-i). These data suggest that a protein of junctional complexes within KV cells is not affected by Cx43.4 knockdown and, further, that KV cells are specified correctly.

A Cx43.4 hemichannel mutant partially rescues L-R patterning defects

We next set forth to determine how Cx43.4 functions during KV morphogenesis to form a fully inflated, functional KV. A number of Cxs are thought to function both as hemichannels and as intercellular channels. To distinguish between these two possibilities, a mutant form of Cx43.4 (C64S) that has been designed to form hemichannels, but not GJ channels, was developed. This construct was patterned after a related mutant of Cx43, in which conserved extracellular cysteines have been shown to be essential for

the docking of hemichannels between cells (Bao et al., 2004). As previously observed, when Cx43.4-targeting MOs were injected alone, 30% of the morphant embryos displayed reversed, left-looping hearts (Fig. 3a). Notably, when rescuing Cx43.4 C64S mRNA was co-injected with MOs, the percentage of embryos with reversed hearts was significantly reduced to 14% (Fig. 3a). These results are quantitatively comparable to previous results showing rescue with Cx43.4 mRNA (Hatler, et al., manuscript submitted). This indicates that Cx43.4 hemichannels are able to rescue the L-R phenotype as efficiently as wildtype Cx43.4 and suggests that Cx43.4-based GJ communication is not an essential function of Cx43.4 during L-R patterning.

To verify that the Cx43.4 C64S hemichannel construct was indeed capable of opening to the extracellular environment and displaying the anticipated permeability, a cell culture system was utilized for dye uptake assays. Wildtype human embryonic kidney (293T) cells (Penuela et al., 2007), were transfected with either WT Cx43.4 or Cx43.4 containing the C64S mutation (Supplementary Information, Fig. S3a,b, respectively) and were assayed for their ability to take up the fluorescent dye, sulforhodamine B. Significant dye uptake above background levels was observed in single, unpaired cells expressing either WT Cx43.4 or Cx43.4 C64S when assayed in the presence of low extracellular Ca^{2+} (Fig. 3b,c). The specificity of the dye uptake through a Cx hemichannel-mediated pathway is supported by a dramatic reduction in the percentage of fluorescent cells when assayed with

normal extracellular Ca^{2+} levels (Fig. 3c and Supplementary Information Fig. S4).

Using the same dye uptake assay, but analyzing groups of cells rather than single cells as above, we next asked whether the Cx43.4 C64S mutation supported a pathway for dye transfer between adjacent cells. Control, untransfected cells had very few instances of clusters containing multiple dye-positive cells, which could reflect dye transfer between cells (Fig. 3d). However, consistent with the presence of GJ-mediated dye transfer between cells, the cells expressing WT Cx43.4 displayed twice as many cell clusters with multiple dye-positive cells as background levels (Fig. 3d). Of critical importance, the number of clusters of cells with multiple dye-positive cells, indicative of dye transfer, was not significantly different from background levels when Cx43.4 C64S was expressed, suggesting that any dye transfer in these transfected cells was mediated by endogenous channels. Note that this means of analyzing cell-to-cell transfer is expected to underestimate the extent of transfer, given the size of many cell clusters. Taken together, the results of the dye uptake assay support the ability of the Cx43.4 C64S mutant to function only as a hemichannel, and not as a cell-cell channel as in the case of the WT Cx43.4.

Cx43.4 hemichannels interact with P2Y receptors for L-R patterning

To address the mechanism of Cx43.4 hemichannel action during L-R patterning in KV cells, we theorized that Cx43.4 hemichannels function at the apical, lumen-facing membrane of KV cells. Since Cx hemichannels have been reported to release ATP into the extracellular environment (Kang et al., 2008), we tested a model where Cx43.4 could be involved in an ATP-dependent pathway to stimulate lumen expansion. Extracellular ATP can activate certain (P2) purinergic receptors, which are found in the apical membranes of most luminal epithelia (Leipziger, 2003). In response to luminal ATP, P2 receptor activation results in a rise in intracellular Ca^{2+}, which induces ion secretion and the movement of H_2O into the luminal space (Leipziger, 2003).

To test whether P2Y receptors have a role in KV lumen formation, knockdown embryos were evaluated using PKC antibodies. In $P2Y_5$-deficient embryos, PKC was localized to apical membranes but KV was disorganized (Fig. 4a). Interestingly, when comparing relative KV areas, Cx43.4-deficient embryos were about one third the size of wildtype and $P2Y_5$ knockdown KVs averaged half those of wildtype. These data reveal that $P2Y_5$ depletion phenocopies the KV defects associated with Cx43.4 knockdown and suggest that these two genes interact in a the same developmental process.

To address whether $P2Y_5$ functioned within KV cells versus a role in mesodermal cells surrounding KV, for example, chimaeric embryos were studied in which $P2Y_5$ was knocked down only in KV cells using a DFC-targeted

MO injection approach (Amack & Yost, 2004). Compared to previously published results of Cx43.4 depletion in KV cells (34%), DFC-targeted $P2Y_5$ knockdown resulted in a significant number 29% (n=130, $p<0.016$) of embryos with aberrant heart looping, which serves as a readout for L-R patterning. These results place $P2Y_5$ function at the same time and place, in KV, as Cx43.4 during L-R patterning. Additionally, to our knowledge, this is the first report linking a purinergic receptor to the morphogenesis of KV and the development of the L-R axis.

Finally, we asked whether Cx43.4 and $P2Y_5$ interact during L-R development. In these experiments, low doses of either Cx43.4 (3 ng) or $P2Y_5$ (1.5 ng) MOs were injected into embryos, resulting in no significant effect on heart looping at 30 hpf when compared to uninjected controls. In contrast, co-injection of these two low doses of Cx43.4 and $P2Y_5$ MOs produced a synergistic effect on L-R patterning: nearly 30% of embryos had reversed, left-looping hearts (Fig. 4c). These results support a model where Cx43.4 hemichannels and $P2Y_5$ function together in KV cells to produce a functional, fully inflated, luminal epithelium (Fig. 5).

Although this model is generally supported given the role of ATP release through Cx43 hemichannels in ovarian granulosa cells and the importance of P2 receptors in these cells (Tong et al., 2007), it remains unclear whether ATP is in fact a ligand for $P2Y_5$, the receptor considered here to be important for KV morphogenesis. The chick $P2Y_5$ binds ATP with high affinity (Webb et al.,

1996), while ATP stimulation of turkey $P2Y_5$ did not significantly activate the downstream signaling components IP_3 or cAMP (Li et al., 1997). Additionally, a recent study evaluating human $P2Y_5$ (Pasternack et al., 2008) did not find that nucleotides were able to activate $P2Y_5$ (although ATP was not included in the analysis of potential ligands). However, consistent with the initial observation that the chick $P2Y_5$ receptor binds ATP, when the human $P2Y_5$ receptor was expressed in *Xenopus* oocytes a subtle response to ATP was observed (King & Townsend-Nicholson, 2000), suggesting that the absence of activation in other studies may be related to experimental limitations. Additional variation in P2Y receptor ligand binding is exemplified by human $P2Y_4$, which is stimulated by UTP and antagonized by ATP, whereas the murine orthologs are stimulated by both nucleotides, despite 89% amino acid conservation between human and rodent $P2Y_4$ sequences (King & G, 2002).

All of these observations indicate that the role of $P2Y_5$ in nucleotide signaling may vary across species, so it is possible that zebrafish $P2Y_5$ is capable of binding ATP and activating downstream signaling events. Further studies are necessary to determine whether ATP can physiologically activate the zebrafish $P2Y_5$ ortholog, particularly during KV morphogenesis. From the data presented here, it is clear that $P2Y_5$ is required for L-R patterning through its function during KV morphogenesis.

Importantly, given our observations supporting a function for Cx43.4 hemichannels and $P2Y_5$ receptors during the process of lumen formation in KV

morphogenesis, it is possible that this mechanism is not restricted to KV. Previous studies have described luminal membrane localization of mammalian Cx30 in distal nephrons (McCulloch et al., 2005) and Cx43 in the apical membrane of the developing epiphysis during lumen expansion (Yancey et al., 1992). Given that P2Y receptors are widespread across epithelia, it is possible that these, and other apically-localized Cx family members, could interact with various purinergic receptors to regulate lumen formation in a similar mechanism as shown here for Cx43.4 during KV morphogenesis.

MATERIALS AND METHODS

Morpholino knockdown

One-cell wildtype zebrafish embryos, obtained from natural matings, were injected with the following morpholinos according to published methods (Nasevicius & Ekker, 2000).

Cx43.4 MO: 5'-TCAAGAAGTACCACCGTCTCAGTCC-3'

$P2Y_5$ MO: 5'-TCTCTTTAATGTGTTGCTTCTGTTC-3'

Chimaeric knockdown embryos were generated by a morpholino injection strategy to target the DFCs (Amack & Yost, 2004). Briefly, MOs were injected into the yolks of embryos between the 256- and 1000-cell stages to preferentially knockdown gene expression in KV cells.

mRNA rescue

The Cx43.4 coding sequence was cloned using the following 5' primer 5'-ATGAGtTGGAGcTTcCTaACGCGGTTGTTG-3'. This fragment was generated with silent mutations (shown in lower case letters) to prevent recognition by start codon-targeting MOs. The cytosine in amino acid position 64 was then changed to a serine using a site-directed mutagenesis PCR method and the full construct was cloned into the transcription vector, pT3TS. A human Cx45 plasmid was provided by E. Beyer (Kanter et al., 1994) (University of Chicago). Full-length, capped mRNA was synthesized using Ambion's mMessage Machine (Austin, TX) transcription kit. Cx43.4 C64S or human Cx45 mRNA

was injected into one-cell embryos at doses ranging from 20-200 pg/embryo. For MO-mRNA co-injection experiments, a dose of 60 or 100 pg/embryo was used.

In situ hybridization

Shield stage wildtype embryos were fixed in 4% paraformaldehyde and processed for *in* situ hybridization according to previously published methods (Essner et al., 1996). Proteinase K treatment for permeabilization was limited to 30 seconds and embryos were incubated with antisense digoxigenin-labeled *ntl* probes at 65°C.

Whole-mount immunofluorescence

KV development was monitored using whole-mount immunofluorescence methods as described (Amack et al., 2007). Here, apical cell membranes were labeled with rabbit anti-PKC antibodies (Santa Cruz sc-216, Santa Cruz, CA), and cilia in KV were labeled with anti-acetylated tubulin (Sigma T7451, St. Louis, MO). ZO-1 antibodies (Zymed, Carlsbad, CA) were used to analyze junctional complexes. Cx43.4 rabbit polyclonal antibodies (Desplantez et al., 2003) were used at 10 μg/ml. Secondary antibodies used were goat anti-rabbit Alexa Fluor 586 and goat anti-mouse Alexa Fluor 488 (Molecular Probes, Carlsbad, CA). Embryos were mounted in Prolong Antifade (Molecular Probes, Carlsbad, CA) and z-series images were collected using a Zeiss microscope

fitted with an Apotome and analyzed using ImageJ software (NIH, Bethesda, MD).

Cell culture

Wildtype human embryonic kidney cells (293T) were obtained from Sylvia Penuela (Penuela et al., 2007). Cells were cultured in DMEM supplemented with 10% FBS, penicillin, and streptomycin at 37°C in 5% CO_2. Trypsin (0.25%, 1 mM EDTA) was used to release cells from the dishes prior to passage or plating for Cx functional assays.

Transient transfections

20,000 cells 293T cells were plated in 35 mm dishes 24 hours prior to transfection. Transfection was then carried out in Opti-MEM1 medium (Invitrogen, Carlsbad, CA) containing TransIT-LT1 transfection reagent (Mirus, Madison, WI) and 4 ug plasmid DNA were prepared using a QIAGEN miniprep kit (Valencia, CA). Transfection efficiency was evaluated 24 hours later using a fluorescent microscope to visualize the Cx-EGFP fusion proteins.

Wildtype Cx43.4 or Cx43.4 C64S (described above) were sub-cloned into the mammalian expression vector, pEGFP-N3 (BD Biosciences), downstream of the human cytomegalovirus (CMV) promoter.

Dye uptake analysis of hemichannel function

Transiently transfected or untransfected 293T cells were evaluated for Cx hemichannel function using a dye uptake assay as described (Li et al., 1996; Penuela et al., 2007). 24 hours post-transfection, dishes of cells were rinsed with cold Dulbecco's-PBS (D-PBS) and stimulated on ice with fluorescent dye. For this, a steady stream of 800 ul of 1 mg/ml sulforhodamine B (558.66 MW, Invitrogen, Carlsbad, CA) in Dulbecco's PBS with or without Ca^{2+} was added to a 1/4 inch target area from a height of 25 mm. The cells were incubated on ice in the dye for five minutes and the dye was then washed using D-PBS +/- Ca^{2+}. Dye positive cells within the target were scored using a Zeiss fluorescent microscope, imaged using DCViewer, and processed with ImageJ software (NIH, Bethesda, MD). Three independent Cx43 and five independent Cx43.4 C64S transfections were assayed for dye uptake.

Acknowledgements

Thank you to Sylvia Penuela (University of Western Ontario) for generously providing 293T cells and to Mark Stenglein (University of Minnesota) for providing mammalian expression vectors and transfection reagents and for invaluable discussions of transfection methods.

FIGURE 1:

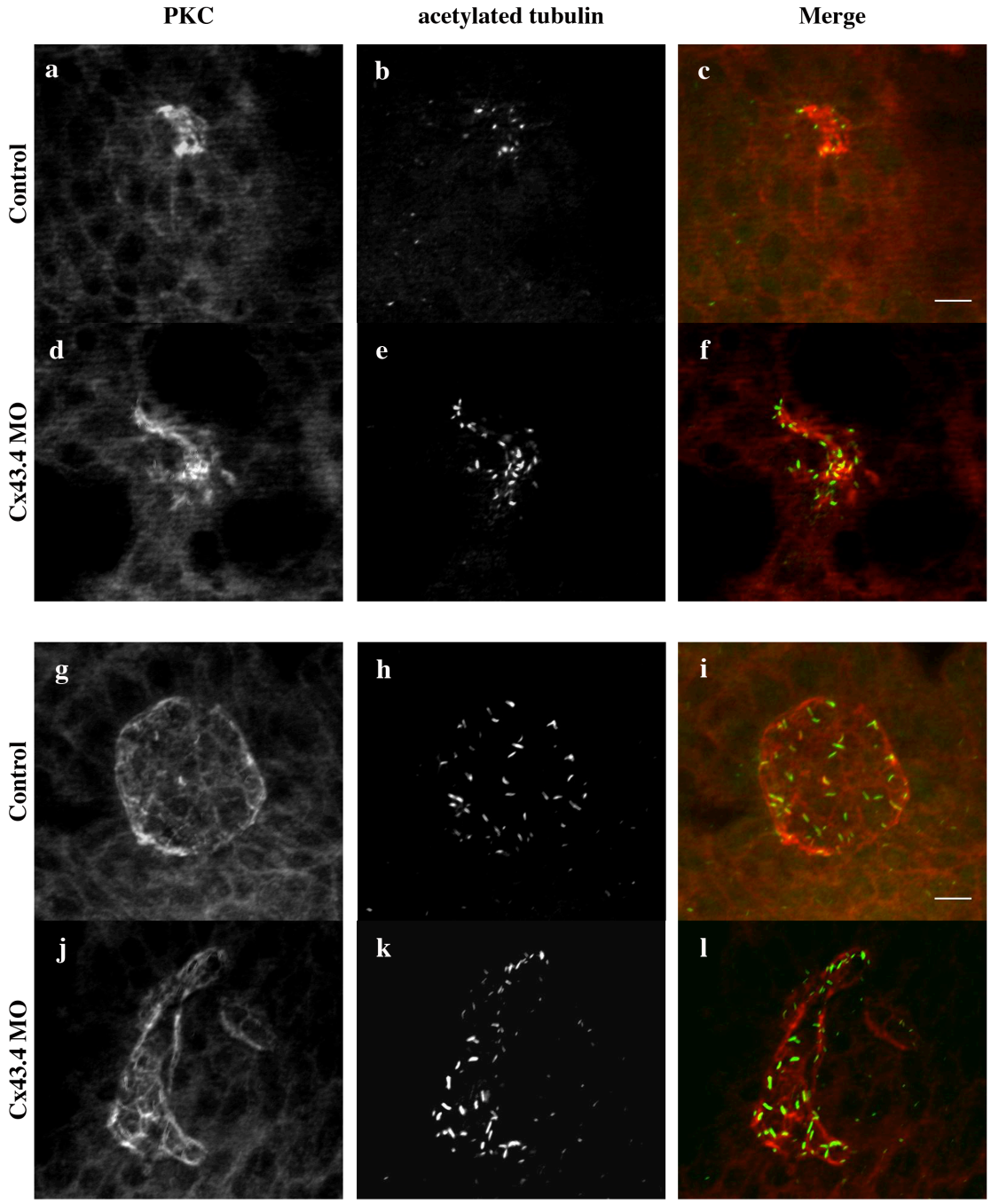
PKC
acetylated tubulin
Merge
Control
Cx43.4 MO
Control
Cx43.4 MO
a
b
c
d
e
f
g
h
i
j
k
l

FIGURE 1:

Cx43.4 is required for KV morphogenesis. “Confocal-like” imaging of double fluorescent immunostaining using antibodies for PKC (red and acetylated tubulin (green) during apical clustering of KV cells at the 2 SS (a-f) and KV lumen formation at the 4 SS (g-l). PKC labeled the apical surface of KV cells and tubulin labeled cilia protruding into the developing lumen. Cx43.4 morphant embryos (j-l) consistently lacked a fully inflated KV lumen. Scale bar in f and l = 25 microns.

FIGURE 2:

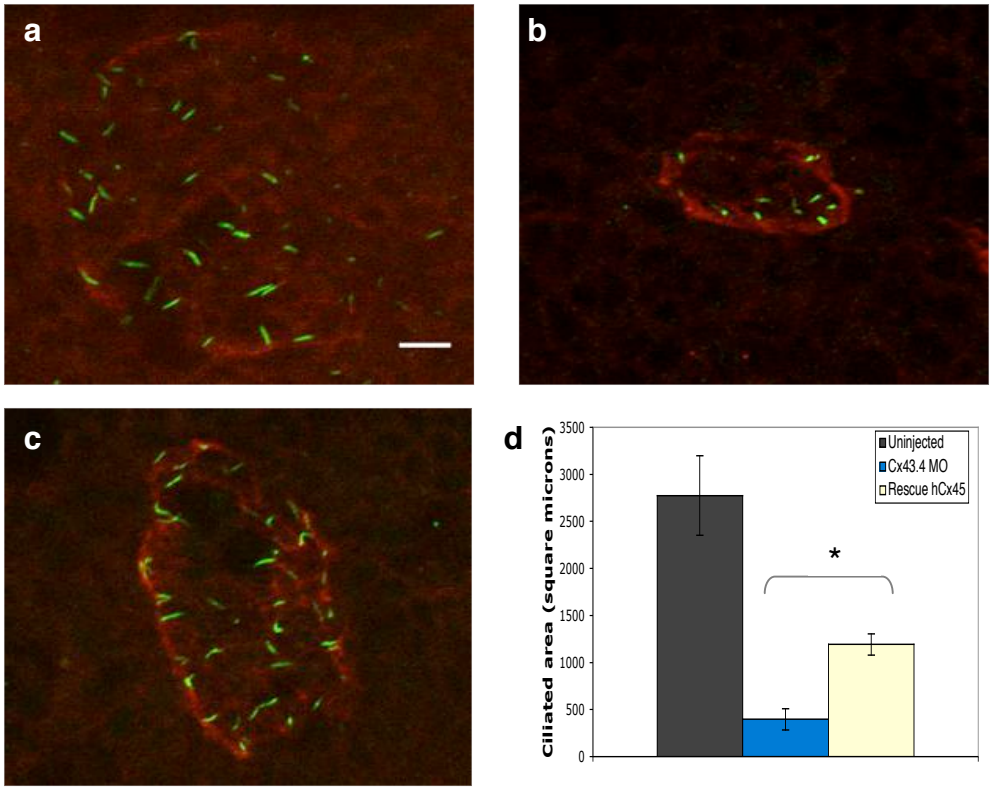
a
b
c
d
Ciliated area (square microns)
3500
3000
2500
2000
1500
1000
500
0
Uninjected
Cx43.4 MO
Rescue hCx45
*

FIGURE 2:

Lumen formation defect is partially rescued by human Cx45 mRNA. Co-labeling with PKC (red) and tubulin (green) antibodies (a-c) reveals a well-developed sphere in a wildtype embryo (a), a severe reduction in lumen expansion in a Cx43.4 morphant embryo (b), and a partial rescue of lumen formation in an embryo co-injected with Cx43.4 MOs and human *cx45* mRNA (c). The ciliated area of multiple KVs (d) in one representative rescue experiment (out of three) is represented as averages +/- s.e.m., *$p<0.01$.

Figure 3:

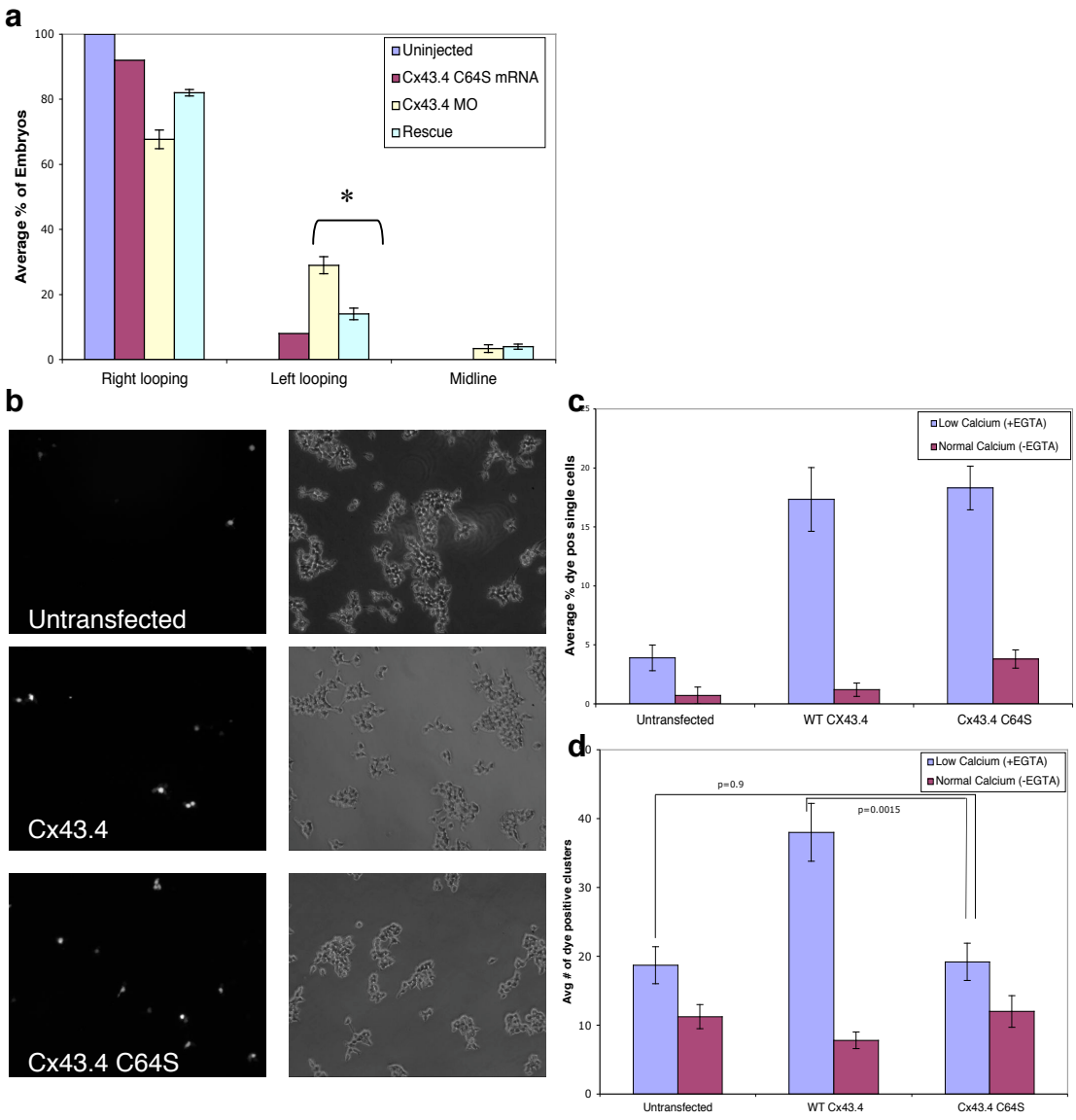
a
Average % of Embryos
100
80
60
40
20
0
Uninjected
Cx43.4 C64S mRNA
Cx43.4 MO
Rescue
*
Right looping
Left looping
Midline
b
Untransfected
Cx43.4
Cx43.4 C64S
c
Average % dye pos single cells
Low Calcium (+EGTA)
Normal Calcium (-EGTA)
Untransfected
WT CX43.4
Cx43.4 C64S
d
Avg # of dye positive clusters
Low Calcium (+EGTA)
Normal Calcium (-EGTA)
p=0.9
p=0.0015
Untransfected
WT Cx43.4
Cx43.4 C64S

Figure 3:

Cx43.4 hemichannels are sufficient to rescue L-R patterning defects. (a) Quantification of three independent experiments shows no alterations in heart looping when Cx43.4 C64S mutant mRNA is injected alone. Co-injection of human Cx43.4 C64S mRNA with Cx43.4 MOs significantly rescues aberrant heart looping, *p=0.009. Data are represented as averages +/- s.e.m. (b) sulforhodamine B dye uptake (left panels) is increased in Cx transfected 293T cells, entire cell field (right panels). (c) Quantification of single cell dye uptake in low versus normal Ca2+ are represented as averages +/- s.e.m. (d) Average number of dye-positive cell clusters is significantly increased in WT Cx43.4 expressing cells compared to Cx43.4 C64S or untransfected cells, error bars are +/- s.e.m.

Figure 4:

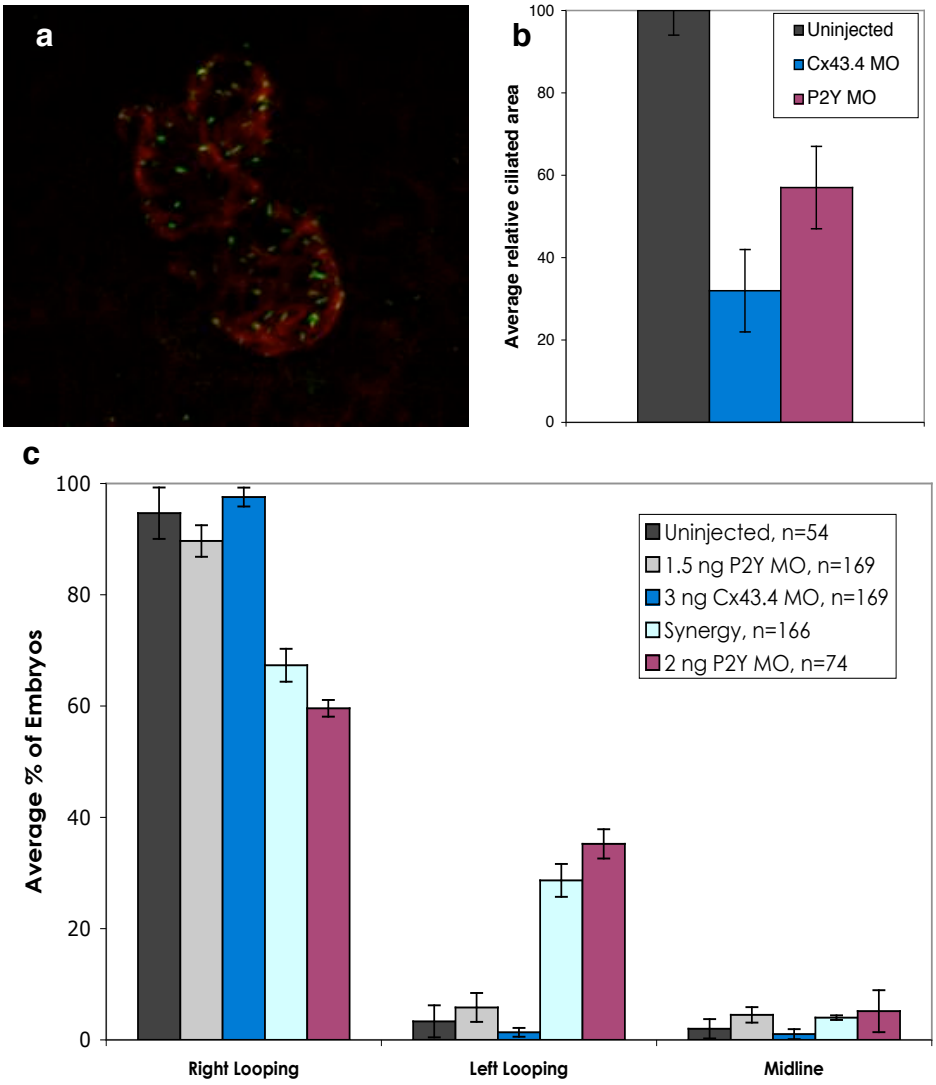
a
b
Uninjected
Cx43.4 MO
P2Y MO
Average relative ciliated area
100
80
60
40
20
0
c
Uninjected, n=54
1.5 ng P2Y MO, n=169
3 ng Cx43.4 MO, n=169
Synergy, n=166
2 ng P2Y MO, n=74
Average % of Embryos
Right Looping
Left Looping
Midline

Figure 4:

$P2Y_5$ MO phenocopies KV lumen development defect and acts synergistically with Cx43.4. (a) Immunofluorescence of a representative $P2Y_5$ embryo co-labeled with PKC (red) and tubulin (green) antibodies. Multiple fluorescence images of 4-somite stage KVs labeled with tubulin antibodies were analyzed using ImageJ software (b) and data were plotted as the average relative area +/- s.e.m. (d) Heart looping was not altered in embryos injected with low doses of $P2Y_5$ or Cx43.4 MOs, while co-injection produced a synergistic effect on heart looping. Data are averages +/- s.e.m.

Figure 5:

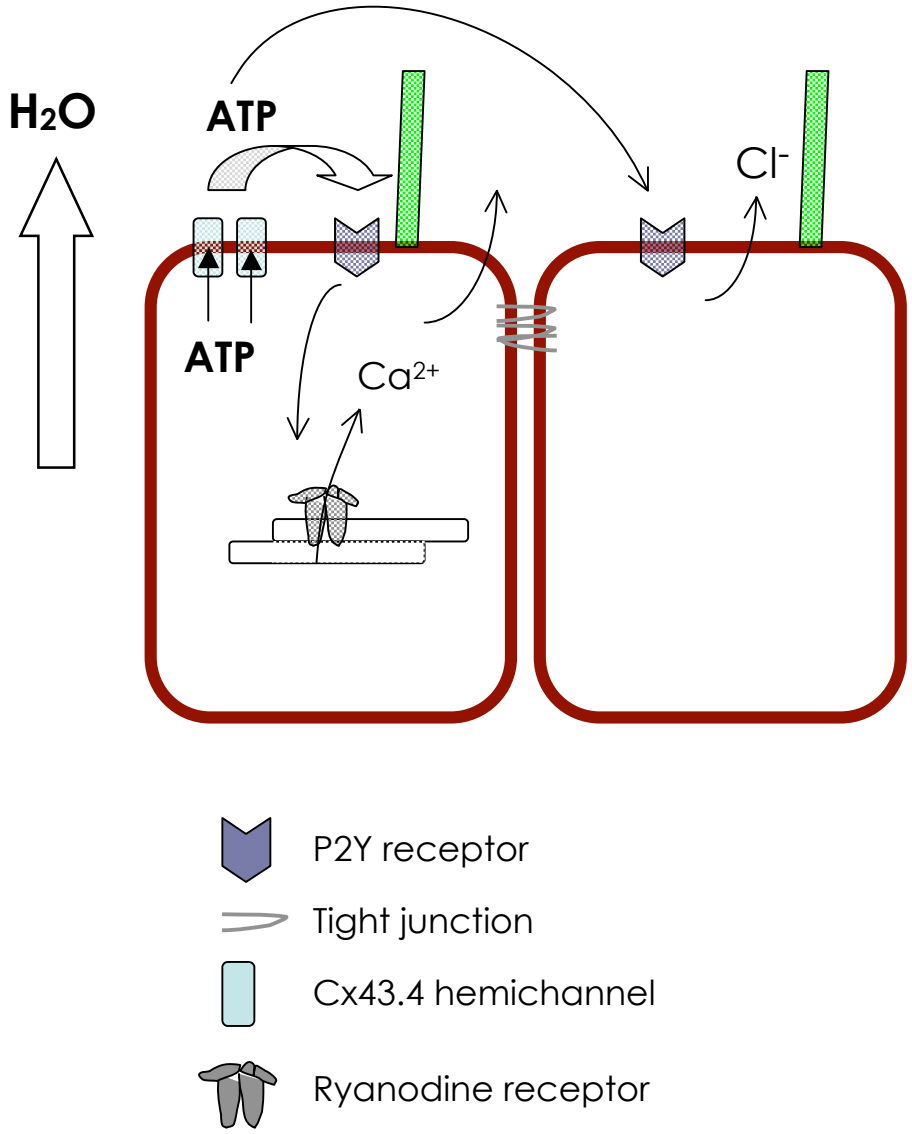
H2O
ATP
ATP
Ca2+
Cl-
P2Y receptor
Tight junction
Cx43.4 hemichannel
Ryanodine receptor

Figure 5:

Proposed model of Cx43.4 hemichannel function in KV morphogenesis: Apically localized Cx43.4 hemichannels open to the developing luminal space and, upon activation (potentially through mechanical stimulation), release ATP. ATP then binds to and activates P2Y G-protein coupled receptors also localized to the apical membrane of KV cells. This activation could stimulate Ca^{2+} release from internal stores (possibly through ryanodine receptors[3]) and the subsequent activation of Ca^{2+}-sensitive Cl^- channels. An increase in Cl^- (and other ions) in the developing luminal space would result in osmotically driven fluid flow, thereby further driving apart apical membranes and increasing the volume of KV.

Supplementary Figure 1

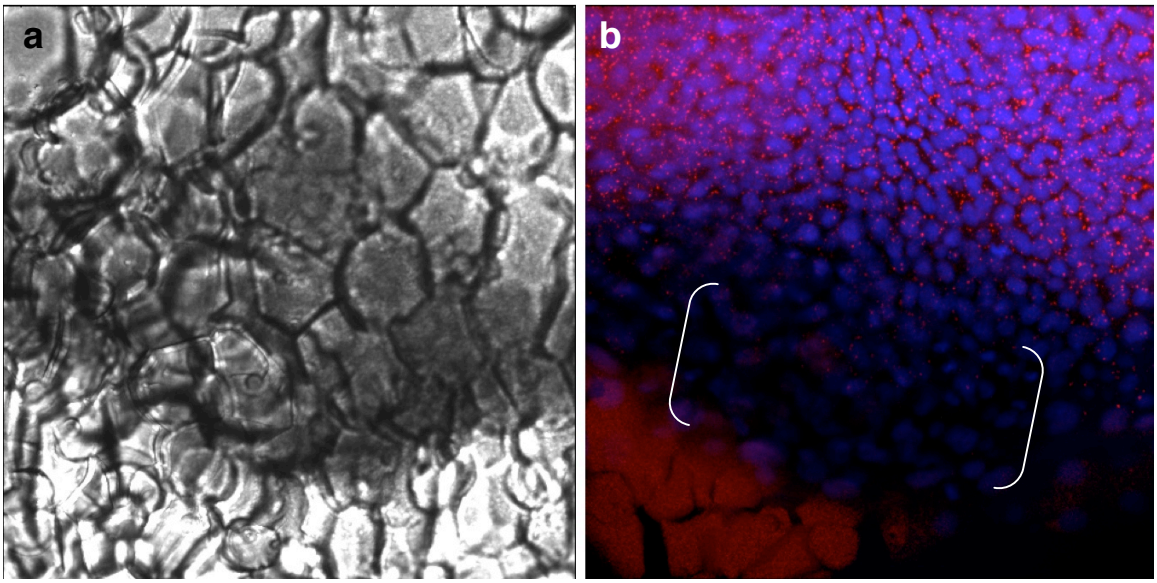

Supplementary Figure 1

Cx43.4 is not expressed in DFCs at the shield stage. (a) A shield stage embryo processed for whole-mount *in situ* hybridization and labeled with an antisense *ntl* probe. (b) The same embryo as (a) labeled with Cx43.4 polyclonal antibodies shows distinct puncta throughout the animal, although the DFC area is devoid of Cx43.4-positive puncta (bracket).

Supplementary Figure 2

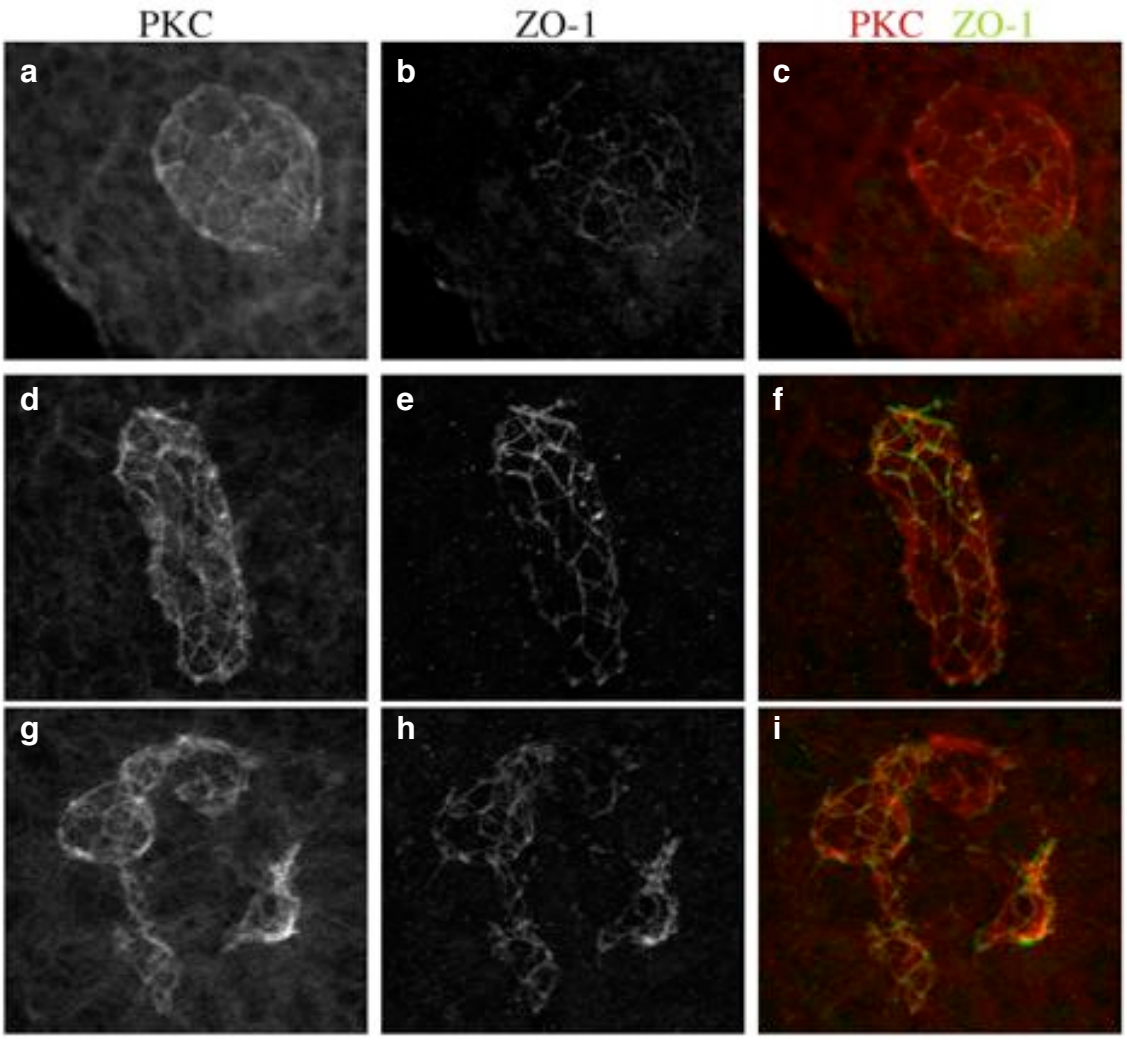

Supplementary Figure 2

Junctional complexes are not altered in Cx43.4 morphants. (a-j) Immunolabeling with PKC (red) and ZO-1 (green) antibodies. A 6-somite stage uninjected control embryo (a-c) displays PKC and ZO-1 staining at the junctions. Two Cx43.4 morphant embryos (d-f) and (g-I) both retain PKC and ZO-1 localization despite disrupted KV morphology.

Supplementary Figure 3

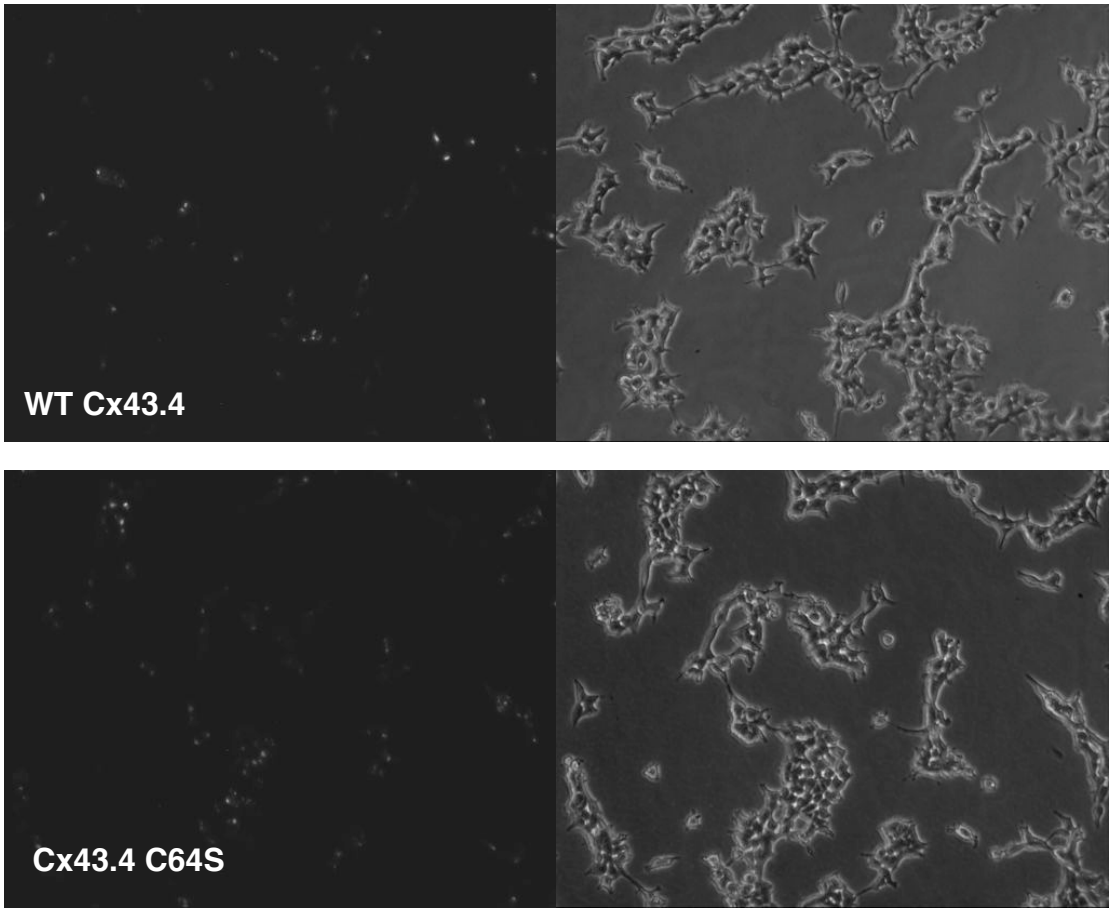

Supplementary Figure 3

Expression of transfected Cx constructs in 293T cells. Cx43.4-GFP and Cx43.4 C64S-GFP fusion proteins are visualized by fluorescent microscopy (left panels). Entire cell field as seen in bright light (right panels).

Supplementary Figure 4

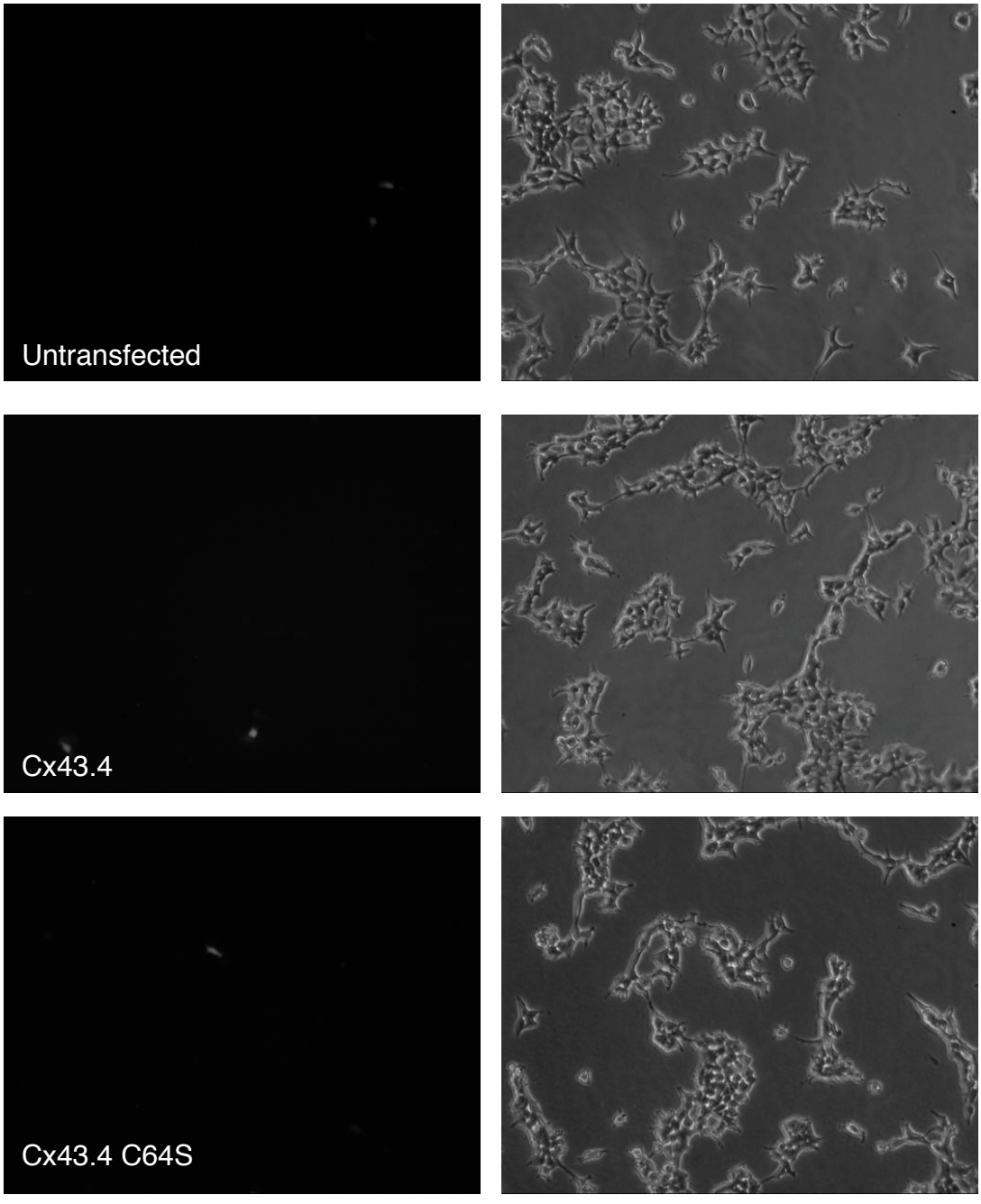

Supplementary Figure 4

Cx43.4-mediated dye uptake in 293T cells is sensitive to Ca^{2+} levels. Very few 293T cells take up sulforhodamine B dye in the presence of low extracellular Ca^{2+} (left panels) even when transfected with Cx43.4 or Cx43.4 C64S expression vectors. Entire cell field as seen in bright light (right panels).

Chapter IV

Summary and Discussion

Role of Cx43.4 during L-R patterning

GJs have long been speculated to play important roles during development. In support of this idea, mouse knockout studies have provided many examples of Cx requirements during organ morphogenesis and function (Willecke et al., 2002). However, earlier developmental requirements for Cxs (e.g. during patterning events) and their functions have been less understood. Patterning of the L-R axis is thought to be influenced by Cxs, however the exact Cx isoforms that are required, in which tissue(s) do Cxs function, and the mechanisms by which Cxs regulate L-R patterning are not clear.

The data presented in this thesis provide several major findings that increase our understanding of the role of Cxs during early vertebrate development: 1) Cx43.4 is specifically required during L-R patterning, 2) a Cx protein has been shown, for the first time, to be required within a specific tissue, KV, the L-R organizer of zebrafish, 3) KV lumen formation requires the function of Cx43.4 hemichannels.

How does an uninflated KV lead to defects in patterning?

We have shown that the primary role of zebrafish Cx43.4 during L-R patterning is in the formation of a fully inflated KV (see Chapter II). A fluid-filled inflated, spherical KV structure is likely important for normal fluid flow, but it was initially unclear how cilia could produce a net directional flow within KV or in the mouse node. One could imagine that if cilia were positioned vertically, rotation about that axis would not result in a net leftward flow. Rather, a vortex or

whirlpool would be present about each cilium. In order to generate a leftward flow, it was proposed, based on mathematical simulations, that cilia are actually tilted toward the posterior of the node (Cartwright et al., 2004). In this case, a directional fluid flow would be observed closest to the surface of the node.

These mathematical models were verified by an *in vivo* study demonstrating a conserved mechanism of nodal flow in mouse, rabbit, and medakafish that relied on the cilia tilting at a 40° +/- 10 angle toward the posterior (Okada et al., 2005). Posteriorly tilted cilia mean that they brush along the apical surface of the cell on the rightward stroke. This drag makes their movement very inefficient at moving fluid. On the leftward stroke, however, the cilia are unencumbered and the beat effectively pushes fluid in the leftward direction. In addition to this finding, the cilia were also positioned toward the posterior within the plane of the apical cell membrane of all nodal cells, raising the possibility that planar cell polarity signaling is also involved in L-R asymmetry.

The data presented here suggest that in Cx43.4 morphant embryos, the primary defect leading to randomized L-R patterning is an uninflated KV. Given the previous studies of fluid flow and ciliary beating described above, it is possible that the cilia within Cx43.4-deficient KVs encounter a cell surface on the rightward and/or leftward strokes. This would render the cilia incapable of generating a robust movement of fluid on the leftward stroke since the surface of an apposing cell is likely in very close proximity.

Are Cx43.4 hemichannels sufficient for L-R patterning?

In order to determine how Cx43.4 influenced KV morphogenesis, specifically in terms of lumen formation, the role of a Cx43.4 hemichannel (C64S) was tested. The results showed that Cx43.4 hemichannels were capable of rescuing aberrant L-R patterning following Cx43.4 knockdown (see Chapter III). This important finding raises new questions about the roles of Cx proteins in development. For example, since Cx hemichannels are known to respond to mechanical stimulation in tissue culture experiments, is it possible that hemichannels could function as transducers of fluid flow within KV? Also, what signaling molecules may pass through hemichannels to mediate L-R patterning within KV?

The results presented in this thesis demonstrate that rescues of heart looping (a readout of normal L-R patterning) using various Cx constructs are feasible experiments. Using this approach it is possible to ask the following questions to determine whether Cx43.4 hemichannel opening is necessary for L-R patterning:

1) Does a closed hemichannel mutant rescue the Cx43.4 morphant phenotype?

Cx43 expression has been shown to be necessary for the localization of N-cadherin at the cell membrane (although whether the formation of a GJ is a necessary step has not been elucidated) (Wei et al., 2005). Therefore, it is possible that simple expression of Cx43.4 in MO-treated embryos, rather than

the opening of hemichannels, is required for L-R patterning. To test this idea, a closed hemichannel mutant could potentially be engineered by mutating a conserved tyrosine residue (Beahm et al., 2006) that is adjacent to the amino acid known to be critical for channel opening. If hemichannel opening is not deemed critical for L-R patterning, this would lend support to a model involving interaction with adhesion proteins or other signaling molecules through the C-terminus.

2) Is the C-terminus of Cx43.4 critical for normal L-R patterning?

Mutating an extracellular loop cysteine (C64S) was designed to interfere with the docking of hemichannels between apposed plasma membranes. This would block the formation of the cell-to-cell channels found in GJs, as well as adhesive bonds between cells. Recent experiments using a closed GJ channel construct suggested that adhesion was a critical function for Cxs during neural migration in the cortex (Elias et al., 2007). However, it is possible that eliminating the docking capabilities of Cx43.4 is not sufficient to alter the endogenous function of Cx43.4 in L-R patterning. That is, the C-terminal domain, which is important for signaling events through phosphorylation and protein-protein interactions, remained intact and it is possible that this domain is the required component during L-R patterning. Truncation mutants have been used to evaluate the roles of phosphorylation and protein interactions in various cell systems, and a similar approach could be tested in zebrafish embryos to determine whether the C-terminus is critical for L-R asymmetry.

Implications for Cxs and P2 receptors in epithelial development and lumen biogenesis

The primary defect associated with Cx43.4 depletion and L-R patterning anomalies in zebrafish is a lack of KV lumen formation (see Chapter III). Importantly, these findings have implicated the function of a Cx hemichannel in the establishment of a functional, specialized epithelium, KV. In order to form a fluid-filled KV, Cx43.4 and $P2Y_5$ are both required within the epithelial cells. Given the extensive expression of P2 receptors across epithelia (Leipziger, 2003) and the presence of Cx isoforms in apical membranes, it is possible that these proteins function together for epithelial development and lumen biogenesis in a variety of tissues.

The proposed model for epithelial tube or lumen biogenesis includes: 1) the acquisition of apical-basal polarity, 2) the fusion of ion channel-containing vesicles with the apical surface, and 3) the accumulation of extracellular fluid to separate apical membranes and create a fluid-filled space (Lubarsky & Krasnow, 2003). There are many potential roles for Cx and P2 receptor functions during these stages of lumen biogenesis and some will be briefly discussed here.

First, the acquisition of apical-basal polarity is a necessary prerequisite for the formation of a lumen. Cells that have established apical-basal polarity have essentially created distinct sub-cellular membrane domains to which various proteins can be specifically targeted. For example, intercellular

junctions provide adhesion between neighboring cells (e.g. apical junctional complexes), and a sealed paracellular space between epithelial cells (tight junctions). Cx proteins could influence this early stage of epithelial development by directing and stabilizing adhesion (Cotrina et al., 2008) through protein-protein interactions with components of intercellular junctions (Giepmans, 2004). Additionally, specific P2 receptors are polarized with respect to their localization within the apical or basolateral membranes of epithelial cells, (Wolff et al., 2005). While the regulation of this trafficking remains unclear, it is possible that the polarized localization of these receptors is an early step in epithelial development.

Second, the fusion of ion channel-containing vesicles with the apical membrane is necessary for expansion of the developing lumen. Given that Cx hemichannels can facilitate ion transport, in addition to the release of small molecules such as ATP, they are probable candidates for localization to the developing apical membrane. This will be an important trafficking question, because hemichannels may also be required basolaterally to provide for GJ communication between neighboring cells. P2Y receptors are also likely to be found in vesicles fusing with the apical membrane, given that they modulate ion flow through downstream signaling mechanisms. Future studies will be necessary to determine whether Cxs and/or P2 receptors are localized to vesicles prior to fusion with the apical membrane in a variety of developing epithelia.

Third, the accumulation of extracellular fluid is required to separate apical membranes and create a fluid-filled space. In the lung, this is achieved by chloride ion transport which sets up an osmotic gradient to draw water into the lumen (Lubarsky & Krasnow, 2003). It is possible that Cx hemichannels could function in the apical membrane as an avenue for fluid flow into the lumen space (Goodenough & Paul, 2003). In addition, the importance of ion transport, mediated by luminal P2 receptor activation, and subsequent fluid flow are well-established for the function of sweat glands, the gastrointestinal tract, and the conjunctiva of the eye (Leipziger, 2003). However, the roles of P2 receptors during the development of lumen-containing tissues early in embryogenesis remain largely unexplored.

Final conclusions

The results presented here demonstrate several key contributions to the fields of embryonic patterning and cell-cell communication. Importantly, these findings implicate the function of a Cx hemichannel during early vertebrate development, specifically in the morphogenesis of the specialized epithelium, KV, which is required for L-R patterning. Additionally, an interesting relationship between Cxs and P2 receptors in the development of a functional epithelial compartment has been uncovered. Given the many questions remaining in the Cx and P2 receptor fields, particularly with respect to what passes through hemichannels and what ligands activate recetprors, future studies addressing

these aspects will provide additional insight as to the mechanisms of Cx function in epithelia and tissue morphogenesis.

Chapter V

Knockdown of Zebrafish Connexin43.4 Perturbs Angiogenesis Through an Affect on Netrin Signaling

SUMMARY

The notochord plays an essential role in directing axial development and patterning the adjacent vascular system through the production of Sonic Hedgehog (Shh) and a cascade of gene expression in the adjacent somites involving vascular endothelial growth factor (VEGF). We are asking whether GJ communication is required for notochord signaling and, if so, what role does it play? We have shown that three connexins (Cx) are expressed in the notochord of zebrafish embryos: Cx43 and apparent orthologs of mammalian Cx45, Cx43.4 and Cx44.2. Dose-dependent reductions in circulation were documented by injection of Cx antisense morpholinos (MOs) into transgenic embryos, which carried a *fli1*-EGFP marker for endothelial cells and a *gata1*-dsRed marker for cells of the blood lineage. We found that circulation was depressed and in some cases completely absent. Based on studies in mice, MO knockdowns of the Cx43 and Cx45 orthologs are expected to have an impact on cardiac function. However, embryos with major defects in circulation displayed actively beating hearts. Anomolies were also observed in the migration of endothelial cells giving rise to intersomitic vessels and the secondary vessel, the parachordal vessel. These effects on vessel sprouting and migration coincide with an increase in Netrin signaling, which is known to influence axonal migration and, in this case, endothelial cell migration. These

results provide a working model for the mechanism of Cx function during vascular development.

INTRODUCTION

Development of the vasculature is a highly regulated process that is required for the growth, differentiation, and function of tissues within a developing embryo and for homeostasis in adults. The vascular network serves as a conduit for the delivery of nutrients and oxygen to organs and tissues, the removal of wastes, and as a microenvironment for hormone signaling. Normal vascular development has been separated into two distinct processes: (1) vasculogenesis, or the migration and coalescence of angioblasts into 'cords' followed by subsequent lumenization of the main vessels and (2) angiogenesis, which is defined as the reorganization and sprouting of new vessels from the pre-existing vasculature (Patan, 2000).

Although these basic morphological processes have been described for some time, the signaling pathways that regulate cell fate decisions, migration, and differentiation during vasculogenesis and angiogenesis have only been studied more recently. Hypoxia-induced vascular endothelial growth factor (VEGF) is perhaps the best-known vascular signal; it influences the proliferation, migration, and survival of endothelial cells (Ferrara et al., 1996). Additionally, VEGF is known to induce angiogenesis under conditions of hypoxia in adult tissues (Shweiki D, 1992), so understanding this pathway is also important for biomedical purposes.

In developing zebrafish embryos, the expression of VEGF is required for vasculogenesis, angiogenesis, and decisions affecting arterial and venous fates

(Lawson et al., 2002). Sonic hedgehog (Shh) expression along the midline is essential for the regulation of VEGF levels in the adjacent somites of the early embryo (Lawson et al., 2002). Therefore, mutations in *shh* or downregulation of Shh using chemical inhibitors result in an increase in venous cell fate at the expense of the dorsal aorta.

In zebrafish, the regulation of arterial cell fate decisions is mediated by Notch signaling, which is downstream of the Shh/VEGF signaling pathway. Activation of the Notch pathway promotes arterial endothelial cell fate decisions through activation of the membrane-bound ligand, *ephrin2b* (*efnb2*) and represses venous cell fate by inhibiting the expression of the venous-specific gene, *flt4* (a tyrosine kinase receptor for the VEGF ligand), in future arterial cells (Lawson & Weinstein, 2002a).

More recent advances in understanding the signaling pathways involved in vascular development have examined the roles of molecules previously known to be involved in axonal guidance during neural development. When examining the migration patterns of nerves and blood vessels, it was noted that the two paths were oftentimes indistinguishable (Carmeliet & Tessier-Lavigne, 2005). These observations led to the prediction that the same molecules could direct the migration of both endothelial cells and axons during development. Further studies provided evidence that angiogenic molecules, such as VEGF, could regulate axonal migration (Schwarz et al., 2004); and previously identified axonal migration cues, such as the Netrin family of ligands and their receptors

UNC5B and Deleted in colon cancer (DCC), are required for the appropriate migration of endothelial cells during angiogenesis (Lu et al., 2004). Likewise, Ephrin signaling is known to provide guidance cues during both axonal pathfinding and vasculogenesis (Eichmann et al., 2005). Observations of this type suggest that there is considerable overlap in the signaling cascades that regulate vascular remodeling and axonal guidance.

In addition to the requirement of vascular development during embryogenesis, significant vascular remodeling is known to occur postnatally. For example, vasculogenesis can be stimulated during adulthood in response to tissue ischemia (Murasawa & Asahara, 2005). Importantly, heart failure occurs after myocardial infarction and the mobilization of bone marrow-derived endothelial progenitor cells (EPCs) is subsequently activated (Shintani et al., 2001; Massa et al., 2005). Myocardial regeneration following infarct relies on the migration and differentiation of EPCs, which promote neovascularization (Numaguchi et al., 2006).

In adults, the stimulation of angiogenesis is rare (usually restricted to wound healing events) and is therefore associated with disease states. For example, angiogenesis is required for at least two phases of cancer progression: tumor growth and metastasis. First, tumor growth requires a significant nutrient supply. Many tumors, specifically breast cancers, meet this need by secreting pro-angiogenic factors including VEGF in order to remodel the local, endogenous vasculature and thereby increase blood supply to the

tumor (Fox et al., 2007). Second, one of the final steps in tumor progression is metastasis, which is also the cause of death for many cancer patients. A common mechanism used by cancer cells to metastasize to other tissues is intravasation – the invasion of cancer cells into blood vessels (Condeelis & Segall, 2003). Therefore, the presence of neovasculature surrounding a tumor also serves as an avenue for metastasis, whereby cells slough off the tumor and enter the circulatory system (Jahroudi & Greenberger, 1995). Because of the clinical ramifications of vascular remodeling through vasculogenesis and angiogenesis pathways, it is critical to understand how the normal vascular development and remodeling programs are regulated so that rational therapeutics can be designed to better treat cardiovascular diseases and cancers.

Despite the advances in describing which signaling molecules are required for normal vasculogenesis and angiogenesis and instances where mis-regulation of these processes is associated with disease, our understanding of how vascular-specific signaling pathways are regulated is incomplete. An important, largely unanswered question in vascular development is whether cells utilize short range, direct cell-to-cell transfer of signals or other small molecules via gap junctions (GJs) in order to regulate the formation of the vasculature.

GJs are known to be critical for cardiovascular development in mice, based on targeted deletion of particular GJ protein subunits, members of the

Connexin (Cx) family. Specifically, in terms of the Cx considered in this project, Cx43.4, the orthologous knockout (Cx45) in mice produced embryonic lethality with effects on both heart and vascular development (Kruger et al., 2000; Kumai et al., 2000). While Cxs are well-known for their role in mediating the spread of electrical impulses that synchronize the contraction of the adult heart (Wei et al., 2004), less is known about their roles during cardiac development. Kumai at al. studied the hearts of Cx45 knockout embryos and found that the endocardial cushion failed to develop. This developmental defect was associated with a failure in the epithelial-mesenchymal transformation of the cardiac endothelium, possibly due to a mislocalization of the Ca^{2+}-dependent transcription factor, NF-ATc1. This suggests that for proper heart development, Cx45 is necessary for intracellular Ca^{2+} levels to be high enough to activate NF-ATc1 and facilitate its translocation to the nucleus.

In another Cx45 knockout study, Kruger et al. found that vasculogenesis seemed unaffected in Cx45 knockout embryos, while remodeling of the vasculature into a branched network was impaired in three embryonic blood vessel systems. Since these defects were similar to embryos with impaired TGF-β signaling, the authors suggested that Cx45 might regulate TGF-β upstream of vascular development. However, in two of the three vascular systems affected by Cx45 knockout, only one system had reduced levels of TGFβ receptor expression.

Although these two studies clearly demonstrate that Cx45 is necessary for normal cardiovascular development, the signaling pathways that Cx45 influences to direct vascular development remain unclear, especially given that TGF-β expression was not altered in all defective vessel systems. Moreover, with respect to the vasculature, the mechanisms by which GJ communication contributes to vasculogenesis, angiogenesis, and endothelial cell fate decisions are largely unknown.

To understand the mechanisms by which GJs influence these aspects of vascular development, we have chosen to utilize the zebrafish as a model. The zebrafish is advantageous for these studies because injections for morpholino-knockdown of Cx proteins are straightforward and transgenic embryos are ideal for studies of vascular formation. Additionally, while a functional cardiovascular system develops rapidly after just 24 hours post fertilization (hpf), this network is dispensable throughout embryogenesis and the first larval stages. During this time period, it is possible to analyze developmental abnormalities since the fish are able to receive oxygen through simple diffusion.

The expression patterns of zebrafish Cxs have implicated them in the specification of mesoderm and the function of the notochord (Essner et al., 1996; Chatterjee et al., 2005), which is an axial mesoderm-derived structure that becomes progressively specified from late blastula periods to somite forming periods. The notochord provides two functions in the embryo. First, the notochord fulfills a major structural role in the embryo that in most

vertebrates is replaced by vertebrae later in development. Second, from gastrulation through somite forming periods the cells that comprise this structure are a rich source of signaling molecules, such as Shh, that are important for patterning the surrounding tissues (Stemple, 2005). Therefore, it is possible that Cx function in the notochord is important for regulating vascular development through an influence on Shh signals emanating from the notochord.

These studies, primarily of the Cx45-related protein in zebrafish, Cx43.4, are aimed at revealing the mechanisms underlying the role of GJ communication during vascular development. We present data here showing that cells in different developmental states within the notochord express Cx43 or Cx45 orthologs. We also show that Cx function in the notochord is developmentally necessary, since vascular defects were observed in Cx-deficient embryos. Moreover, we show that the vascular defects arose as a consequence of aberrant midline signaling suggesting that appropriate levels of GJ communication in the notochord are required to regulate vascular-specific developmental signaling cascades.

RESULTS

Cx43.4, Cx44.2, and Cx43 are expressed in the zebrafish notochord

It has been shown previously that zebrafish *cx43* (Chatterjee et al., 2005) and *cx43.4* (Essner et al., 1996) transcripts are expressed in the notochord during various developmental stages. In order to identify potential Cx family members that are localized in the notochord and could therefore contribute to embryonic patterning events, the spatial and temporal expression patterns of zebrafish Cx43, Cx43.4 and *cx44.2* were analyzed. Using polyclonal antibodies, Cx43.4 was localized to stereotypical punctate structures throughout the 10-somite stage embryo, particularly in the developing notochord, along the entire anterior-posterior axis (Fig. 1a). Later during somitogenesis, at the 20-somite stage, Cx43.4-positive puncta were localized dorsally along the presumptive neural tube and throughout the axial mesoderm (Fig. 1b). Notably, Cx43.4 expression remained distributed throughout the entire length of the notochord, as in the 10-somite stage embryo (Fig. 1b). At 24 hours post-fertilization (hpf), however, Cx43.4 localization was restricted to the most posterior notochord cells (Fig. 1c). These observations suggest that Cx43.4 expression is tightly regulated throughout developmental progression, since the most posteriorly located cells are “younger” and less differentiated than those found more anteriorly.

Cx43 is also known to be expressed in the notochord, but its localization is not spatially restricted. Rather, cells along the entire length of the notochord

expressed Cx43 at 24 hpf (Fig. 1e). Since Cx43 is found in all notochord cells, the expression of this Cx isoform does not have significant spatio-temporal regulation during maturation of the notochord. Taken together, the Cx spatio-temporal expression patterns show that individual Cx family members have differentially regulated expression patterns during the development of the notochord and suggest that each isoform has a unique functional role in patterning embryonic tissues.

In the absence of antibodies for Cx44.2, the expression pattern of this previously uncharacterized Cx was evaluated using whole-mount *in situ* hybridization methods. *cx44.2* is closely related to *cx43.4* and likely arose as a result of a genome duplication event that occurred in an ancestral ray-finned fish that eventually gave rise to zebrafish (Amores et al., 1998; Taylor et al., 2003). *in situ* labeling experiments showed that *cx44.2* is localized to the dorsal region of the early gastrula at about 70% epiboly; expression remained higher dorsally throughout gastrulation (data not shown). Similar to *cx43.4*, during somite stages, *cx44.2* is expressed in the paraxial mesoderm with enrichment in the posterior region (Fig. 1g). Upon sectioning, *cx44.2* expression is clearly observed in the notochord (Fig. 1h). The expression of *cx44.2* mRNA in the notochord is transient as 24 hpf embryos do not stain positively in this tissue.

Cx43.4 and Cx44.2 are required for vascular function

Based on the evaluation of Cx expression in the notochord, we next asked how Cx function in this tissue influenced embryonic development. Since the notochord is known to be a source of signals that are required for the patterning of adjacent tissues, and the vasculature clearly showed developmental anomalies in the Cx43 and Cx45 (Kruger et al., 2000; Kumai et al., 2000) knockouts in mice, the remaining studies focused on an analysis of vascular development in Cx43.4 and Cx44.2 knockdown embryos, largely due to an early lethality phenotype in Cx43 morphant embryos.

To analyze the functional roles of Cx43.4 and Cx44.2 during development, morpholino (MO) antisense methods were utilized. For both Cx43.4 and Cx43, MO efficacy was verified by the loss of immunoreactivity in MO-injected embryos (Fig. 1d and 1f, respectively). Additionally, a complete lack of punctate staining with Cx43.4 pre-immune serum verified the specificity of the antibody (data not shown).

Following MO knockdown, one evident defect was greatly reduced circulation throughout the trunk and tail of Cx43.4 and Cx44.2 morphants at both 30 and 50 hpf. To more specifically characterize the circulation defects, transgenic animals in which dsRed is driven by the blood cell-specific promoter, *gata1* (Traver et al., 2003), were utilized. In uninjected control Tg*(gata1:dsRed)* embryos at 30 hpf, a continuous circulatory loop was visualized (Fig. 2a). After

being pumped through the heart, dsRed-labeled blood cells were observed along the dorsal aorta (DA) to the very posterior of the embryo. Here, the blood cells turn back toward the anterior and move through the branched plexus of the caudal vein. Finally, the blood coalesces into the single tube of the posterior cardinal vein (PCV) vein, which returns the blood back to the heart (Fig. 2a).

Observation of Tg*(gata1:dsRed)* morphant embryos revealed a variety of defects in circulation. Most Cx43.4 morphant embryos (Fig. 2b) displayed a severe reduction in *gata1*:dsRed fluorescence in the DA and PCV. The complexity of the vascular plexus was also reduced (compare with Fig. 2a) in these embryos. Cx44.2 knockdown (Fig. 2c) produced a less dramatic affect on circulation, since fluorescent blood cells were observed circulating through the DA and PCV. However, the vascular plexus in these animals also lacked significant branching. Additionally, blood clots or pools were often observed in the trunk of Cx43.4- and Cx44.2-deficient embryos. The extent of defective circulation in a representative experiment was 80% of Cx43.4 morphant embryos (n=5) and 77% (n=13) in the Cx44.2 MO-treated embryos at 30 hpf, while standard control MO embryos showed normal circulation (n=6) (Tables 1,3). These observations suggest that Cx43.4 and Cx44.2 are required to establish a fully functional circulatory system.

Since Cx43.4 and Cx44.2 are closely related and may both be considered to be orthologs of mammalian Cx45, we asked whether the

knockdown of both isoforms was additive. That is, do Cx43.4 and Cx44.2 have redundant or unique functions in cardiovascular development? MOs against both isoforms were co-injected into Tg*(gata1:dsRed)* embryos and circulation was analyzed as above. Depletion of both Cx43.4 and Cx44.2 (Fig. 2d) resulted in a similar phenotype as knockdown of a single isoform: reduced circulation was observed in the DA and PCV and the vascular plexus was under-developed. The lack of an additive effect when both Cx43.4 and Cx44.2 are knocked down together suggests that these two Cxs function in the same pathway towards cardiovascular development.

When circulation was analyzed at 50 hpf, the uninjected control Tg*(gata1:dsRed)* embryos had a complete circulatory loop from the DA through the PCV. At this developmental stage, the circulatory network was more complex containing blood flow through the intersegmental vessels (ISVs). In both the Cx43.4 and Cx44.2 morphants, however, reduced circulation was observed throughout the trunk and tail (Tables 2 and 4, respectively). Included in these defects was a reduction in the number of ISVs that facilitated active blood flow. In the double Cx knockdown embryos, the circulation defects were not more severe than in the Cx43.4 morphants (Tables 5,6). This suggests that Cx43.4 plays a more prominent role than Cx44.2 in the development of the vasculature. Moreover, Cx43.4 may have a role in promoting angiogenesis, given that circulation in the ISVs was severely impaired in a high percentage of Cx43.4 morphants.

To evaluate the specificity of MOs against Cx43.4 and Cx44.2, multiple MO doses were injected and defects in circulation were analyzed. The results are summarized in Tables 1-6 and demonstrate that the defects are MO dose-dependent. Depending on the MO dose, the defects ranged from reduced red blood cell movement through the trunk or tail to severe cases in which little *gata1*:dsRed fluorescence was detected in the vessels and significant blood pooling was observed. Since these severe defects induced by high MO doses were associated with gross morphological defects (data not shown) including undulated notochords and small heads, they may represent off-target effects caused by toxicity. In the majority of uninjected control embryos, blood cells could be observed circulating throughout the entire vasculature, while an average of 7% (n=34) displayed slight defects that were limited to lack of circulation in a few ISVs at 30 hpf or slight areas of blood pooling at 50 hpf. For all experiments described elsewhere, 4 ng of MO were injected as this dose resulted in high phenotypic penetrance with low toxicity.

One possible explanation for the defective circulation in Cx knockdown embryos is impaired heart function or blood pressure, especially since the mammalian Cx ortholog is expressed and functions in the heart. In all Cx morphant embryos tested, however, an active heartbeat was observed. When heart rates were measured at 24 hpf, the Cx43.4 morphant embryos had similar rates as controls. In contrast, at 48 hpf, Cx43.4-deficient embryos showed a slightly, but significantly, slower average rate than controls (Fig. 3). However,

this slower heart rate is likely not severe enough to account for the dramatic loss in functional ISVs at 30 hpf and PAV development at 50 hpf (see below) in Cx43.4-deficient embryos. This is consistent with a previous report which demonstrated that the fluid force created by a pumping heart is not necessary for the development of the primary vasculature (Isogai et al., 2003).

Endothelial cell development during vasculogenesis and angiogenesis

We hypothesized that the defects in circulation could be due to problems during vasculogenesis, angiogenesis, or both. To discriminate between these possibilities and to evaluate the development of the vasculature, morpholinos were injected into embryos from a transgenic line, Tg*(fli1:EGFP)*, in which EGFP is expressed under the control of *fli1*, an endothelial cell-specific promoter (Lawson & Weinstein, 2002b). The results of these treatments showed defects in the overall layout of the vasculature in 93% (n=30) of the Cx43.4 morphants and in 42% (n=24) of the Cx44.2 morphants. With respect to the DA and PCV that are formed during vascuologenesis, *fli1*:EGFP expressing endothelial cells lining the major vessels appeared normal, suggesting that vasculogenesis is not affected in Cx-deficient embryos.

Angiogenesis in the zebrafish is a precisely patterned event such that each ISV sprouts from the DA (Fouquet et al., 1997) and migrates dorsally between pairs of somites to reach the dorsal longitudinal anastomotic vessel (DLAV) where the vascular network is connected (Childs et al., 2002). Since

this ISV network is highly stereotypical, deviations from the normal patterning are easily visible using transgenic embryos. Specifically, Cx-deficient Tg*(fli1:EGFP)* embryos showed defects in angiogenesis demonstrated by delayed endothelial cell migration, abnormal branching morphology, and incomplete anastomoses in the forming ISVs 30 hpf (Fig. 4c,e,g), while only 5% (n=46) of uninjected control embryos displayed modest defects (Fig. 4a). When analyzed further at 50 hpf, the ISVs had largely resolved their migrations dorsally in most of the Cx-morpholino injected embryos (Fig. 4d,f,h), suggesting that the initial impairment in ISV migration at 30 hpf may reflect a developmental delay, possibly due to the MO injection procedure.

A second round of angiogenic sprouting normally occurs from the posterior cardinal vein at 36 hpf and results in formation of the parachordal vessel (PAV) (Wilson et al., 2006). In control embryos at 50 hpf, the PAV can clearly be seen by horizontal bands of EGFP expression along the horizontal myoseptum (Figure 4b, arrowhead) between intersomitic vessels. The PAV of Cx morphants, however, failed to develop in the vast majority of segments as seen by the absence of intersegmental fluorescence in the Tg(*fli1*:EGFP) background (Figure 4d,f,h). Lack of a well-developed PAV at 50 hpf suggests that this defect is not due to a simple developmental delay, since PAV sprouting can be observed as early as 36 hpf. Rather, Cx function is required for this secondary angiogenic sprouting event.

To further assess the vascular defects, mature endothelial cell fates were studied by *in situ* hybridization in control and Cx morphant embryos. At 24 hpf in all control embryos, *ve-cadherin* (*cadh5*) (Larson et al., 2004) expression was localized to the DA and PCV, as well as a few developing ISV sprouts (Fig. 5a). However, in 75% (n=20) of Cx43.4 and 60% (n=20) of Cx44.2 morphants, *cadh5* was misexpressed (Fig. 5b and c, respectively). Specifically, *cadh5* was preferentially expressed in the DA and was either not observed or was discontinuously localized in the PCV. When Cx43.4 and Cx44.2 were knocked down in the same embryo, *cadh5* was similarly misexpressed (Fig. 5d). These data suggest that connexins are required for appropriate maturation of axial vessel endothelial cells, particularly those of the PCV.

Vascular defects in Cx morphants are endothelial cell non-autonomous

Given the observed vascular defects and the widespread extent of Cx43.4-positive puncta in mesodermal tissues adjacent to the notochord during somite stages, it is possible that Cx43.4 is required in the migrating angioblasts during vasculogenesis or in the endothelial cells during angiogenesis. To test whether Cx43.4 is required cell-autonomously in the developing vasculature, we examined the localization of Cx43.4 during vasculogenesis and angiogenesis. Cx43.4-positive puncta were observed in the notochord domain, as seen previously, as well as in the axial tissue of 18-somite stage embryos (Fig. 6a). At this stage, the angioblasts (marked by *fli1*:EGFP expression) are located in

the axial mesoderm (Fig. 6c) and are beginning to migrate toward the midline where they will coalesce to form the dorsal aorta and posterior cardinal vein. Co-localization of Cx43.4 and *fli1*:EGFP was not observed (Fig. 6c,e). These results suggest that Cx43.4 is unlikely to function endothelial cell-autonomously within the angioblasts during vasculogenesis.

Similarly, at 30 hpf when angiogenesis is progressing, Cx43.4 staining was not observed to co-localize with *fli1*:EGFP expression in the developing ISVs (Fig. 6 d,f). Specific puncta in the posterior-most notochord cells served as an internal positive control (Fig. 6b, bracket). Interestingly, a regular, repeating pattern of puncta was observed beneath the notochord along the length of the anterior-posterior axis (Fig. 6b, arrowheads). The nature of this staining and the identity of the labeled structures are yet to be determined. Taken together, the lack of vascular cell-specific Cx43.4 expression during vasculogenesis and angiogenesis are not consistent with a cell-autonomous role for Cx43.4 in the developing vasculature.

Cx43.4 and Cx44.2 knockdowns lead to altered midline signaling

Since significant expression of Cx43.4 was not detected in endothelial cells, we hypothesized that GJ communication in the notochord influences adjacent vascular development. Since sonic hedgehog (shh) signaling through VEGF is known to regulate both vasculogenesis and angiogenesis in zebrafish (Lawson et al., 2002) and other systems, we investigated this and related

signaling genes in Cx morphant embryos. The knockdown of Cx43.4 (and Cx44.2 to a lesser extent) resulted in an apparent upregulation of *shh* in the notochord of morphant embryos (data not shown) compared to wildtype expression levels (Fig. 7a). Embryos in which both Cx43.4 and Cx44.2 had been knocked down showed the most intense *shh* staining (Fig. 7b). Additionally, the notochord, *shh*-positive domain in these embryos was undulated. The receptor for Shh, Patched1 (Ptc1), is positively regulated by Shh in the adjacent somites and serves as a readout for Shh-signaling. Interestingly, the *in situ* signal of *ptc* was also more intense in Cx43.4 morphant embryos (data not shown), suggesting that the increase in *shh* could be functionally relevant.

We theorized that if Shh signaling were elevated, then the downstream effector molecule, VEGF, might also be increased, which could explain the observed angiogenesis defects. In Cx morphant embryos, however, no difference in *vegf* expression was seen compared to controls at the 12- (Fig. 7c-e) or 18-somite stages (data not shown). Additionally, the expression of two other signaling molecules, the arterial marker, *ephB2* (data not shown), and the venous marker, *flt4* (Fig. 7f-h), that are indicative of arteriovenous specification downstream of Shh signaling were not altered in Cx-knockdown embryos. These results suggest that the Shh-signaling cascade is intact and that cells are competent to send and receive vascular-specific signals appropriately in the absence of Cx43.4 and/or Cx44.2.

Netrin signaling is upregulated in Cx43.4 morphants

Given that functional analysis of the vasculature by visualization of blood cell movement in Tg*(gata1:dsRed)* embryos showed lumen formation in the major axial vessels that develop during vasculogenesis, and signaling molecules downstream of Shh did not appear to be altered when analyzed by *in situ* hybridization, we next asked whether defects in angiogenesis signals could account for the circulation defects. It is possible that appropriate regulation of Netrin expression is required for development of the major vessels and could also influence angiogenesis since both processes involve extensive cell migration. Since previous reports have implicated Netrin signaling downstream of the Shh signaling pathway (Strahle et al., 1997; Lauderdale et al., 1998) and *shh* expression appeared to be altered in Cx-deficient embryos, we hypothesized that Cx43.4 is required for the regulation of *netrin* expression.

The expression of *netrin1b (net1b)* was analyzed by *in situ* hybridization and an increased signal was observed in the floorplate of Cx-deficient embryos compared with controls (Fig. 8 a-d). The morphology of the floorplate was also altered in Cx43.4/Cx44.2 co-injected morphant embryos. These results suggest that Cx function is required to appropriately regulate Netrin signaling during angiogenesis.

To test whether *net1b* upregulation in Cx-deficient embryos was specific to MO knockdown and not an off-target effect of injection, a rescue experiment

was performed. As seen previously, knock down of Cx43.4 resulted in an increase in *net1b*-specific staining in the floorplate compared with controls (Fig. 9a,b). When Cx43.4 MOs and a Cx43.4 DNA construct were co-injected, the elevated *net1b* levels were partially rescued back to wildtype levels (Fig. 9c). In these rescue experiments, an average of only 30% of Cx43.4 morphant embryos had wildtype levels of *net1b* expression, while 56% of rescued embryos appeared to have normal *net1b* (Fig. 9d). These results suggest that Cx43.4 is specifically required for the regulation of *net1b* expression and implicate a connexin protein in a novel signaling pathway for vascular development.

Cx-deficient embryos have quantitative differences in gene expression levels

Given the apparent upregulation of *shh* and *net1b* expression in Cx morphants observed by *in situ* hybridization methods, a more quantitative approach was necessary to determine whether the increase in this signaling cascade was significant. Real-time quantitative PCR (RT-qPCR) methods were utilized and no significant differences in the levels of *shh* mRNA in Cx43.4 or Cx43 knockdown embryos were observed when compared to controls (Fig. 10). Additionally, *vegf* expression was not significantly altered in Cx43.4 morphants, which is consistent with the observed staining by *in situ* hybridization. Together, the lack of alteration in *shh* or *vegf* expression levels suggests that

disruptions in the canonical vascular signaling cascade are not responsible for the angiogenesis defects in Cx-deficient embryos.

RT-PCR methods were also utilized to evaluate the expression levels of *net1b* and *net1a* (closely related to *net1b)* given the more intense *in situ* hybridization signal in Cx-deficient embryos (Figs. 8,9). In these experiments, both *net1a* and *net1b* mRNA was increased nearly two-fold in Cx43.4 morphants compared to uninjected control embryos ($p<0.003$ and $p<0.001$, respectively). Cx43 knockdown resulted in no significant differences in the expression levels of *shh*, *vegf*, *net1a*, or *net1b*. These results show that the Netrin signaling cascade is regulated by Cx43.4 but not by Cx43. Moreover, these RT-PCR data suggest that the unique notochord expression of Cx43.4 has very different effects on vascular patterning and gene expression regulation compared with Cx43.

DISCUSSION

Connexins in vascular development

GJ communication is known to be important for cardiac function by facilitating the transfer of electrical signals that synchronize the beating of the heart (Wei et al., 2004). Because of this critical role in the adult heart, it was postulated that Cx function might also be important during embryonic cardiovascular function and/or development. Indeed, Cx45 knockout mice have defects in both heart formation and angiogenesis.

Here, we sought to understand whether Cx knockdown had an effect on the signaling systems that regulate vasculogenesis, angiogenesis, or the specification of endothelial cells into arterial or venous cells. We found that Cx knockdown impaired circulation and produced defects in angiogenesis. Specifically, Cx-deficient embryos failed to undergo the secondary angiogenic sprouting event, formation of the PAV. This angiogenesis defect was associated with a quantitative increase in *netrin* expression levels, suggesting that previously identified neural guidance cues are also important for vascular development and are regulated by Cxs.

Is increased netrin signaling consistent with vascular defects in Cx morphants?

Previous reports in the literature have implicated Netrin signaling in angiogenesis (Freitas et al., 2008). However, these studies have not served to

clarify the exact mechanism of Netrin function during angiogenesis: competing studies have suggested that the signals have attractive and repressive effects on migrating endothelial cells (Lu et al., 2004; Wilson et al., 2006). While Lu et al. reported defects in the migratory paths of ISVs in the absence of the ligand netrin1a or its receptor, Unc5b, Wilson et al. focused their analyses later in development and found that the ISVs had resolved their migration. However, Wilson et al. showed that the PAV failed to develop in netrin1a morphant embryos, a phenotype that is similar to the angiogenesis defects reported here in Cx-deficient embryos.

In contrast to these previous reports showing the effects of netrin depletion, the Cx knockdown studies presented here show defects in angiogenesis that are associated with an increase in netrin expression. This prompts the questions: Could over-expression of netrin signaling yield the same phenotype as reduced netrin expression?

Netrin molecules are known to function as chemoattractants for angiogenesis events at low levels, while inhibiting migration at higher concentrations (Yang et al., 2007). The application of purified netrin proteins to cultured endothelial cells has been shown to inhibit migration and tube formation (Nacht et al., 2009). These results suggest that a precisely regulated level of netrin signaling is required for appropriate cell migration during angiogenesis.

The regulation of netrin signaling is also tightly controlled during axon guidance, where netrins were first studied. Once neurons reach their target migration point, the signaling pathway is desensitized so that migration halts. The molecular mechanism of this halt in signaling is thought to be mediated by a self-inhibitory system, whereby Netrin protein induces the ubiquitination of its receptor, DCC, which targets it for degradation by the proteasome (Kim et al., 2005). In Cx-deficient embryos, overexpression of net1b could result in premature degradation of DCC prior to the complete migration of the developing PAV.

Because of the effects on angiogenesis and vascular remodeling, Netrin signaling has been recognized for its potential as a degenerative disease therapeutic or an anti-cancer target. It is possible that netrins, in appropriately regulated amounts, could promote neovascularization in order to facilitate the regeneration of diseased tissues (Wilson et al., 2006). Alternatively, since netrin signaling has also been shown to inhibit vascular tube formation and tumor cell growth in culture through a phosphorylation mechanism (Nacht et al., 2009), an anti-cancer therapeutic agent could be rationally designed.

Is the notochord-specific expression of Cx proteins involved in netrin signaling and angiogenesis?

Since Cx43.4 and Cx43 have effects on vascular development through a non-endothelial cell autonomous mechanism, we hypothesized that the

expression of these two Cxs in the notochord is required to regulate vascular-specific signaling cascades. In zebrafish, Shh signaling from the notochord is known to activate VEGF in the adjacent somites and stimulate a vascular signaling cascade to promote the migration of angioblasts and the differentiation of endothelial cells (Lawson et al., 2002). In Cx-deficient embryos, an apparent upregulation in *shh* expression in the notochord was observed by *in situ* hybridization. However, this upregulation was not verified by RT-PCR. It is possible that the increase in *shh* probe reactivity visualized by *in situ* hybridization is reflective of a shortened and widened midline. In this case, an alteration in spatial Shh protein due to defects in the structure of the midline could aberrantly upregulate netrin signaling.

Significance and future directions

These experiments have provided additional support for a requirement of Cx proteins during vascular development. In contrast to previously published work on the roles of mammalian Cx45, the data presented here provide insight into the early establishment of the vasculature. Importantly, these data are the first to associate Cx function with the newly identified role for netrins in angiogenesis.

Although a non-endothelial cell autonomous role was described here for Cx43.4, it remains unclear whether the notochord-specific expression of Cx43.4 and/or Cx43 is required for vascular development. To test directly whether GJ

communication in the notochord is necessary for vascular patterning, pseudogenetic mosaic zebrafish embryos could be analyzed. In these experiments, donor embryos would be co-injected with Biotin-dextran to mark the cells and Cx-specific MOs to knockdown the Cx in those cells only. Blastomeres from the labeled donor embryo would then be transplanted into an unlabeled, wildtype Tg(*fli1*:EGFP) host. After transplantation, those embryos with significant dextran-labeled notochord cells would be analyzed for defects in angiogenesis using fluorescence microscopy. It should be possible to ask whether angiogenesis is normal or not in regions running along the notochord where a high proportion of donor, Cx-deficient cells are located. In addition, RT-PCR experiments could be used to detect any changes in the expression levels of vascular-specific genes. These experiments could provide valuable insights into the role of connexins in angiogenesis.

MATERIALS AND METHODS

Zebrafish stocks and embryo culture

WT *Danio rerio* strains were obtained from Segrest Farms. Tg*(fli1:EGFP)* and Tg*(gata1:dsRed)* strains were obtained from the colonies of Dr. Steve Ekker. All animals were housed according to established methods at 28.5°C. Embryos were collected from natural matings, cultured in fish water and staged according to morphological markers (Kimmel et al., 1995) prior to analyses or fixation.

Morpholino injections

The following morpholino antisense oligonucleotides targeting cx43.4, cx44.2, and cx43 were purchased from Gene-Tools (Corvallis, OR):

Cx43 #2 MO: 5'-AGGGAGTTCTAGCTGGAAAGAAGTA-3'

Cx43.4 #1 MO: 5'-CCGCGTAAGAAAACTCCAGCTCATG-3'

Cx43.4 #2 MO: 5'-TCAAGAAGTACCACCGTCTCAGTCC-3'

Cx43.4 mismatch MO: 5'-TCAtGAAcTACCACCGTCaCAGaCC-3'

Cx44.2 MO: 5'-AACGTGTCAAGAAGCTCCAACTCAT-3'

Zebrafish embryos were microinjected between the one- and four-cell stages with various MO doses as described (Nasevicius and Ekker, 2000).

Phenotypic analyses of transgenic embryos

Dechorionated *fli1*:EGFP/*gata1*:dsRed double-transgenic embryos were anesthetized at 30 hpf and 50 hpf for analysis of vasculature morphology and circulation using epifluorescence. Vasculature was documented using a Zeiss Apotome "grid-confocal" microscope and circulation was recorded with a Sony Handicam using Apple iMovie software. Gross morphology and heart function were scored using a Zeiss dissecting microscope.

Gene expression studies

Whole-mount *in situ* hybridization studies used antisense digoxigenin-labeled RNA probes and were conducted according to published methods (Essner et al., 1996). Embryos were permeabilized with Proteinase K and hybridization proceeded at 65°C. Upon detection of probe reactivity, embryos were placed in PBST to quench the reaction, and images were collected on a Zeiss dissecting microscope using a Nikon digital camera. The analysis of *cx44.2* expression used a probe that was complimentary to the full length coding sequence of *cx44.2*. Other probes included those for sonic hedgehog (*shh*), patched (*ptc*), vascular epithelial growth factor (*vegf*), ephrin (*ephB2*), fms-related tyrosine kinase 4 (*flt4*), ve-cadherin (*cadh5*) (Larson et al., 2004.), netrin1a (*net1a*) and netrin1b *(net1b)***.**

Whole-mount immunofluorescence was conducted as previously described (Essner et al., 1996). Briefly, embryos were fixed using 4% paraformaldehyde and were dehydrated in EtOH. Following rehydration

through a methanol series, embryos were incubated in blocking solution (5% goat serum, 2% BSA, 1% DMSO in PBS + 0.1% Tween 20) for 2 hours at room temperature. Primary antibodies (rabbit polyclonal Cx43.4 antibodies raised to amino acid residues 338-350 (Desplantez et al., 2003) or rabbit Cx43 (gift from Kathy Iovine, Lehigh University) were added to the blocking solution and embryos were incubated overnight at 4°C. Embryos were washed in 1% BSA, 1% DMSO in PBST and Alexa Fluor 568 goat anti-rabbit (Molecular Probes A-11011, Eugene, OR) secondary antibodies at 1:500 were added to blocking solution and incubated overnight at 4°C. Following PBST washes, embryos were mounted in Prolong Antifade (Molecular Probes) and images were collected using a Zeiss "grid-confocal" microscope.

Rescue

The Cx43.4 coding sequence was cloned using the following 5' primer 5'-ATGAGtTGGAGcTTcCTaACGCGGTTGTTG-3'. This fragment was generated with silent mutations (shown in lower case letters) to prevent recognition by start codon-targeting MOs and cloned into the vector, pFRM2.1. pFRM2.1 contains a carp β–actin promoter, which drives expression of Cx43.4 when injected into zebrafish embryos at the one-cell stage. 20 pg or 60 pg of rescuing DNA per embryo were used in these experiments.

Quantitative real-time PCR

Total RNA was isolated from zebrafish embryos at the 10-somite stage or 30 hpf using TRIzol reagent (Invitrogen). 500ng of RNA was reverse transcribed using SuperScript II (Invitrogen) and OligodT primers. 3 ng of template from the reverse transcription reaction was amplified with SYBR green reagent (BioRad) and the following gene specific primers:

shh: 5'-acaatcccgacattatctttaagga-3' and 5'-tgtctttgcatctctgtgtcatga-3'

vegf: 5'-tccaggagtatcccgatgag-3' and 5'-gctttgacttctgcctttgg-3'

net1a: 5'-caggtaagctggtgggtgat-3' and 5'-cagagtttgcccatgtgttg-3'

net1b: 5'-cctgccttgtctcctttcag-3' and 5'-gggaccagagtgtgacaggt-3'

s6K: 5'-ggcacagtgacccacacttt-3' and 5'-aggtccctggcttcttgtgt-3'

The relative level of gene expression was quantified by the comparative cycle threshold (Ct) method for quantification following normalization to S6K. All experiments were performed with at least three different RNA preparations and Ct reactions were conducted in triplicate for each sample.

FIGURES

Figure 1: Multiple connexin isoforms are expressed in the notochord

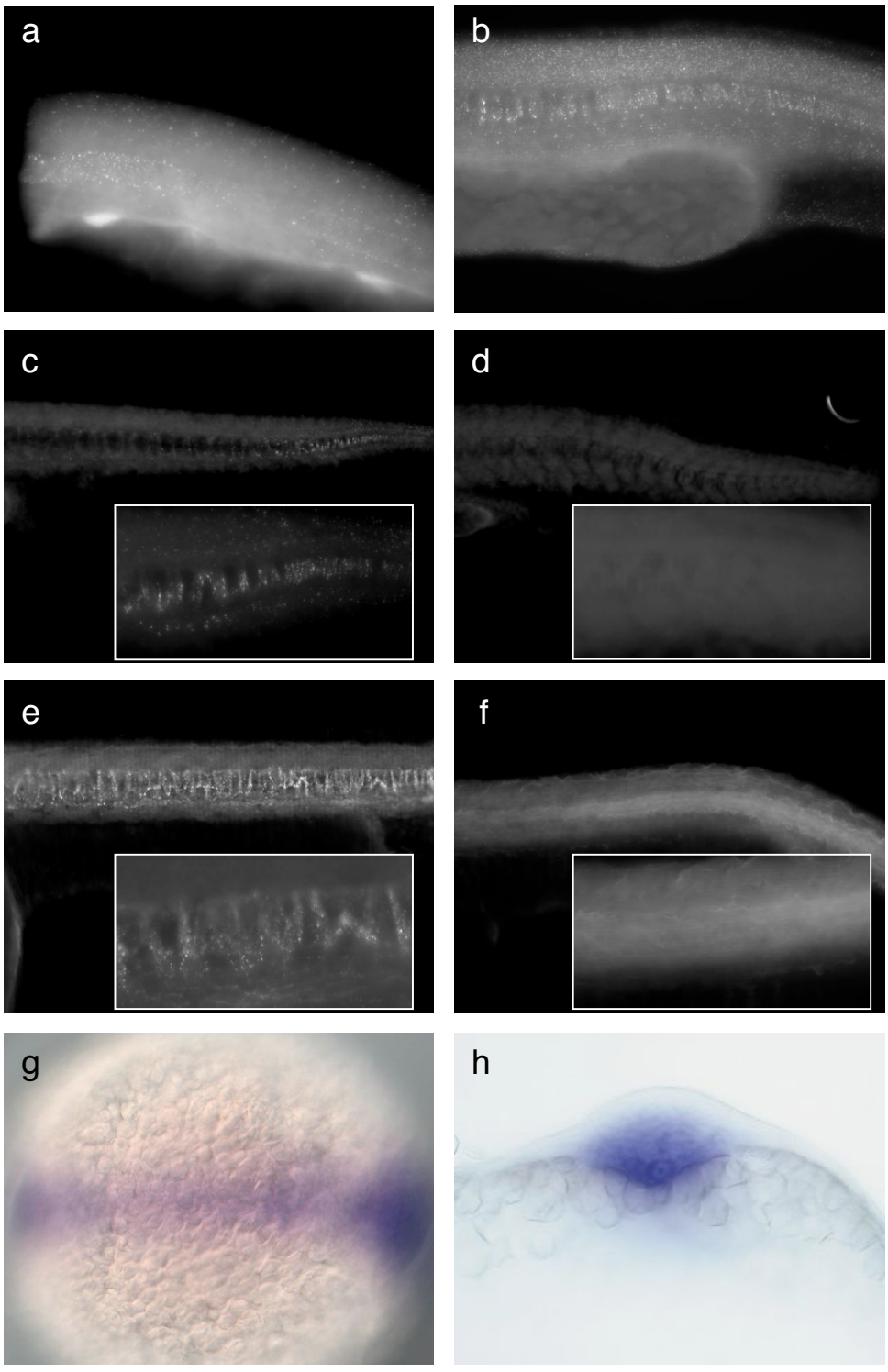

Figure 1: Multiple connexin isoforms are expressed in the notochord

Lateral views of embryos with anterior to the left and dorsal up were processed for whole-mount immunofluorescence (a-f). Cx43.4 labeling (a-d) in a 10-somite stage embryo (a) shows puncta throughout the midline and lateral tissue. At 20 somites (b), Cx43.4 labeling is seen throughout the length of the notochord, anterior to the yolk extension. Cx43.4 puncta are restricted to the posterior notochord cells at 24 hpf (c). The localization of Cx43.4 at 24 hpf is abolished by MOs (d). Cx43-specific labeling is seen throughout the notochord of a control embryo (e) at 24 hpf. Punctate staining in notochord cells (and elsewhere) is abolished after injections of Cx43 MOs (f). Insets (c-f) are higher magnifications. *cx44.2* transcripts, visualized by *in situ* hybridization methods, are localized to the midline at 10 somites (g). A cross section (h) shows *cx44.2* expression in the notochord.

Figure 2: Cx-deficient embryos have abnormal circulation

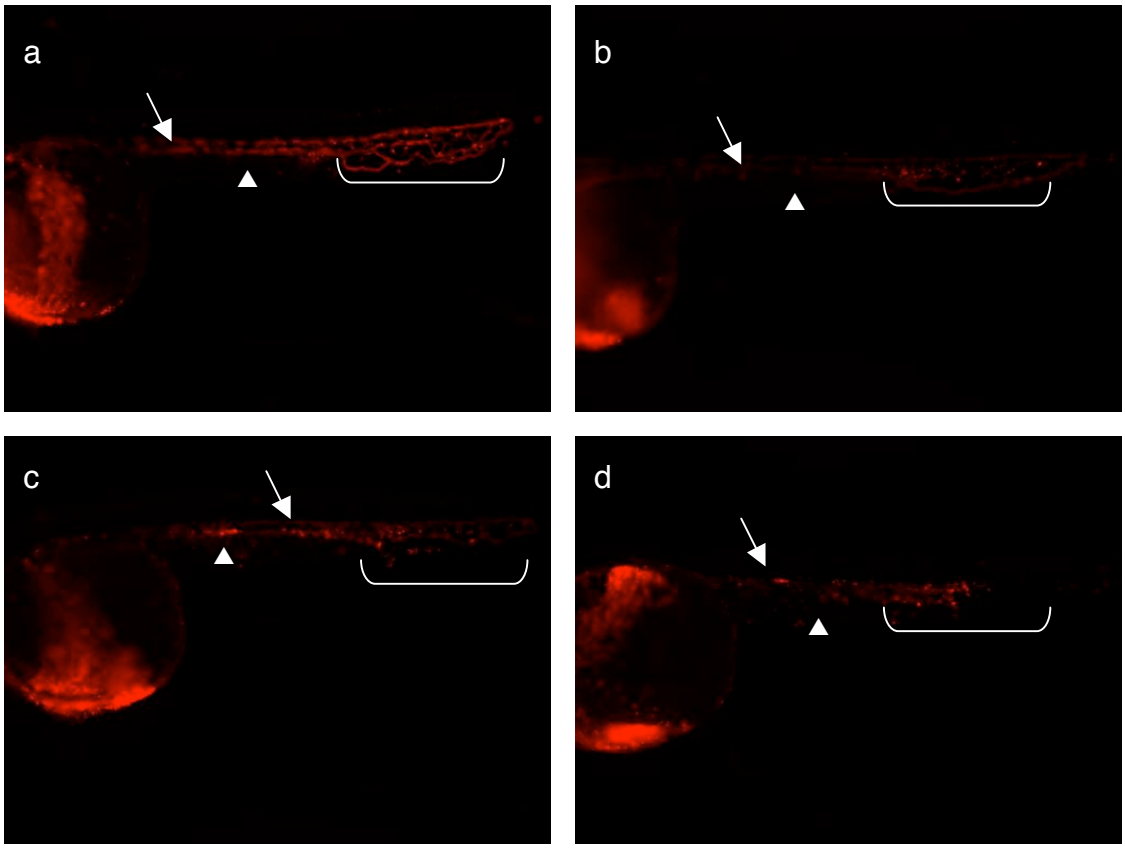

Figure 2: Cx-deficient embryos have abnormal circulation

Lateral views of *Tg(gata1:*dsRed*)* embryos at 30 hpf, anterior is to the left. The circulation of a 30 hpf uninjected control embryo (a) is continuous through the DA (arrow) and the PCV (arrowhead). The vascular plexus (bracket) is branched and well-developed. Knock down of Cx43.4 (b) or Cx44.2 (c) affects circulation through the major vessels. Co-injection of Cx43.4 and Cx44.2 MOs (d) shows similar disruptions in circulation.

Figure 3: Cx43.4 morphants have slower heart rates at 48 hpf

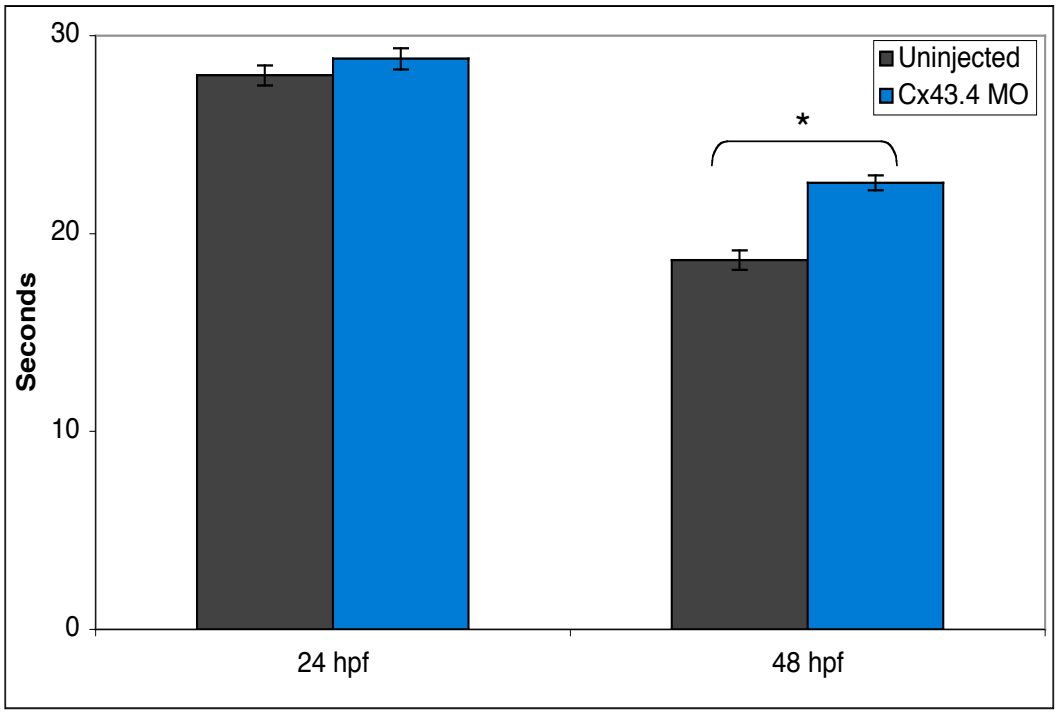

Figure 3: Cx43.4 morphants have slower heart rates at 48 hpf

The amount of time elapsed for the hearts of uninjected control and Cx43.4 knockdown embryos to beat 50 times was measured in two independent experiments. Data are representative and are calculated from embryos within one injection experiment. Data are plotted as averages +/- s.e.m, *$p<1.7 \times 10^{-7}$.

Figure 4: Cx43.4- and Cx44.2-deficient embryos have defects in angiogenesis

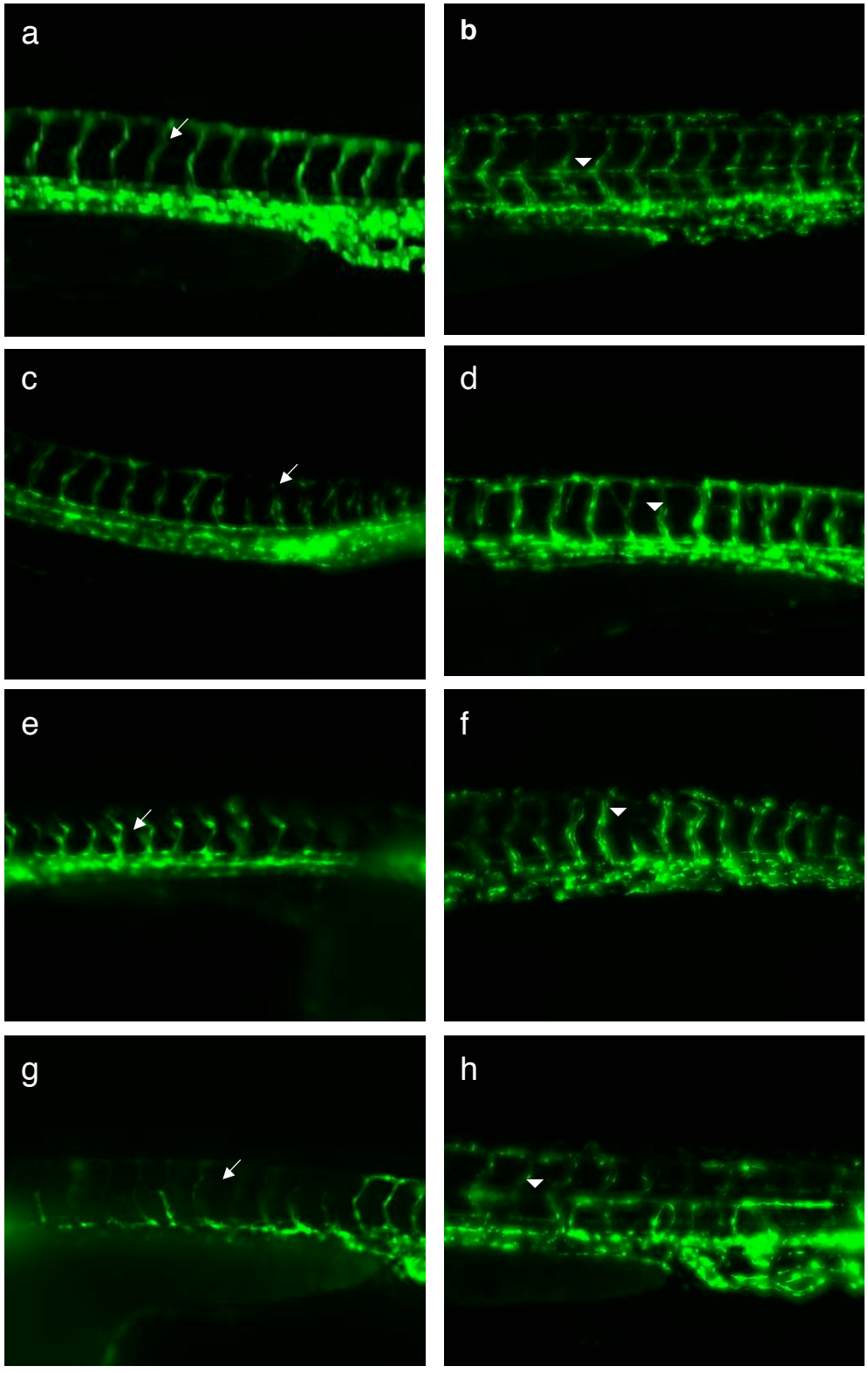

Figure 4: Cx43.4- and Cx44.2-deficient embryos have defects in angiogenesis

Lateral views of *Tg(fli1:egfp)* embryos at 30 hpf (a,c,e,g) and at 50 hpf (b,d,f,h), anterior is to the left. The vasculature of a 30 hpf uninjected control embryo (a) is stereotypically organized and the ISVs (arrow) are well-developed and continuous with the major vessels. Knock down of Cx43.4 (c) or Cx44.2 (e) affects migration of the ISVs (arrows). Co-injection of Cx43.4 and Cx44.2 MOs (g) shows similar disruptions in ISV development. At 50 hpf, uninjected control embryos (b) show a well-developed PAV (arrowhead). Cx43.4 (d) and Cx44.2 (f) morphants show some resolution of ISV migration, however, the PAV is discontinuous (arrowhead). Cx43.4/Cx44.2 double-knockdown embryos (h) have a disorganized vasculature with mis-patterning of the PAV (arrowhead) and ISVs.

Figure 5: *cadh5* expression is reduced in the PCV of Cx morphant embryos

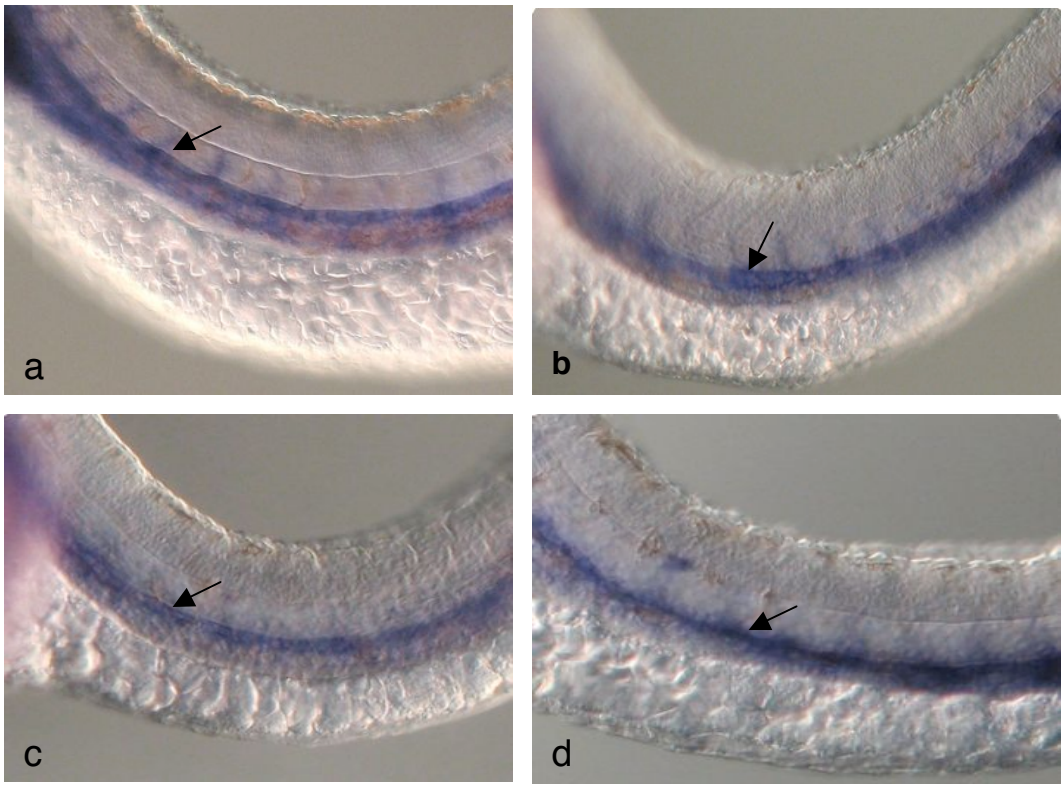

Figure 5: *cadh5* expression is reduced in the PCV of Cx morphant embryos

Lateral views (anterior to the left) of 30 hpf embryos processed for whole-mount *in situ* hybridization (a-d). An uninjected control embryo (a) has *cadh5* expression in the dorsal aorta (arrow) and posterior cardinal vein (arrowhead). Cx43.4 (b), Cx44.2 (c), and Cx43.4/Cx44.2 (d) morphant embryos have *cadh5* expression in the dorsal aorta, but lack expression in the vein.

Figure 6: Cx43.4 is not expressed in the developing vasculature of *Tg(fli:egfp)* embryos

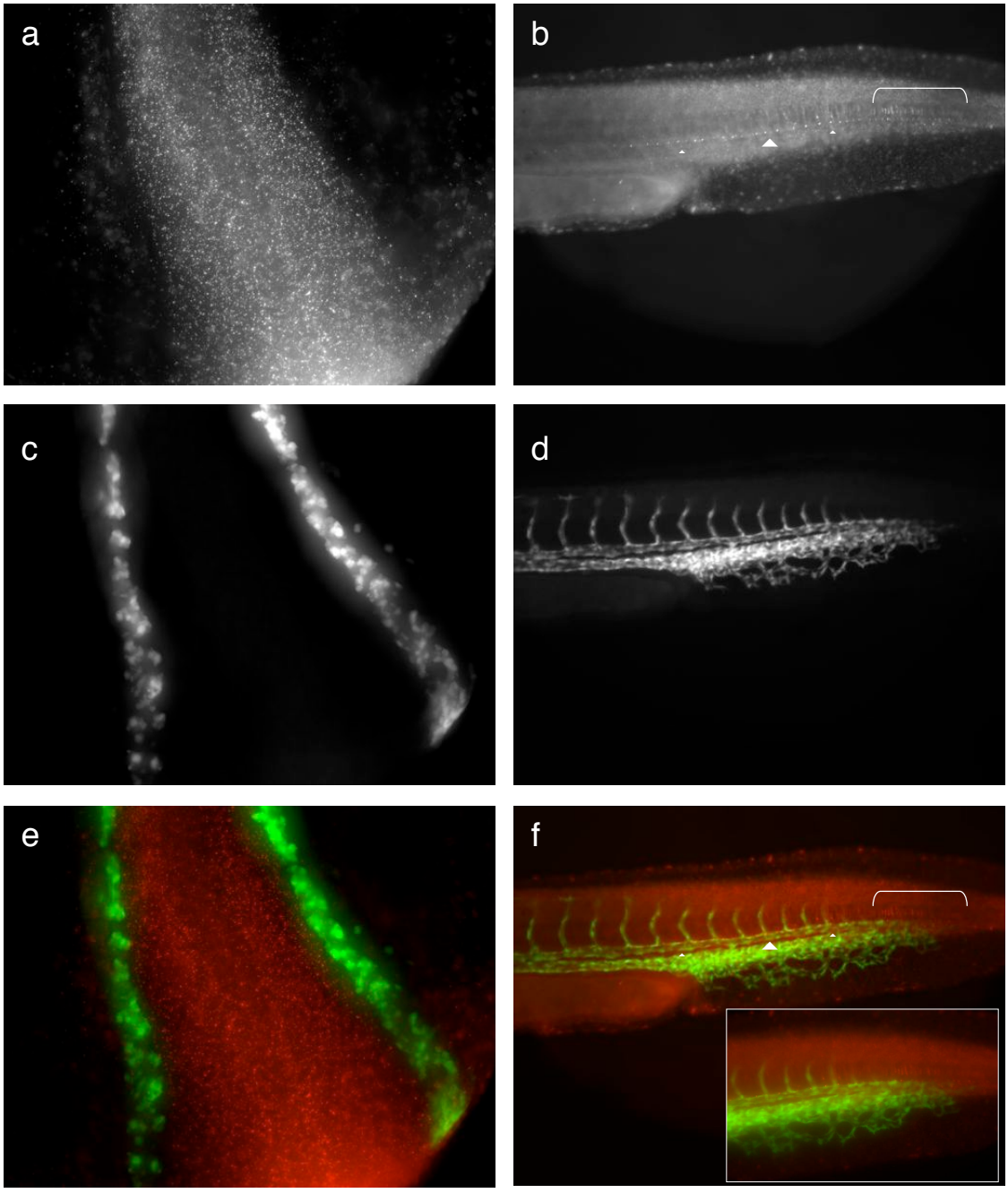

Figure 6: Cx43.4 is not expressed in the developing vasculature of *Tg(fli:egfp)* embryos

Co-localization of Cx43.4 and endothelial cells was analyzed during vasculogenesis at 18 somites (a,c,e) and angiogenesis at 30 hpf (b,d,f). Dorsal view (anterior up) of Cx43.4 labeling (a) seen throughout the axial mesoderm. *fli1*-expressing angioblasts (b), marked by EGFP, are positioned lateral to the notochord. (e) Merged image of (a) and (c). Lateral view (anterior to the left) of Cx43.4 labeling in a 30 hpf embryo (b) shows Cx43.4-positive puncta in the posterior notochord cells (bracket) and a regular punctate pattern below the notochord (arrowheads). Endothelial cells (d) in the primary vasculature and developing ISVs are marked by EGFP. (f) Merged image of (b) and (d).

Figure 7: Vascular-specific *shh* signaling cascade in Cx-deficient embryos

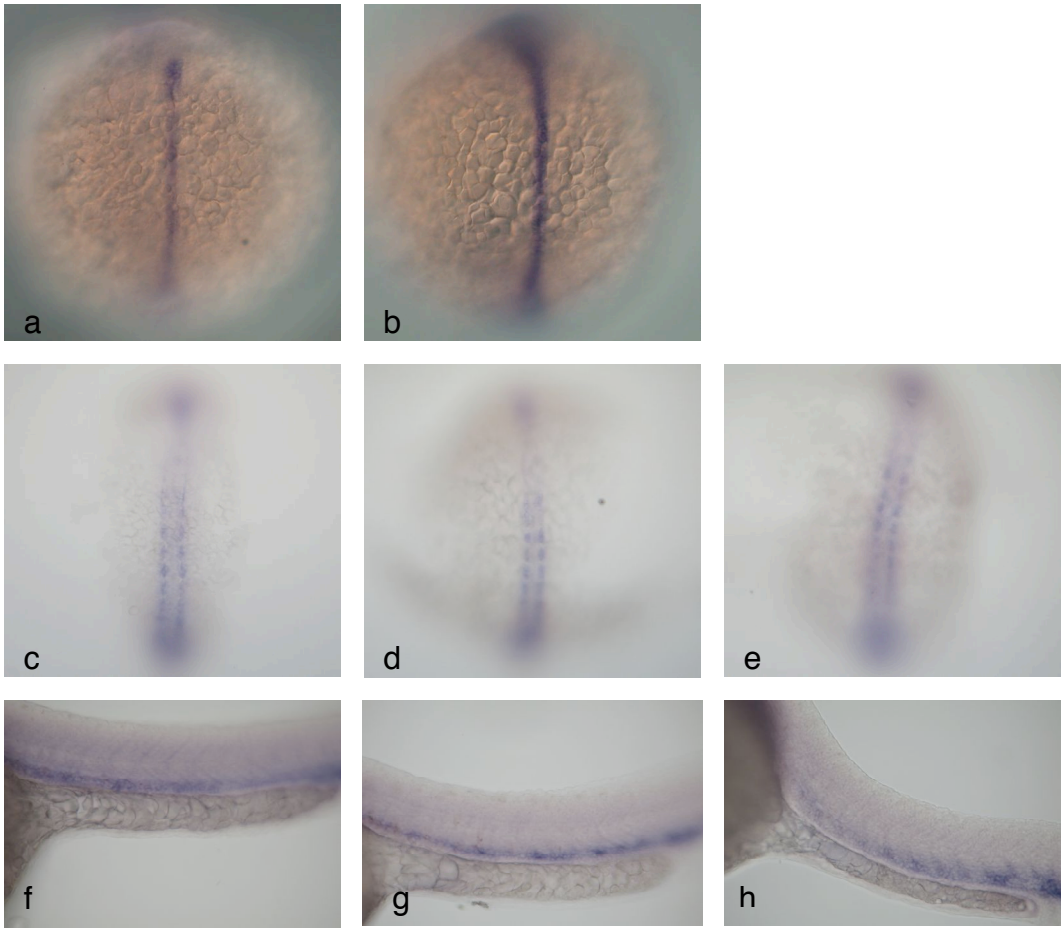

Figure 7: Vascular-specific *shh* signaling cascade in Cx-deficient embryos

Whole-mount *in situ* hybridization using probes for genes in the *shh* signaling cascade (a-h). A 10-somite stage, uninjected control embryo (a) has normal *shh* expression in the notochord. A representative Cx43.4/Cx44.2 double knockdown embryo (b) has a more intense *shh* signal in the notochord (compare with a). *vegf* expression in the somites of a control embryo (c) is comparable to a Cx44.2 (d) and a Cx43.4/Cx44.2 morphant embryo (e). *flt4* expression in the posterior cardinal vein of a control embryo at 30 hpf (f) is similar to a Cx43.4 (g) and a Cx43.4/Cx44.2 morphant embryo (h).

Figure 8: *net1b* expression is upregulated in Cx morphants

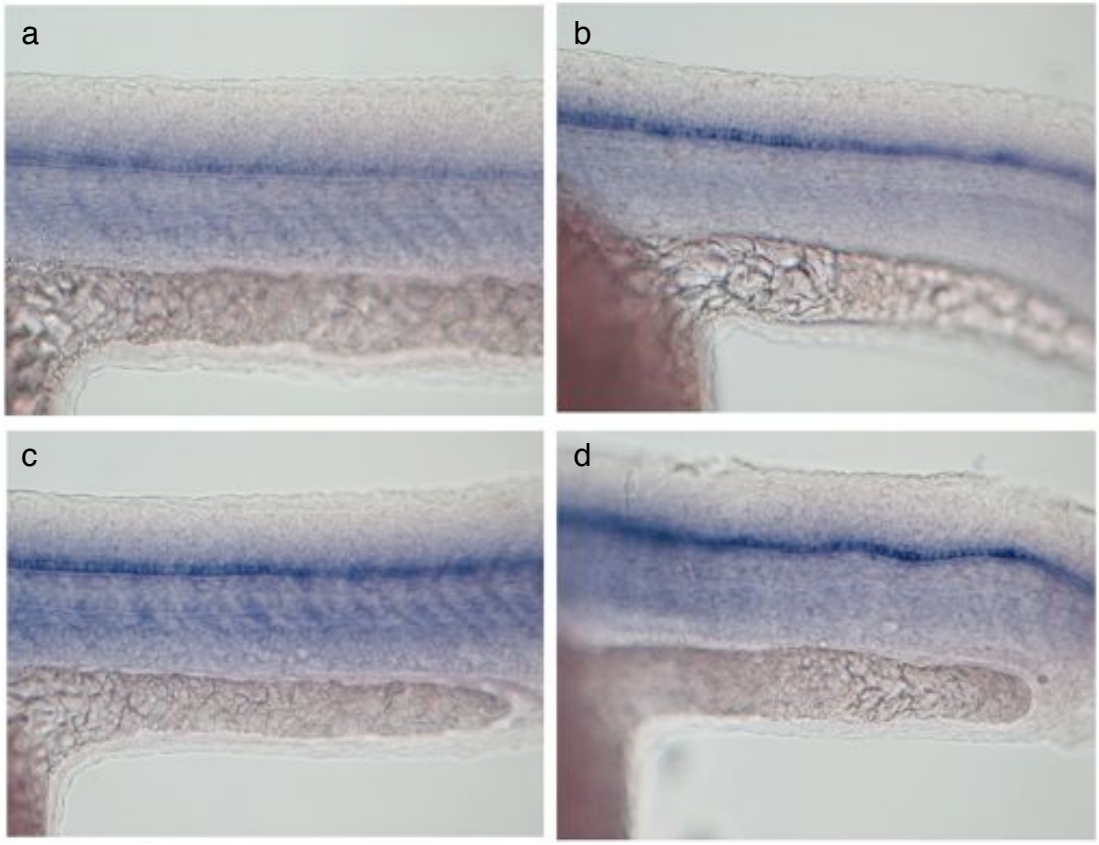

Figure 8: *net1b* expression is upregulated in Cx morphants

30 hpf embryos were processed for whole-mount *in situ* hybridization (a-d), lateral views with anterior to the left. *net1b* labeling in the floorplate cells of an uninjected control embryo (a). *net1b* staining is darker in representative Cx43.4 (b), Cx44.2 (c), and Cx43.4/Cx44.2 (d) morphant embryos.

Figure 9: Increased *net1b* staining is partially rescued by Cx43.4 DNA

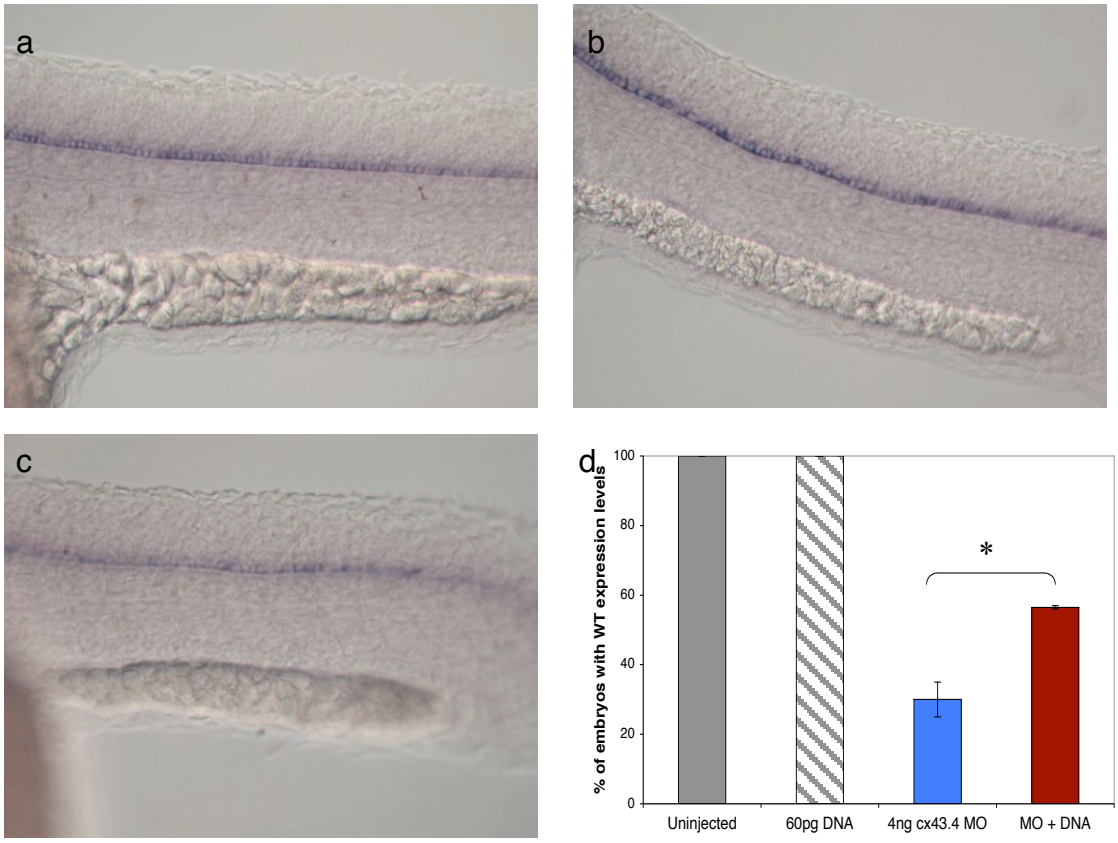

Figure 9: Increased *net1b* staining is partially rescued by Cx43.4 DNA

30 hpf embryos were processed for whole-mount *in situ* hybridization (a-c), lateral views with anterior to the left. *net1b* labeling in the floorplate cells of an uninjected control embryo (a). *net1b* staining is darker in a representative Cx43.4 morphant embryo (b). Co-injection of Cx43.4 MOs and rescuing Cx43.4 DNA (c) shows *net1b* staining that is similar to wildtype (compare with a). Multiple rescue experiments were scored for the percentage of embryos with *net1b* staining similar to wildtype levels. (d) Data are represented as averages from two independent experiments +/- s.e.m., *$p<0.03$.

Figure 10: Quantitative PCR reveals differences in gene expression in Cx43.4 morphants

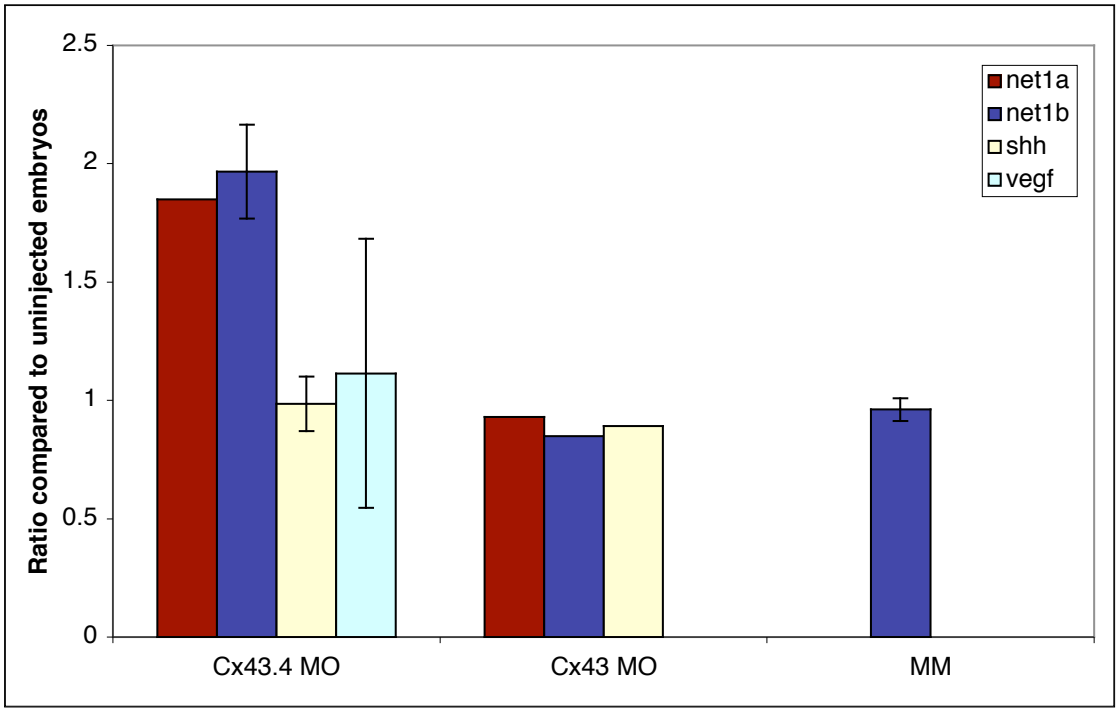

Figure 10: Quantitative PCR reveals differences in gene expression in Cx43.4 morphants

RNA was extracted from 30 hpf embryos and analyzed by RT-qPCR. Data are represented as ratios compared to uninjected control embryos after normalizing to the levels of a standardized gene, S6K. Mismatched (MM) control MOs show no difference compared to control levels. Data are plotted as averages of independent experiments, +/- s.e.m.

Table 1: Circulation defects in Cx43.4-deficient embryos at 30 hpf

	Cx43.4 Morpholino dose (ng)			
	Uninjected	2	4	8
Slow blood flow	0	20	0	0
Non-existent	0	0	0	85.7
Trunk or vasc. bed: reduced/absent	0	20	60	85.7
Heart and/or head only	0	0	20	14.3
Blood pooling	0	0	40	71
Overall abnormalities	**0 (3)**	**40 (5)**	**80 (5)**	**100 (7)**
ISV: migration/absent	0	60	80	
PCV: reduced/absent	0 (8)	20 (10)	10 (10)	

Table 2: Circulation defects in Cx43.4-deficient embryos at 50 hpf

	Cx43.4 Morpholino dose (ng)			
	Uninjected	2	4	8
Slow blood flow	0	0	0	14.3
Non-existent	0	0	0	14.3
Trunk or vasc. bed: reduced/absent	0	66.7	55	85
Heart and/or head only	0	0	0	0
Blood pooling	0	44	33.3	100
Overall abnormalities	**0 (8)**	**66.7 (9)**	**77.8 (9)**	**100 (7)**
ISV: migration/absent	0 (10)	46 (11)	90 (11)	100 (11)

Table 3: Circulation defects in Cx44.2-deficient embryos at 30 hpf

	Cx44.2 Morpholino dose (ng)			
	Uninjected	2	4	8
Slow blood flow	0	0	0	17
Non-existent	0	0	8	0
Trunk or vasc. bed: reduced/absent	0	23	70	33
Heart and/or head only	0	0	0	0
Blood pooling	0	23	70	100
Overall abnormalities	**0 (9)**	**23 (13)**	**77 (13)**	**100 (6)**
ISV: migration/absent	0 (9)	33 (15)	40 (15)	71 (7)

Table 4: Circulation defects in Cx44.2-deficient embryos at 50 hpf

	Cx44.2 Morpholino dose (ng)			
	Uninjected	2	4	8
Slow blood flow	0	0	7	0
Non-existent	0	0	0	0
Trunk or vasc. bed: reduced/absent	0	21	28	50
Heart and/or head only	0	0	0	0
Blood pooling	0	7	7	38
Overall abnormalities	**0 (8)**	**21 (14)**	**21 (14)**	**50 (8)**
ISV: migration/absent	0 (9)	13 (15)	13 (16)	88 (8)

Table 5: **Co-injection of Cx43.4 and Cx44.2 MOs affect the circulation at 30 hpf**

	Total Cx Morpholino dose (ng)			
	Uninjected	2	4	8
Slow blood flow	0	0	40	0
Non-existent	0	0	0	10
Trunk or vasc. bed: reduced/absent	0	25	30	30
Heart and/or head only	0	0	0	0
Overall abnormalities	**0 (10)**	**50 (8)**	**90 (10)**	**90 (10)**
ISV: migration/absent	0 (10)	46 (11)	90 (11)	100 (11)

Table 6: Co-injection of Cx43.4 and Cx44.2 MOs affect the circulation at 50 hpf

	Uninjected	2	4	8
Slow blood flow	0	0	36	9
Non-existent	0	0	0	9
Trunk or vasc. bed: reduced/absent	0	66.7	54	81
Heart and/or head only	0	0	0	0
Blood pooling	0	40	27.3	45
Overall abnormalities	**0 (9)**	**40 (5)**	**64 (11)**	**64 (11)**
ISV: migration/absent	11 (10)	71 (7)	63 (8)	100 (12)
	Total Cx Morpholino dose (ng)			

Appendix I

Reprint Permissions

ELSEVIER LICENSE
TERMS AND CONDITIONS

Apr 20, 2009

This is a License Agreement between Julia M Hatler ("You") and Elsevier ("Elsevier") provided by Copyright Clearance Center ("CCC"). The license consists of your order details, the terms and conditions provided by Elsevier, and the payment terms and conditions.

All payments must be made in full to CCC. For payment instructions, please see information listed at the bottom of this form.

Supplier	Elsevier Limited The Boulevard,Langford Lane Kidlington,Oxford,OX5 1GB,UK
Registered Company Number	1982084
Customer name	Julia M Hatler
Customer address	4536 42nd Ave S Minneapolis, MN 55406
License Number	2173190339757
License date	Apr 20, 2009
Licensed content publisher	Elsevier
Licensed content publication	Cell
Licensed content title	Nodal Flow and the Generation of Left-Right Asymmetry
Licensed content author	Nobutaka Hirokawa, Yosuke Tanaka, Yasushi Okada and Sen Takeda
Licensed content date	7 April 2006
Volume number	125
Issue number	1
Pages	13
Type of Use	Thesis / Dissertation
Portion	Figures/table/illustration /abstracts
Portion Quantity	1
Format	Both print and electronic

BIBLIOGRAPHY

ADAMS, D. S., ROBINSON, K. R., FUKUMOTO, T., YUAN, S., ALBERTSON, R. C., YELICK, P., KUO, L., MCSWEENEY, M. & LEVIN, M. (2006). Early, H+-V-ATPase-dependent proton flux is necessary for consistent left-right patterning of non-mammalian vertebrates. *Development* **133,** 1657-1671.

AI, Z., FISCHER, A., SPRAY, D. C., BROWN, A. M. & FISHMAN, G. I. (2000). Wnt-1 regulation of connexin43 in cardiac myocytes. *J Clin Invest* **105,** 161-171.

AMACK, J. D., WANG, X. & YOST, H. J. (2007). Two T-box genes play independent and cooperative roles to regulate morphogenesis of ciliated Kupffer's vesicle in zebrafish. *Dev Biol* **310,** 196-210.

AMACK, J. D. & YOST, H. J. (2004). The T box transcription factor no tail in ciliated cells controls zebrafish left-right asymmetry. *Curr Biol* **14,** 685-690.

AMORES, A., FORCE, A., YAN, Y. L., JOLY, L., AMEMIYA, C., FRITZ, A., HO, R. K., LANGELAND, J., PRINCE, V., WANG, Y. L., WESTERFIELD, M., EKKER, M. & POSTLETHWAIT, J. H. (1998). Zebrafish hox clusters and vertebrate genome evolution. *Science* **282,** 1711-1714.

BAO, X., CHEN, Y., REUSS, L. & ALTENBERG, G. A. (2004). Functional expression in Xenopus oocytes of gap-junctional hemichannels formed by a cysteine-less connexin 43. *J Biol Chem* **279,** 9689-9692.

BARRIO, L. C., CAPEL, J., JARILLO, J. A., CASTRO, C. & REVILLA, A. (1997). Species-specific voltage-gating properties of connexin-45 junctions expressed in Xenopus oocytes. *Biophys J* **73,** 757-769.

BASU, B. & BRUECKNER, M. (2008). Cilia multifunctional organelles at the center of vertebrate left-right asymmetry. *Curr Top Dev Biol* **85,** 151-174.

BEAHM, D. L., OSHIMA, A., GAIETTA, G. M., HAND, G. M., SMOCK, A. E., ZUCKER, S. N., TOLOUE, M. M., CHANDRASEKHAR, A., NICHOLSON, B. J. & SOSINSKY, G. E. (2006). Mutation of a conserved threonine in the third transmembrane helix of alpha- and beta-connexins creates a dominant-negative closed gap junction channel. *J Biol Chem* **281,** 7994-8009.

BISGROVE, B. W., ESSNER, J. J. & YOST, H. J. (1999). Regulation of midline development by antagonism of lefty and nodal signaling. *Development* **126,** 3253-3262.

BISGROVE, B. W., MORELLI, S. H. & YOST, H. J. (2003). Genetics of human laterality disorders: insights from vertebrate model systems. *Annu Rev Genomics Hum Genet* **4,** 1-32.

BOITANO, S., DIRKSEN, E. R. & SANDERSON, M. J. (1992). Intercellular propagation of calcium waves mediated by inositol trisphosphate. *Science* **258,** 292-295.

BRITZ-CUNNINGHAM, S. H., SHAH, M. M., ZUPPAN, C. W. & FLETCHER, W. H. (1995). Mutations of the Connexin43 gap-junction gene in patients with heart malformations and defects of laterality. *N Engl J Med* **332,** 1323-1329.

CARMELIET, P. & TESSIER-LAVIGNE, M. (2005). Common mechanisms of nerve and blood vessel wiring. *Nature* **436,** 193-200.

CARTWRIGHT, J. H., PIRO, O. & TUVAL, I. (2004). Fluid-dynamical basis of the embryonic development of left-right asymmetry in vertebrates. *Proc Natl Acad Sci U S A* **101,** 7234-7239.

CARUSO, R. L., UPHAM, B. L., HARRIS, C. & TROSKO, J. E. (2005). Biphasic lindane-induced oxidation of glutathione and inhibition of gap junctions in myometrial cells. *Toxicol Sci* **86,** 417-426.

CHATTERJEE, B., CHIN, A. J., VALDIMARSSON, G., FINIS, C., SONNTAG, J. M., CHOI, B. Y., TAO, L., BALASUBRAMANIAN, K., BELL, C., KRUFKA, A., KOZLOWSKI, D. J., JOHNSON, R. G. & LO, C. W. (2005). Developmental regulation and expression of the zebrafish connexin43 gene. *Dev Dyn* **233,** 890-906.

CHILDS, S., CHEN, J. N., GARRITY, D. M. & FISHMAN, M. C. (2002). Patterning of angiogenesis in the zebrafish embryo. *Development* **129,** 973-982.

CONDEELIS, J. & SEGALL, J. E. (2003). Intravital imaging of cell movement in tumours. *Nat Rev Cancer* **3,** 921-930.

COOPER, M. S. & D'AMICO, L. A. (1996). A cluster of noninvoluting endocytic cells at the margin of the zebrafish blastoderm marks the site of embryonic shield formation. *Dev Biol* **180,** 184-198.

COTRINA, M. L., LIN, J. H. & NEDERGAARD, M. (2008). Adhesive properties of connexin hemichannels. *Glia* **56,** 1791-1798.

CRUCIANI, V. & MIKALSEN, S. O. (2006). The vertebrate connexin family. *Cell Mol Life Sci* **63,** 1125-1140.

CRUCIANI, V. & MIKALSEN, S. O. (2007). Evolutionary selection pressure and family relationships among connexin genes. *Biol Chem* **388,** 253-264.

DANOS, M. C. & YOST, H. J. (1996). Role of notochord in specification of cardiac left-right orientation in zebrafish and Xenopus. *Dev Biol* **177,** 96-103.

DE VUYST, E., DECROCK, E., DE BOCK, M., YAMASAKI, H., NAUS, C. C., EVANS, W. H. & LEYBAERT, L. (2007). Connexin hemichannels and gap junction channels are differentially influenced by lipopolysaccharide and basic fibroblast growth factor. *Mol Biol Cell* **18,** 34-46.

DEBRUS, S., TUFFERY, S., MATSUOKA, R., GALAL, O., SARDA, P., SAUER, U., BOZIO, A., TANMAN, B., TOUTAIN, A., CLAUSTRES, M., LE PASLIER, D. & BOUVAGNET, P. (1997). Lack of evidence for connexin 43 gene mutations in human autosomal recessive lateralization defects. *J Mol Cell Cardiol* **29,** 1423-1431.

DESPLANTEZ, T., MARICS, I., JARRY-GUICHARD, T., VETEIKIS, R., BRIAND, J. P., WEINGART, R. & GROS, D. (2003). Characterization of zebrafish Cx43.4 connexin and its channels. *Exp Physiol* **88,** 681-690.

EASTMAN, S. D., CHEN, T. H., FALK, M. M., MENDELSON, T. C. & IOVINE, M. K. (2006). Phylogenetic analysis of three complete gap junction gene families reveals lineage-specific duplications and highly supported gene classes. *Genomics* **87,** 265-274.

EICHMANN, A., MAKINEN, T. & ALITALO, K. (2005). Neural guidance molecules regulate vascular remodeling and vessel navigation. *Genes Dev* **19,** 1013-1021.

ELIAS, L. A., WANG, D. D. & KRIEGSTEIN, A. R. (2007). Gap junction adhesion is necessary for radial migration in the neocortex. *Nature* **448,** 901-907.

ESSNER, J. J., AMACK, J. D., NYHOLM, M. K., HARRIS, E. B. & YOST, H. J. (2005). Kupffer's vesicle is a ciliated organ of asymmetry in the zebrafish embryo that initiates left-right development of the brain, heart and gut. *Development* **132,** 1247-1260.

ESSNER, J. J., LAING, J. G., BEYER, E. C., JOHNSON, R. G. & HACKETT, P. B., JR. (1996). Expression of zebrafish connexin43.4 in the notochord and tail bud of wild-type and mutant no tail embryos. *Dev Biol* **177,** 449-462.

ESSNER, J. J., VOGAN, K. J., WAGNER, M. K., TABIN, C. J., YOST, H. J. & BRUECKNER, M. (2002). Conserved function for embryonic nodal cilia. *Nature* **418,** 37-38.

FEISTEL, K. & BLUM, M. (2008). Gap junctions relay FGF8-mediated right-sided repression of Nodal in rabbit. *Dev Dyn* **237,** 3516-3527.

FERRARA, N., CARVER-MOORE, K., CHEN, H., DOWD, M., LU, L., O'SHEA, K. S., POWELL-BRAXTON, L., HILLAN, K. J. & MOORE, M. W. (1996). Heterozygous embryonic lethality induced by targeted inactivation of the VEGF gene. *Nature* **380,** 439-442.

FOUQUET, B., WEINSTEIN, B. M., SERLUCA, F. C. & FISHMAN, M. C. (1997). Vessel patterning in the embryo of the zebrafish: guidance by notochord. *Dev Biol* **183,** 37-48.

FOX, S. B., GENERALI, D. G. & HARRIS, A. L. (2007). Breast tumour angiogenesis. *Breast Cancer Res* **9,** 216.

FREITAS, C., LARRIVEE, B. & EICHMANN, A. (2008). Netrins and UNC5 receptors in angiogenesis. *Angiogenesis* **11,** 23-29.

GEBBIA, M., TOWBIN, J. A. & CASEY, B. (1996). Failure to detect connexin43 mutations in 38 cases of sporadic and familial heterotaxy. *Circulation* **94,** 1909-1912.

GIEPMANS, B. N. (2004). Gap junctions and connexin-interacting proteins. *Cardiovasc Res* **62,** 233-245.

GOODENOUGH, D. A. & PAUL, D. L. (2003). Beyond the gap: functions of unpaired connexon channels. *Nat Rev Mol Cell Biol* **4,** 285-294.

GRANDE, C. & PATEL, N. H. (2009). Nodal signalling is involved in left-right asymmetry in snails. *Nature* **457,** 1007-1011.

HIROKAWA, N., TANAKA, Y., OKADA, Y. & TAKEDA, S. (2006). Nodal flow and the generation of left-right asymmetry. *Cell* **125,** 33-45.

HUANG, G. Y., COOPER, E. S., WALDO, K., KIRBY, M. L., GILULA, N. B. & LO, C. W. (1998). Gap junction-mediated cell-cell communication modulates mouse neural crest migration. *J Cell Biol* **143,** 1725-1734.

ISOGAI, S., LAWSON, N. D., TORREALDAY, S., HORIGUCHI, M. & WEINSTEIN, B. M. (2003). Angiogenic network formation in the developing vertebrate trunk. *Development* **130,** 5281-5290.

JAHROUDI, N. & GREENBERGER, J. S. (1995). The role of endothelial cells in tumor invasion and metastasis. *J Neurooncol* **23,** 99-108.

KANG, J., KANG, N., LOVATT, D., TORRES, A., ZHAO, Z., LIN, J. & NEDERGAARD, M. (2008). Connexin 43 hemichannels are permeable to ATP. *J Neurosci* **28,** 4702-4711.

KANTER, H. L., SAFFITZ, J. E. & BEYER, E. C. (1994). Molecular cloning of two human cardiac gap junction proteins, connexin40 and connexin45. *J Mol Cell Cardiol* **26,** 861-868.

KAUSALYA, P. J., REICHERT, M. & HUNZIKER, W. (2001). Connexin45 directly binds to ZO-1 and localizes to the tight junction region in epithelial MDCK cells. *FEBS Lett* **505,** 92-96.

KIM, T. H., LEE, H. K., SEO, I. A., BAE, H. R., SUH, D. J., WU, J., RAO, Y., HWANG, K. G. & PARK, H. T. (2005). Netrin induces down-regulation of its receptor, Deleted in Colorectal Cancer, through the ubiquitin-proteasome pathway in the embryonic cortical neuron. *J Neurochem* **95,** 1-8.

KIMMEL, C. B., BALLARD, W. W., KIMMEL, S. R., ULLMANN, B. & SCHILLING, T. F. (1995). Stages of embryonic development of the zebrafish. *Dev Dyn* **203,** 253-310.

KING, B. F. & G, B. (2002). Purinergic receptors. In *Understanding G Protein-Coupled Receptors and Their Role in the CNS*. ed. M, P. & C, D., pp. 422-438. Oxford University Press, Oxford.

KING, B. F. & TOWNSEND-NICHOLSON, A. (2000). Recombinant P2Y receptors: the UCL experience. *J Auton Nerv Syst* **81,** 164-170.

KRAMER-ZUCKER, A. G., OLALE, F., HAYCRAFT, C. J., YODER, B. K., SCHIER, A. F. & DRUMMOND, I. A. (2005). Cilia-driven fluid flow in the zebrafish pronephros, brain and Kupffer's vesicle is required for normal organogenesis. *Development* **132,** 1907-1921.

KREILING, J. A., WILLIAMS, G. & CRETON, R. (2007). Analysis of Kupffer's vesicle in zebrafish embryos using a cave automated virtual environment. *Dev Dyn* **236,** 1963-1969.

KRUFKA, A., JOHNSON, R. G., WYLIE, C. C. & HEASMAN, J. (1998). Evidence that dorsal-ventral differences in gap junctional communication in the early Xenopus embryo are generated by beta-catenin independent of cell adhesion effects. *Dev Biol* **200,** 92-102.

KRUGER, O., PLUM, A., KIM, J. S., WINTERHAGER, E., MAXEINER, S., HALLAS, G., KIRCHHOFF, S., TRAUB, O., LAMERS, W. H. & WILLECKE, K. (2000). Defective vascular development in connexin 45-deficient mice. *Development* **127,** 4179-4193.

KUMAI, M., NISHII, K., NAKAMURA, K., TAKEDA, N., SUZUKI, M. & SHIBATA, Y. (2000). Loss of connexin45 causes a cushion defect in early cardiogenesis. *Development* **127,** 3501-3512.

KUMAR, N. M. & GILULA, N. B. (1996). The gap junction communication channel. *Cell* **84,** 381-388.

LARSON, J. D., WADMAN, S. A., CHEN, E., KERLEY, L., CLARK, K. J., EIDE, M., LIPPERT, S., NASEVICIUS, A., EKKER, S. C., HACKETT, P. B. & ESSNER, J. J. (2004). Expression of VE-cadherin in zebrafish embryos: a new tool to evaluate vascular development. *Dev Dyn* **231,** 204-213.

LAUDERDALE, J. D., PASQUALI, S. K., FAZEL, R., VAN EEDEN, F. J., SCHAUERTE, H. E., HAFFTER, P. & KUWADA, J. Y. (1998). Regulation of netrin-1a expression by hedgehog proteins. *Mol Cell Neurosci* **11,** 194-205.

LAWSON, N. D., VOGEL, A. M. & WEINSTEIN, B. M. (2002). sonic hedgehog and vascular endothelial growth factor act upstream of the Notch pathway during arterial endothelial differentiation. *Dev Cell* **3,** 127-136.

LAWSON, N. D. & WEINSTEIN, B. M. (2002a). Arteries and veins: making a difference with zebrafish. *Nat Rev Genet* **3,** 674-682.

LAWSON, N. D. & WEINSTEIN, B. M. (2002b). In vivo imaging of embryonic vascular development using transgenic zebrafish. *Dev Biol* **248,** 307-318.

LEE, J. D. & ANDERSON, K. V. (2008). Morphogenesis of the node and notochord: the cellular basis for the establishment and maintenance of left-right asymmetry in the mouse. *Dev Dyn* **237,** 3464-3476.

LEIPZIGER, J. (2003). Control of epithelial transport via luminal P2 receptors. *Am J Physiol Renal Physiol* **284,** F419-432.

LEITHE, E. & RIVEDAL, E. (2004). Ubiquitination and down-regulation of gap junction protein connexin-43 in response to 12-O-tetradecanoylphorbol 13-acetate treatment. *J Biol Chem* **279,** 50089-50096.

LEVIN, M. (2005). Left-right asymmetry in embryonic development: a comprehensive review. *Mech Dev* **122,** 3-25.

LEVIN, M. & MERCOLA, M. (1998). Gap junctions are involved in the early generation of left-right asymmetry. *Dev Biol* **203,** 90-105.

LEVIN, M. & MERCOLA, M. (1999). Gap junction-mediated transfer of left-right patterning signals in the early chick blastoderm is upstream of Shh asymmetry in the node. *Development* **126,** 4703-4714.

LEVIN, M. & NASCONE, N. (1997). Two molecular models of initial left-right asymmetry generation. *Med Hypotheses* **49,** 429-435.

LI, H., LIU, T. F., LAZRAK, A., PERACCHIA, C., GOLDBERG, G. S., LAMPE, P. D. & JOHNSON, R. G. (1996). Properties and regulation of gap junctional hemichannels in the plasma membranes of cultured cells. *J Cell Biol* **134,** 1019-1030.

LI, Q., SCHACHTER, J. B., HARDEN, T. K. & NICHOLAS, R. A. (1997). The 6H1 orphan receptor, claimed to be the p2y5 receptor, does not mediate nucleotide-promoted second messenger responses. *Biochem Biophys Res Commun* **236,** 455-460.

LO, C. W., WALDO, K. L. & KIRBY, M. L. (1999). Gap junction communication and the modulation of cardiac neural crest cells. *Trends Cardiovasc Med* **9,** 63-69.

LONG, S., AHMAD, N. & REBAGLIATI, M. (2003). The zebrafish nodal-related gene southpaw is required for visceral and diencephalic left-right asymmetry. *Development* **130,** 2303-2316.

LU, X., LE NOBLE, F., YUAN, L., JIANG, Q., DE LAFARGE, B., SUGIYAMA, D., BREANT, C., CLAES, F., DE SMET, F., THOMAS, J. L., AUTIERO, M., CARMELIET, P., TESSIER-LAVIGNE, M. & EICHMANN, A. (2004). The netrin receptor UNC5B mediates guidance events controlling morphogenesis of the vascular system. *Nature* **432,** 179-186.

LUBARSKY, B. & KRASNOW, M. A. (2003). Tube morphogenesis: making and shaping biological tubes. *Cell* **112,** 19-28.

MASSA, M., ROSTI, V., FERRARIO, M., CAMPANELLI, R., RAMAJOLI, I., ROSSO, R., DE FERRARI, G. M., FERLINI, M., GOFFREDO, L., BERTOLETTI, A., KLERSY, C., PECCI, A., MORATTI, R. & TAVAZZI, L. (2005). Increased circulating hematopoietic and endothelial progenitor cells in the early phase of acute myocardial infarction. *Blood* **105,** 199-206.

MCCULLOCH, F., CHAMBREY, R., ELADARI, D. & PETI-PETERDI, J. (2005). Localization of connexin 30 in the luminal membrane of cells in the distal nephron. *Am J Physiol Renal Physiol* **289,** F1304-1312.

MCGRATH, J. & BRUECKNER, M. (2003). Cilia are at the heart of vertebrate left-right asymmetry. *Curr Opin Genet Dev* **13,** 385-392.

MCGRATH, J., SOMLO, S., MAKOVA, S., TIAN, X. & BRUECKNER, M. (2003). Two populations of node monocilia initiate left-right asymmetry in the mouse. *Cell* **114,** 61-73.

MENO, C., SAIJOH, Y., FUJII, H., IKEDA, M., YOKOYAMA, T., YOKOYAMA, M., TOYODA, Y. & HAMADA, H. (1996). Left-right asymmetric expression of the TGF beta-family member lefty in mouse embryos. *Nature* **381,** 151-155.

MENO, C., SHIMONO, A., SAIJOH, Y., YASHIRO, K., MOCHIDA, K., OHISHI, S., NOJI, S., KONDOH, H. & HAMADA, H. (1998). lefty-1 is required for left-right determination as a regulator of lefty-2 and nodal. *Cell* **94,** 287-297.

MERCOLA, M. (2003). Left-right asymmetry: nodal points. *J Cell Sci* **116,** 3251-3257.

MORENO, A. P. & LAU, A. F. (2007). Gap junction channel gating modulated through protein phosphorylation. *Prog Biophys Mol Biol* **94,** 107-119.

MURASAWA, S. & ASAHARA, T. (2005). Endothelial progenitor cells for vasculogenesis. *Physiology (Bethesda)* **20,** 36-42.

NACHT, M., ST MARTIN, T. B., BYRNE, A., KLINGER, K. W., TEICHER, B. A., MADDEN, S. L. & JIANG, Y. (2009). Netrin-4 regulates angiogenic responses and tumor cell growth. *Exp Cell Res* **315,** 784-794.

NASEVICIUS, A. & EKKER, S. C. (2000). Effective targeted gene 'knockdown' in zebrafish. *Nat Genet* **26,** 216-220.

NEUGEBAUER, J. M., AMACK, J. D., PETERSON, A. G., BISGROVE, B. W. & YOST, H. J. (2009). FGF signalling during embryo development regulates cilia length in diverse epithelia. *Nature* **458,** 651-654.

NONAKA, S., SHIRATORI, H., SAIJOH, Y. & HAMADA, H. (2002). Determination of left-right patterning of the mouse embryo by artificial nodal flow. *Nature* **418,** 96-99.

NONAKA, S., TANAKA, Y., OKADA, Y., TAKEDA, S., HARADA, A., KANAI, Y., KIDO, M. & HIROKAWA, N. (1998). Randomization of left-right asymmetry due to loss of nodal cilia generating leftward flow of extraembryonic fluid in mice lacking KIF3B motor protein. *Cell* **95,** 829-837.

NONAKA, S., YOSHIBA, S., WATANABE, D., IKEUCHI, S., GOTO, T., MARSHALL, W. F. & HAMADA, H. (2005). De novo formation of left-right asymmetry by posterior tilt of nodal cilia. *PLoS Biol* **3,** e268.

NUMAGUCHI, Y., SONE, T., OKUMURA, K., ISHII, M., MORITA, Y., KUBOTA, R., YOKOUCHI, K., IMAI, H., HARADA, M., OSANAI, H., KONDO, T. & MUROHARA, T. (2006). The impact of the capability of circulating progenitor cell to differentiate on myocardial salvage in patients with primary acute myocardial infarction. *Circulation* **114,** I114-119.

OKADA, Y., TAKEDA, S., TANAKA, Y., BELMONTE, J. C. & HIROKAWA, N. (2005). Mechanism of nodal flow: a conserved symmetry breaking event in left-right axis determination. *Cell* **121,** 633-644.

OLSON, D. J., CHRISTIAN, J. L. & MOON, R. T. (1991). Effect of wnt-1 and related proteins on gap junctional communication in Xenopus embryos. *Science* **252,** 1173-1176.

PASTERNACK, S. M., VON KUGELGEN, I., ABOUD, K. A., LEE, Y. A., RUSCHENDORF, F., VOSS, K., HILLMER, A. M., MOLDERINGS, G. J., FRANZ, T., RAMIREZ, A., NURNBERG, P., NOTHEN, M. M. & BETZ, R. C. (2008). G protein-coupled receptor P2Y5 and its ligand LPA are involved in maintenance of human hair growth. *Nat Genet* **40,** 329-334.

PATAN, S. (2000). Vasculogenesis and angiogenesis as mechanisms of vascular network formation, growth and remodeling. *J Neurooncol* **50,** 1-15.

PEETERS, H. & DEVRIENDT, K. (2006). Human laterality disorders. *Eur J Med Genet* **49,** 349-362.

PENUELA, S., BHALLA, R., GONG, X. Q., COWAN, K. N., CELETTI, S. J., COWAN, B. J., BAI, D., SHAO, Q. & LAIRD, D. W. (2007). Pannexin 1 and pannexin 3 are glycoproteins that exhibit many distinct characteristics from the connexin family of gap junction proteins. *J Cell Sci* **120,** 3772-3783.

RAYA, A. & BELMONTE, J. C. (2006). Left-right asymmetry in the vertebrate embryo: from early information to higher-level integration. *Nat Rev Genet* **7,** 283-293.

REAUME, A. G., DE SOUSA, P. A., KULKARNI, S., LANGILLE, B. L., ZHU, D., DAVIES, T. C., JUNEJA, S. C., KIDDER, G. M. & ROSSANT, J. (1995). Cardiac malformation in neonatal mice lacking connexin43. *Science* **267,** 1831-1834.

SAEZ, J. C., BERTHOUD, V. M., BRANES, M. C., MARTINEZ, A. D. & BEYER, E. C. (2003). Plasma membrane channels formed by connexins: their regulation and functions. *Physiol Rev* **83,** 1359-1400.

SARMAH, B., LATIMER, A. J., APPEL, B. & WENTE, S. R. (2005). Inositol polyphosphates regulate zebrafish left-right asymmetry. *Dev Cell* **9,** 133-145.

SCHALPER, K. A., PALACIOS-PRADO, N., RETAMAL, M. A., SHOJI, K. F., MARTINEZ, A. D. & SAEZ, J. C. (2008). Connexin hemichannel composition determines the FGF-1-induced membrane permeability and free [Ca2+]i responses. *Mol Biol Cell* **19,** 3501-3513.

SCHILTHUIZEN, M. & DAVISON, A. (2005). The convoluted evolution of snail chirality. *Naturwissenschaften* **92,** 504-515.

SCHNEIDER, I., HOUSTON, D. W., REBAGLIATI, M. R. & SLUSARSKI, D. C. (2008). Calcium fluxes in dorsal forerunner cells antagonize -catenin and alter left-right patterning. *Development* **135,** 75-84.

SCHWARZ, Q., GU, C., FUJISAWA, H., SABELKO, K., GERTSENSTEIN, M., NAGY, A., TANIGUCHI, M., KOLODKIN, A. L., GINTY, D. D., SHIMA, D. T. & RUHRBERG, C. (2004). Vascular endothelial growth factor controls neuronal migration and cooperates with Sema3A to pattern distinct compartments of the facial nerve. *Genes Dev* **18,** 2822-2834.

SCHWEICKERT, A., WEBER, T., BEYER, T., VICK, P., BOGUSCH, S., FEISTEL, K. & BLUM, M. (2007). Cilia-driven leftward flow determines laterality in Xenopus. *Curr Biol* **17,** 60-66.

SHIN, J. T. & FISHMAN, M. C. (2002). From Zebrafish to human: modular medical models. *Annu Rev Genomics Hum Genet* **3,** 311-340.

SHINTANI, S., MUROHARA, T., IKEDA, H., UENO, T., HONMA, T., KATOH, A., SASAKI, K., SHIMADA, T., OIKE, Y. & IMAIZUMI, T. (2001). Mobilization of endothelial progenitor cells in patients with acute myocardial infarction. *Circulation* **103,** 2776-2779.

SHWEIKI D, I. A., SOFFER D, KESHET E. (1992). Vascular endothelial growth factor induced by hypoxia may mediate hypoxia-initiated angiogenesis. *Nature* **359,** 843-845.

SIMON, A. M., GOODENOUGH, D. A., LI, E. & PAUL, D. L. (1997). Female infertility in mice lacking connexin 37. *Nature* **385,** 525-529.

SOLAN, J. L. & LAMPE, P. D. (2009). Connexin43 phosphorylation: structural changes and biological effects. *Biochem J* **419,** 261-272.

SPRAY, D. C., YE, Z. C. & RANSOM, B. R. (2006). Functional connexin "hemichannels": a critical appraisal. *Glia* **54,** 758-773.

STEMPLE, D. L. (2005). Structure and function of the notochord: an essential organ for chordate development. *Development* **132,** 2503-2512.

STRAHLE, U., FISCHER, N. & BLADER, P. (1997). Expression and regulation of a netrin homologue in the zebrafish embryo. *Mech Dev* **62,** 147-160.

TANAKA, Y., OKADA, Y. & HIROKAWA, N. (2005). FGF-induced vesicular release of Sonic hedgehog and retinoic acid in leftward nodal flow is critical for left-right determination. *Nature* **435,** 172-177.

TAYLOR, J. S., BRAASCH, I., FRICKEY, T., MEYER, A. & VAN DE PEER, Y. (2003). Genome duplication, a trait shared by 22000 species of ray-finned fish. *Genome Res* **13,** 382-390.

TONG, D., LI, T. Y., NAUS, K. E., BAI, D. & KIDDER, G. M. (2007). In vivo analysis of undocked connexin43 gap junction hemichannels in ovarian granulosa cells. *J Cell Sci* **120,** 4016-4024.

TRAVER, D., PAW, B. H., POSS, K. D., PENBERTHY, W. T., LIN, S. & ZON, L. I. (2003). Transplantation and in vivo imaging of multilineage engraftment in zebrafish bloodless mutants. *Nat Immunol* **4,** 1238-1246.

WARNER, A. E., GUTHRIE, S. C. & GILULA, N. B. (1984). Antibodies to gap-junctional protein selectively disrupt junctional communication in the early amphibian embryo. *Nature* **311,** 127-131.

WEBB, T. E., KAPLAN, M. G. & BARNARD, E. A. (1996). Identification of 6H1 as a P2Y purinoceptor: P2Y5. *Biochem Biophys Res Commun* **219,** 105-110.

WEI, C. J., FRANCIS, R., XU, X. & LO, C. W. (2005). Connexin43 associated with an N-cadherin-containing multiprotein complex is required for gap junction formation in NIH3T3 cells. *J Biol Chem* **280,** 19925-19936.

WEI, C. J., XU, X. & LO, C. W. (2004). Connexins and cell signaling in development and disease. *Annu Rev Cell Dev Biol* **20,** 811-838.

WHITE, T. W., GOODENOUGH, D. A. & PAUL, D. L. (1998). Targeted ablation of connexin50 in mice results in microphthalmia and zonular pulverulent cataracts. *J Cell Biol* **143,** 815-825.

WILLECKE, K., EIBERGER, J., DEGEN, J., ECKARDT, D., ROMUALDI, A., GULDENAGEL, M., DEUTSCH, U. & SOHL, G. (2002). Structural and functional diversity of connexin genes in the mouse and human genome. *Biol Chem* **383,** 725-737.

WILSON, B. D., II, M., PARK, K. W., SULI, A., SORENSEN, L. K., LARRIEU-LAHARGUE, F., URNESS, L. D., SUH, W., ASAI, J., KOCK, G. A., THORNE, T., SILVER, M., THOMAS, K. R., CHIEN, C. B., LOSORDO, D. W. & LI, D. Y. (2006). Netrins promote developmental and therapeutic angiogenesis. *Science* **313,** 640-644.

WOLFF, S. C., QI, A. D., HARDEN, T. K. & NICHOLAS, R. A. (2005). Polarized expression of human P2Y receptors in epithelial cells from kidney, lung, and colon. *Am J Physiol Cell Physiol* **288,** C624-632.

YANCEY, S. B., BISWAL, S. & REVEL, J. P. (1992). Spatial and temporal patterns of distribution of the gap junction protein connexin43 during mouse gastrulation and organogenesis. *Development* **114,** 203-212.

YANG, Y., ZOU, L., WANG, Y., XU, K. S., ZHANG, J. X. & ZHANG, J. H. (2007). Axon guidance cue Netrin-1 has dual function in angiogenesis. *Cancer Biol Ther* **6,** 743-748.

YELON, D., HORNE, S. A. & STAINIER, D. Y. (1999). Restricted expression of cardiac myosin genes reveals regulated aspects of heart tube assembly in zebrafish. *Dev Biol* **214,** 23-37.

YEN, H. J., TAYEH, M. K., MULLINS, R. F., STONE, E. M., SHEFFIELD, V. C. & SLUSARSKI, D. C. (2006). Bardet-Biedl syndrome genes are important in retrograde intracellular trafficking and Kupffer's vesicle cilia function. *Hum Mol Genet* **15,** 667-677.

YOST, H. J. (2003). Left-right asymmetry: nodal cilia make and catch a wave. *Curr Biol* **13,** R808-809.